Multimerization and Membrane Interactions of Bromovirus 1a Protein in RNA Replication Complex Assembly and Function

By

Bryan S. Sibert

A dissertation submitted in partial fulfillment of
the requirements for the degree of

Doctor of Philosophy
(Cellular and Molecular Biology)

at the
UNIVERSITY OF WISCONSIN-MADISON
2016

Date of final oral examination: 4/15/2016
The dissertation is approved by the following members of the Final Oral Committee:
Paul Ahlquist, Professor, Oncology and Plant Pathology
Jon Audhya, Associate Professor, Biomolecular Chemistry
William Bement, Professor, Zoology
James Keck, Professor, Biomolecular Chemistry
Ann Palmenberg, Professor, Biochemistry

ABSTRACT

Positive-strand RNA ((+)RNA) viruses, which include many important human, animal and plant pathogens, all replicate their genomic RNAs in membrane-associated complexes that sequester RNA replication from host defenses and coordinate transitions between RNA translation, replication, and encapsidation. Such RNA replication is a proven, valuable target for (+)RNA virus control. Moreover, conserved requirements for replication complex assembly, including de novo lipid synthesis and viral protein multimerization, are potential targets for the highly valuable goal of broad-spectrum antivirals.

To investigate early steps in (+)RNA virus genome replication, including viral RNA replication protein multimerization, membrane targeting, and membrane rearrangement, we studied an advanced model system, brome mosaic virus (BMV). The large (961 aa), highly multifunctional BMV 1a protein is the only viral factor necessary to induce replication compartment membrane rearrangements in its natural plant hosts and the model yeast S*accharomyces cerevisiae*. Previous studies showed that 1a's N-terminal, 557 aa RNA capping domain (1aN) is sufficient for localizing to endoplasmic reticulum membranes, the normal site of BMV RNA replication. Moreover, in vivo, 1aN multimerizes into tubules that link with membranes and each other through yet unmapped interactions that are nevertheless strongly implicated in replication complex assembly.

We used deletion and mutational analysis to identify additional BMV 1aN regions, beyond a previously identified amphipathic helix, that contribute to membrane binding and proper 1a localization to endoplasmic reticulum membranes in particular. We further showed that known 1a functions, including RNA replication complex assembly, can also be reconstituted in yeast for another bromovirus, cowpea chlorotic mottle virus (CCMV). In yeast, the CCMV 1aN fragment also formed tubule lattices, whose conservation and dominant negative effects on CCMV genome replication further support the importance of 1aN-1aN interactions for RNA replication.

Using BMV-CCMV 1a protein hybrids, we found two distal segments of 1aN, separated by 170 aa, whose compatibility is required for proper 1a intracellular localization, the earliest known step in RNA replication. Moreover, by co-immunoprecipitation analysis, we found that

1aN fragments containing these two distal segments interacted heterotypically, and each multimerized homotypically. Notably, these distal interacting regions each contain sequence motifs not only conserved across bromovirus 1a proteins, but across the entire alphavirus-like superfamily of human, animal, and plant viruses, implying that their underlying functions and interactions are of early and fundamental importance to RNA replication.

Overall, these and other data in this thesis indicate that the earliest steps of bromovirus RNA replication complex assembly, 1a localization, membrane association, and multimerization, are likely linked and require contributions from segments that we mapped throughout the 1aN domain. Our data further provide evidence that viral protein multimerization is essential for (+)RNA virus replication and is a valuable therapeutic target. Since BMV 1a shares significant structural and functional similarities with proteins in and beyond the alphavirus-like superfamily of (+)RNA viruses, the interactions identified here may provide insight into RNA replication complex assembly in a broad range of viruses.

ACKNOWLEDGEMENTS

First and foremost, I would like to thank my advisor Paul Ahlquist for his mentorship, support, and for allowing me the opportunities to develop as a scientist. I would like to thank all of the members of the Ahlquist lab who have contributed to this project in innumerable ways. Thanks to Johan den Boon, Brandi Gancarz, Ling Liu, Masaki Nishikiori, Rob Pugh, Xiaofeng Wang, and the rest of the BMV subgroup for providing protocols and reagents, scientific discussions, and helpful suggestions. Thanks to Megan Bracken, Jim Bruce, Mark Horswill, Justin Massey, Amanda Navine, Kathleen Wessels, and Debbie Van De Velde for all of their assistance and for making the lab a great place to work. I would like to especially thank Arturo Diaz for passing along so much of his knowledge to me, for always being available to answer any questions I had, and for being a great office mate. Thanks to Ben August, Desirée Benefield, Randall Massey, and Janice Pennington for their assistance with electron microscopy and their constant willingness to discuss and attempt new strategies for better sample preparation. Thanks to Lance Rodenkirch and Sarah Swanson for their assistance with confocal and super resolution microscopy. Thanks to Robyn Roberts and the lab of Aurelie Rakotondrafara for providing the oat cell culture system and continued assistance with its use and maintenance. Special thanks to my committee members, Drs. Jon Audyha, Bill Bement, Jim Keck, and Ann Palmenberg, for all of their guidance and helpful suggestions over the years. Finally, I would like to thank my parents and the rest of my family for their constant support, encouragement, and motivation. Thanks to all of my friends in CMB and in Madison for the great times we had together outside of the lab. I am especially grateful for Holly Basta, Tyler Peterson, Rup Chakravorty, Jess Ciomperlik, Adam Swick, and Hannah Delong who were like a family away from home.

This research was partially supported by US National Institutes of Health (NIH) grant R01-GM35072 and by NIH training grant 5T32-GM007215. Paul Ahlquist is an investigator of the Howard Hughes Medical Institute.

TABLE OF CONTENTS

Abstract……..i

Acknowledgements……...iii

List of figures……...v

Abbreviations……vii

Chapter 1: General introduction…….....1

Chapter 2: Bromovirus 1a protein contains multiple determinants for
membrane association and localization of the RNA replication complex…….....21

Chapter 3: Bromovirus hybrids reveal host-specific effects
in viral RNA template recruitment and replication…….37

Chapter 4: Analysis of bromovirus 1a protein hybrids reveals
1a-1a interactions essential for RNA replication complex assembly…….64

Chapter 5: Summary and future directions……...90

List of references……98

LIST OF FIGURES

Figure		Page
Figure 1.1	Positive-strand RNA virus lifecycle	3
Figure 1.2	Structure of spherule-type replication complexes	5
Figure 1.3	Structure of DMV-type replication complexes	7
Figure 1.4	Electron microscopy and model of BMV spherules	9
Figure 1.5	Parallels between (+)RNA virus spherules and retrovirus and dsRNA virus capsids	14
Figure 1.6	BMV genome	16
Figure 2.1	BMV 1a retains strong membrane association after deletion of helix A	24
Figure 2.2	Deletions near the N-terminus of BMV 1a reduce 1a membrane association	27
Figure 2.3	BMV 1a perinuclear localization is disrupted by deletions near the N-terminus	28
Figure 2.4	Mutations at several positions in 1a disrupt ER localization	29
Figure 2.5	Decreased membrane association and aberrant localization are correlated with decreased 1aN interaction by Y2H	31
Figure 3.1	DNA based BMV RNA3 expression and replication	38
Figure 3.2	RNA template specific differences in the ability of BMV and CCMV to support RNA replication in plants and yeast	41
Figure 3.3	CCMV 2a polymerase is competent for negative-strand RNA synthesis in yeast	43
Figure 3.4	CCMV 1a is defective relative to BMV 1a in recruiting RNA templates to membranes	45
Figure 3.5	CCMV 1a localizes to the perinuclear ER and recruits CCMV 2a	47
Figure 3.6	CCMV 1a is sufficient to induce spherule membrane rearrangements along the ER	49
Figure 3.7	Tomography of BMV 1a membrane rearrangements	50
Figure 3.8	Essential multimerization of the 1a N-terminal domain is conserved between BMV and CCMV	52
Figure 3.9	CCMV 1a and 2a support replication of BMV RNA2 in yeast	54

Figure **Page**

Figure 4.1 BMV and CCMV 1a proteins and their 1aN domains interact homo- and hetero- typically……...…….67

Figure 4.2 BMV 1aN contains a self-interaction within aa367-557…….69

Figure 4.3 BMV 1aN aa367-557 co-immunoprecipitates with aa1-247……..70

Figure 4.4 BMV 1aN contains at least two self-interacting regions……...……72

Figure 4.5 Substitution of BMV 1a sequences in several regions with the corresponding sequence from CCMV 1a abolishes RNA replication ….…….74

Figure 4.6 Substitution of BMV 1a regions 3 & 7 with corresponding CCMV sequence disrupts 1a and 1aN localization……...…….75

Figure 4.7 Hybrid 1a protein B/CC 3 does not induce membrane layer replication complexes along the yeast endoplasmic reticulum……...77

Figure 4.8 Co-substitution of region 3 and 7+ in BMV 1aN with sequence from CCMV restores 1aN localization……..….79

Figure 4.9 Substitution of region 7+ with CCMV sequence in B/CC 3 and B/CC 7 fails to restore RNA replication……....……81

Figure 4.10 Mutations of five amino acids in BMV 1a abolishes 1aN filament formation and inhibits RNA replication…….……82

ABBREVIATIONS

(-)RNA	Negative-strand RNA
(+)RNA	Positive-strand RNA
3D	Three dimensional
BMV	Brome mosaic virus
BrUTP	5-Bromouridine-5′-triphosphate
CCMV	Cowpea chlorotic mottle virus
cDNA	Complementary DNA
CM	Convoluted membrane
Co-IP	Co-immunoprecipitation
DALYs	Disability-adjusted life years
DENV	Dengue virus
DMV	Double membrane vesicle
DNA	Deoxyribonucleic acid
dsRNA	Double-stranded RNA
EM	Electron microscopy
ER	Endoplasmic reticulum
ESCRT	Endosomal sorting complexes required for transport
FHV	Flock house virus
GFP	Green fluorescent protein
h.p.i	Hours post infection
HCV	Hepatitis C virus
HIV	Human immunodeficiency virus
HPF-FS	High pressure freezing and freeze substitution
mRNA	Messenger RNA
NTPase	Nucleotide triphosphatase
ORF	Open reading frame
PI4P	Phosphatidylinositol 4-phosphate

PV	Poliovirus
RCs	Replication compartments
RE	Recruitment element
RHD	Reticulon homology domain
RNA	Ribonucleic acid
RNAi	RNA interference
rRNA	Ribosomal RNA
SARS-CoV	Severe acute respiratory syndrome associated coronavirus
SDS-PAGE	Sodium dodecyl sulfate polyacrylamide gel electrophoresis
SFV	Semliki forest virus
snRNP	Small nuclear ribonucleoprotein
TBSV	Tomato bushy stunt virus
tRNA	Transfer RNA
UTR	Untranslated region
Y2H	Yeast two-hybrid

CHAPTER 1

General Introduction

Viruses are a significant burden on human health. Disability-adjusted life years (DALYs) is a measure of disease burden that accounts for years lost due to mortality and severe illness. In 2010, human immunodeficiency virus (HIV) was estimated to account for over 3% of DALYs globally [1]. Lower respiratory infections caused by influenza and respiratory syncytial viruses were responsible for over 1.5% of DALYs. Acute viral hepatitis caused >0.5% of DALYs not including cirrhosis or liver cancer secondary to infection [1]. Viruses, such as hepatitis B and human papilloma virus, cause over 10% of cancers worldwide [2]. Agricultural plant and animal viruses can cause significant economic burdens and be devastating to developing areas dependent on rural and subsistence farming.

Our primary defense against viruses is prophylactic vaccination; in fact it is the only defense available for many viruses. Vaccines and vaccination campaigns have been tremendously useful, leading the eradication of smallpox, near eradication of poliovirus (PV), and substantial reduction of new infections by viruses such as measles, mumps, rubella, and chickenpox [3]. Unfortunately, there are many significant hurdles and challenges to the treatment and prevention of viruses with vaccines. Vaccine distribution and administration can be challenging in developing areas. Compliance, especially with infant vaccinations, is an issue even in developed countries. Immunocompromised individuals, at greatest risk following infection, are often not candidates for vaccines. Perhaps most significantly, vaccine development is a significant financial and scientific undertaking that is not always successful.

Antiviral drugs are another powerful tool that we have to treat viral infection. Unlike vaccines, which are generally prophylactic, these drugs can be used to treat persistent or acute viral infections. Antiviral drugs have been developed against a number a different stages of the viral lifecycle. Correspondingly, they vary in the range of viruses that they are effective against. Oseltamivir (Tamiflu) is a neuraminidase inhibitor approved for prophylactic and therapeutic treatment of influenza viruses [4]. It is effective against a broad range of influenza

neuraminidase variants providing significant advantage over the vaccine in unpredicted pandemic or zoonotic outbreaks, but it is limited to the treatment of influenza. Ribavirin is a ribonucleoside analog that is used in the treatment of a diverse range of viruses including positive- and negative- strand RNA viruses, such as hepatitis C virus (HCV) and viral hemorrhagic fevers. Ribavirin has been shown to inhibit viral RNA synthesis among other proposed mechanisms of action [5].

Among the greatest success stories of antiviral drugs are combination therapies for the treatment of HIV and HCV, both chronic infections with no vaccine. These therapies combine the use of multiple drugs that target different essential steps of the viral lifecycle. The specific combination of drugs used can be individually tailored by physicians to best treat each patient. Antiretroviral therapy against HIV is highly effective in reducing viral load and preventing progression to acquired immune deficiency syndrome [6]. In clinical trials of a now approved HCV combination therapy, over 90% of patients with genotype 1 HCV had undetectable viral RNA 12 weeks after the end of treatment [7].

A better understanding of the mechanisms of viral replication is essential to our ability to continue to develop effective antiviral drugs. Highly conserved processes are particularly attractive due to their potential to reveal targets for broadly acting antivirals. In this work we used brome mosaic virus (BMV) as a model positive-strand RNA virus to study the essential and conserved process of membrane-associated replication complex assembly.

Positive-strand RNA Viruses

The Baltimore classification system groups viruses into seven classes based upon their genome composition and method of RNA replication. Viruses with DNA as their genomic material are divided into three classes: single-stranded, double-stranded, and reverse-transcribing DNA viruses. RNA viruses are also divided into single-stranded, double-stranded, and reverse-transcribing RNA viruses with single-stranded RNA viruses being further divided into negative- (-) or positive- (+) single-stranded RNA viruses.

(+)RNA viruses have directly translatable genomic RNAs and replicate through negative-strand RNA intermediates. A schematic of a generic (+)RNA virus lifecycle can be seen

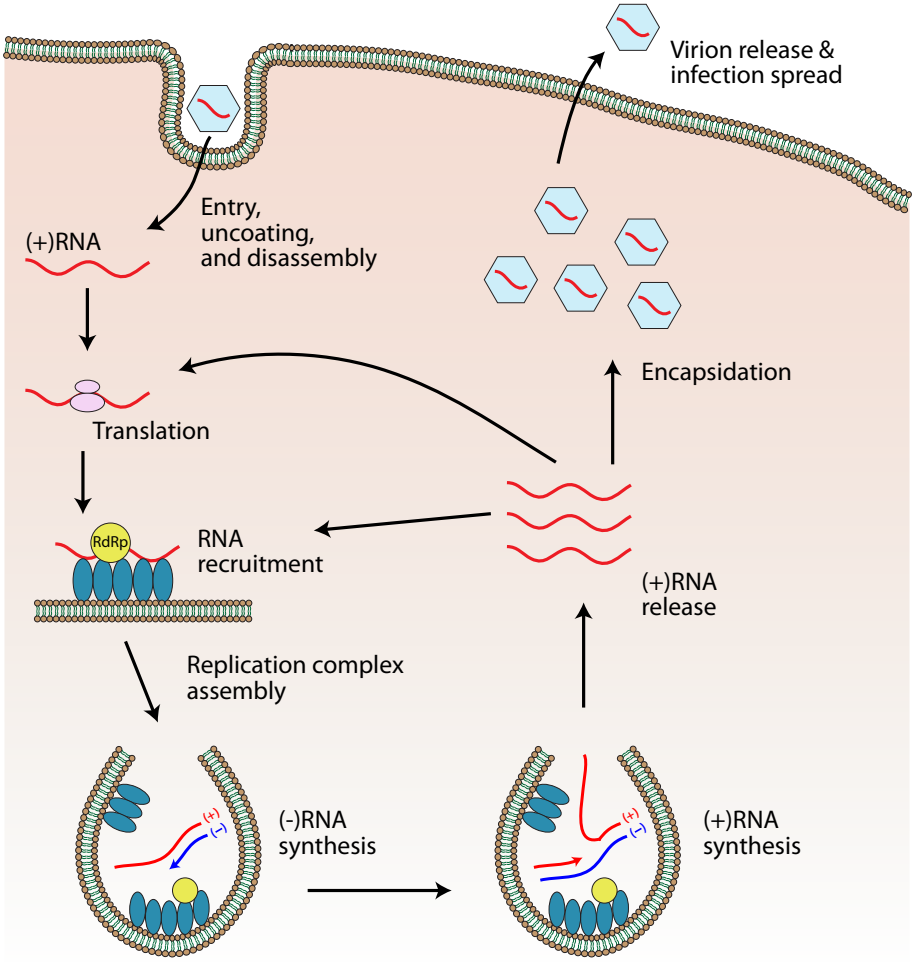

Figure 1.1. Positive-strand RNA virus lifecycle. Image adapted from Nagy P.D. & Pogany J. Nature Reviews Microbiology **10** p.137-149 (2012) Following entry the capsid releases the genomic RNA into the cytoplasm where it is translated by host ribosomes. After a sufficient level of replication proteins have been synthesized the viral proteins recruit the RNA from translation to the membrane and assemble the replication complex. A complementary (-)RNA is synthesized by the viral polymerase that then serves as a template for synthesis of (+) viral genomic and mRNAs. The newly synthesized (+) genomic RNAs may be translated, recruited to a new replication complex, or encapsidated for release.

in figure 1.1. (+)RNA viruses comprise the majority of plant viruses, many of which, such as the barley yellow dwarf viruses [8], can cause significant loss of important agricultural crops . Foot and mouth disease virus [9], porcine reproductive and respiratory syndrome virus [10], and other (+)RNA viruses have economic impacts on animal farming.

(+)RNA viruses also include many important human pathogens such as PV, HCV, severe acute respiratory syndrome associated coronavirus (SARS-CoV), dengue virus (DENV), chikungunya virus, and Zika virus. The geographical distribution of many of these viruses has expanded in recent years and decades, in part due to expanded range of their mosquito vectors [11], increasing their potential impact on human health.

(+)RNA virus genome replication occurs on rearranged membranes

(+)RNA viruses do not package their RNA replication proteins in the virion. After entry, the viral genomic RNA is directly translated by host ribosomes to generate the nonstructural (i.e., non-virion) proteins essential for RNA replication, including the RNA-dependent RNA polymerase. The nonstructural proteins associate with cellular membrane and recruit the host and viral factors necessary for RNA replication. All (+)RNA viruses replicate in the cytoplasm in association with intracellular membranes (Fig. 1.1). The membranes utilized and the topologies of these replication compartments (RCs) vary among viruses (for review see [12]).

The RC membrane rearrangements serve a number of important functions for the virus. The genomic RNA of a (+)RNA virus must function as an mRNA, replication template, and packaging substrate during different stages of infection. (-)RNA synthesis and translation occur in opposite directions along the (+)RNA and thus cannot occur simultaneously. The membrane-bound RC provides physical containment to separate the viral RNA template from these competing processes. The membrane-associated RC also provides a physical scaffold to concentrate and organize viral and host factors essential for RNA replication and to organize the successive steps of RNA replication. As expected, electron microscopy (EM) and immuno-EM studies for a number of viruses have shown that the membrane at the site of RNA replication is generally free of ribosomes and viral coat proteins [13, 14]. The RC further

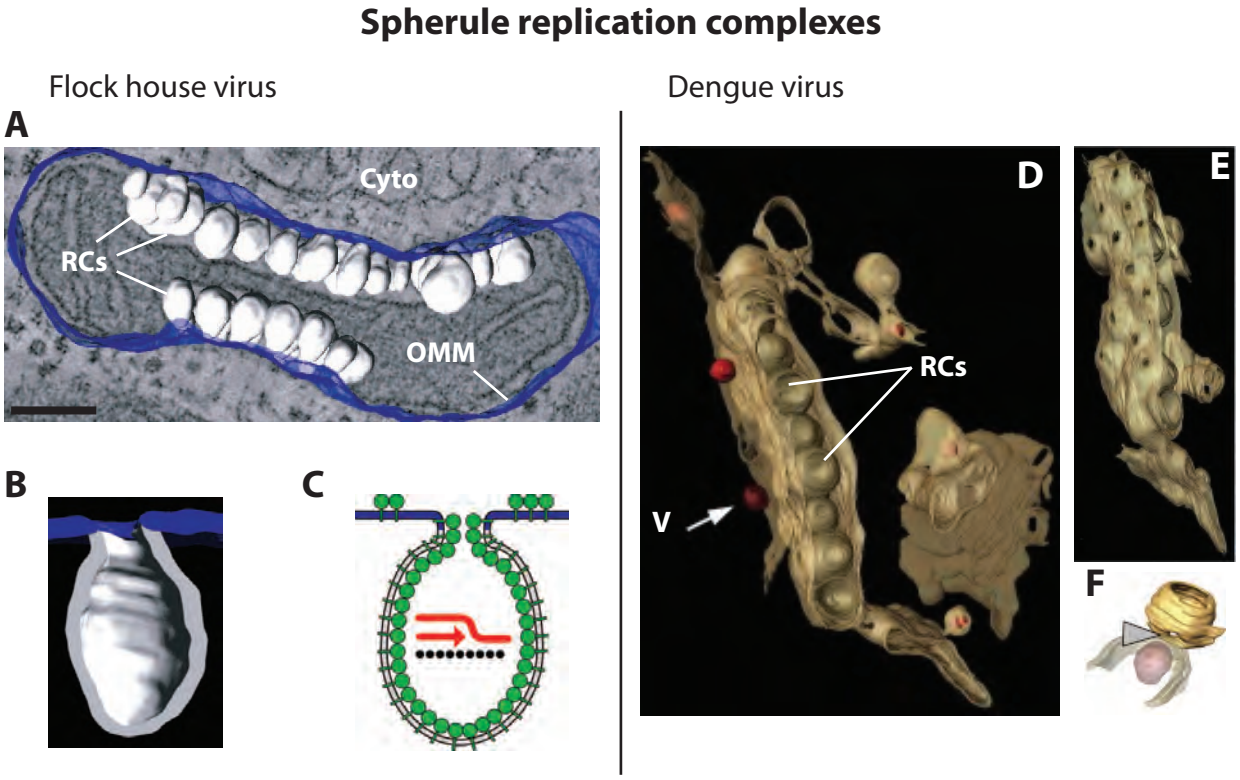

Figure 1.2. Structure of spherule type replication complexes. (A) 3D reconstruction of Flock house virus replication complexes (RCs) along the outer mitochondrial membrane (OMM) assembled from EM tomography. The vesicles pack closely together but do not connect to each other. (B) Cross-section of an FHV spherule showing a ~10 nm neck connecting the spherule interior and the cytoplasm. (C) The FHV spherule contains hundreds of copies of the self-interacting, transmembrane FHV protein A which would be sufficient to coat the vesicle interior as modeled here. (D) 3D reconstruction of dengue virus replication complexes derived from the endoplasmic reticulum. Virions (V, red) are associated with ER closely apposed to the neck of the spherules (also see (F)). (E) The interior of DENV spherules remain connected to the cytoplasm through pores in the membrane. Scale bar is 100 nm. A-C from PLoS Biol 5(9): e220 (2007); D-F from Cell Host Microbe 5(4): 365-375 (2009).

supports RNA replication through retention of the (-)RNA template, which allows for efficient generation and export of (+)RNA produced in far excess to the (-)RNA template.

Assembly of the RC protects the viral RNA and replication factors from degradation by nucleases and proteases in the cytoplasm. Recruitment of RNA to the RC has been shown to protect the RNA from subsequent nuclease digestion in a number of viruses [15-18]. The half-life of a BMV genomic RNA increases from 3-4 minutes in cells lacking viral RNA replication proteins and RCs to significantly over an hour in cells containing RCs [19]. Similarly, HCV proteins in the RC have been shown to be protected from protease treatment of isolated RCs [20]. The RC also serves to protect double-stranded RNA (dsRNA) replication intermediates from recognition by host innate immune responses including RNA interference and interferon responses induced by detection of dsRNA [21].

Though the RC excludes factors essential for translation and packaging from the site of RNA replication, it plays an important role in coordinating these processes. Direct coupling of RNA replication with translation and/or packaging has been demonstrated for a number of (+)RNA viruses [22]. PV RNA, e.g., must be translated prior to recruitment to the RC [23]. EM tomography of DENV revealed that RNA replication, translation, and virion assembly occur in close proximity on a connected network of ER-derived membrane structures [14]. EM tomography of Flock house virus (FHV) revealed large clusters of virions in close proximity to RC containing mitochondria demonstrating that this coordination is not limited to viruses whose RC is associated with the endoplasmic reticulum (ER) [24].

The RCs of different viruses have been divided into two broad classes based upon their overall morphology as observed by EM. Many viruses, including BMV, the focus of this work, form necked invaginations of cytoplasmic membranes with predominantly negative membrane curvature (away from the cytoplasm). These are commonly referred to as spherule-type RCs (Fig. 1.2). The invaginations vary in size among different viruses, but their interiors always remain connected to the cytoplasm. The vesicular nature and open necks of the spherules (Fig. 1.2B,E) can be clearly seen in 3D reconstructions from electron tomography of spherule-type RCs of FHV and DENV (Fig. 1.2). It is well established through immuno-EM studies in several viruses that RNA replication occurs inside of these spherules [14, 17, 25, 26].

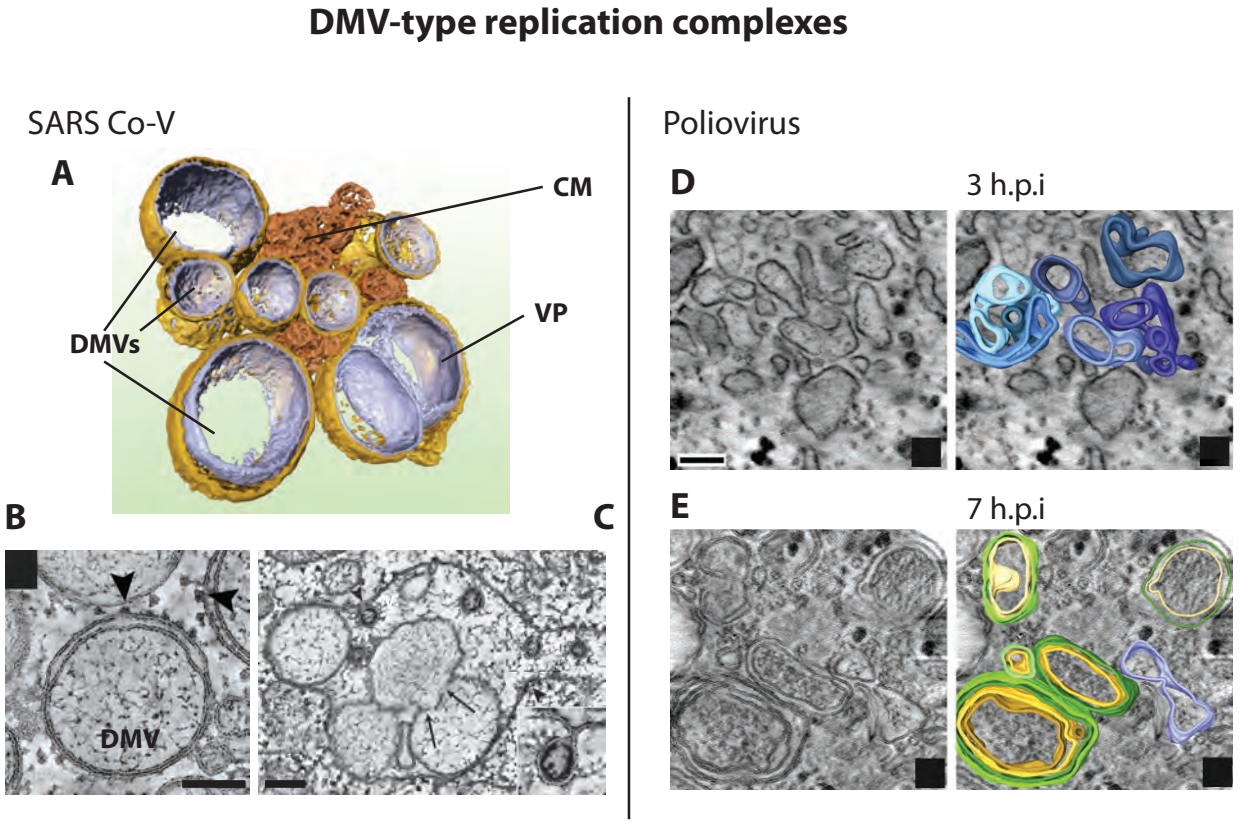

Figure 1.3. Structure of DMV-type replication complexes. (A) 3D EM tomography reconstruction of the SARS-CoV replication complex containing DMVs, a vesicle packet (VP) containing two single-membrane vesicles, and convoluted membrane (CM). (B) DMV and VP outer membranes remain contiguous with the rough-ER and often have associated ribosomes (arrowheads); no ribosomes are observed on interior membranes. (C) Virions assemble in association with VP outer membranes during late stages of SARS-CoV infection (arrowheads) . (D) Poliovirus induces single membrane structures (blue) early in infection (3 h.p.i) that are shown to be convoluted tubules by tomography. (E) Late in infection (7 h.p.i.) double membrane structures and vesicles (green - outer membrane, yellow - inner membrane) are predominant. Scale bars are 100 nm. A-C from PLoS Biol 6(9): e226 (2008); D,E from J Virol 86(1): 302-312 (2012).

Other viruses, such as SARS-CoV and PV, form a variety of structures including double-membrane vesicles (DMVs), convoluted membranes, and/or vesicle packets. These varied membrane ultrastructures are collectively referred to as DMV-type RCs. In some cases, different membrane rearrangements occur simultaneously within a single cell, as shown in the 3D reconstruction of a SARS-CoV RC (Fig. 1.3A). Additionally, the predominant membrane rearrangements may change throughout the course of viral replication, as has been shown for PV (Fig. 1.3B). The structures of spherule- and DMV- RCs and the similarities between them are discussed in more detail further below.

Spherule-type replication compartments

Early EM studies of bromovirus infected plant cells revealed invaginations of the endoplasmic reticulum approximately 70 nm in diameter, though their origin and function remained unknown (Fig. 1.4A,B) [27-29]. Schwartz et al. showed that the multifunctional, non-structural, BMV 1a replication protein was sufficient to induce similar membrane rearrangements in the model organism S*accharomyces cerevisiae* in the absence of other viral factors or viral RNA replication (Fig. 1.4C,D) [17]. It was later found that BMV 1a is sufficient to induce membrane rearrangements in plant cells [30], as in yeast [17].

In yeast, BMV 1a induces invaginations of the yeast perinuclear ER approximately 70 nm in diameter that, in at least some cases, remain connected to the cytoplasm by neck-like structures, as in observations of infected plant ER. BMV is fully competent for RNA replication in *S. cerevisiae* [31]. Newly synthesized RNA, labeled with BrUTP, was detected within the spherule interiors by immuno-EM, along with the BMV 1a protein and the 2a RNA-dependent RNA polymerase (Fig. 1.4E) [17]. This provides strong evidence that the spherules are the site of RNA replication.

The first 3D EM tomography of an (+)RNA virus RC was done with FHV infected cells (Fig. 1.2) [25]. FHV induces invaginations of the outer mitochondrial membrane approximately 50 nm in diameter. As mentioned above, the 3D tomographic reconstructions clearly demonstrated that the spherule membrane remains contiguous with the outer mitochondria membrane and the interior volume is connected to the cytoplasm by an ~10 nm neck [25] (Fig.

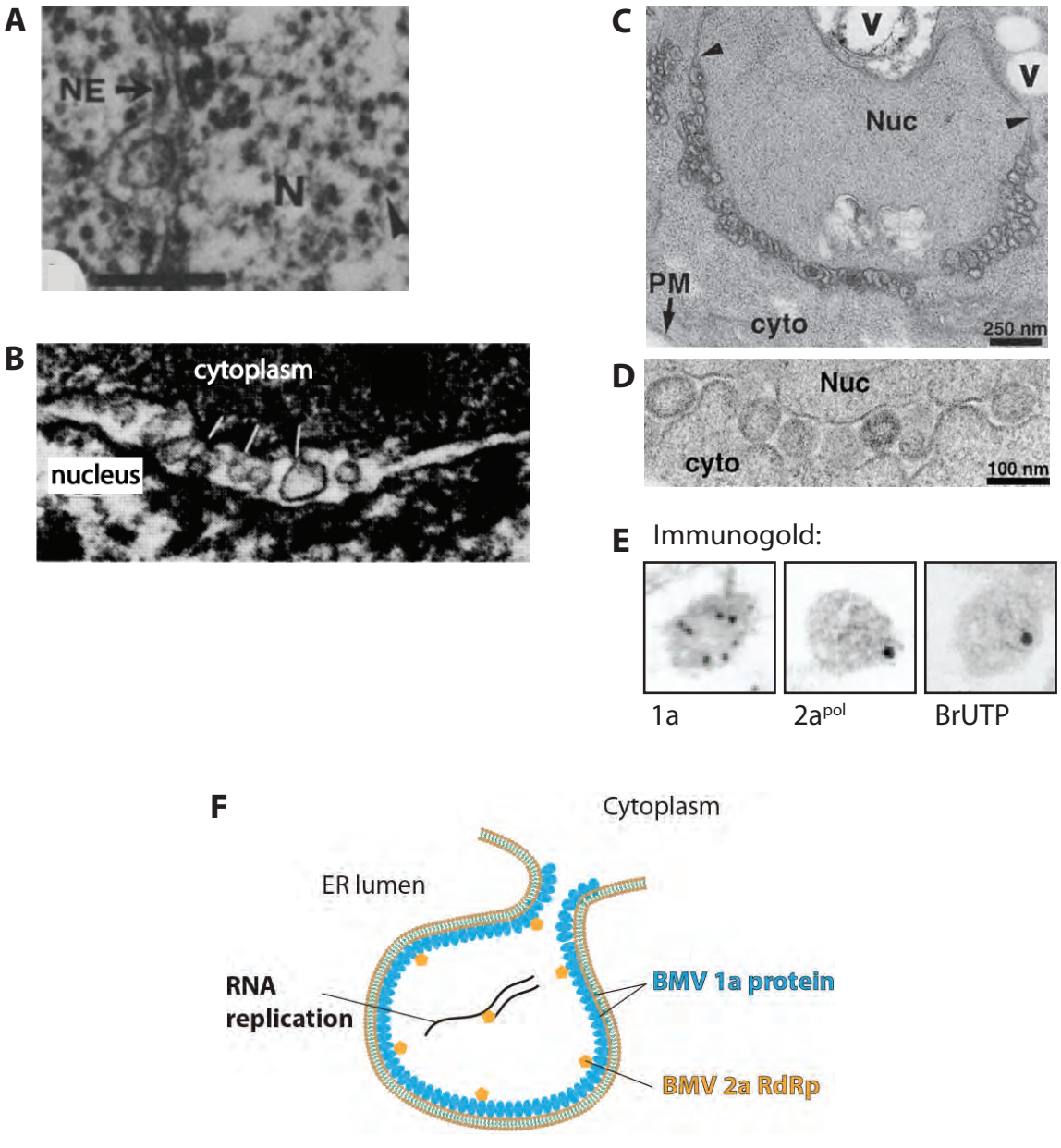

Figure 1.4. Electron microscopy and model of BMV spherules. (A,B) Electron micrographs of perinuclear vesicles induced by infection of plants with the bromoviruses (A) broad bean mottle virus or (B) cowpea chlorotic mottle virus. (C,D,E) Electron micrographs of perinuclear vesicles induced by expression of (C) BMV 1a or (D,E) BMV 1a+2a+RNA3. (E) Immunogold labeling of BMV 1a and 2a proteins and BrUTP. (F) A model of the BMV replication complex based upon imaging and biochemical data that suggest hundreds of membrane associated 1a molecules line the spherule interior and each spherule contains ~10 2a proteins. N/nuc = nucleus; NE = nuclear envelope; cyto = cytoplasm; PM = plasma membrane; V = vacuole. A is from The Plant viruses. Virus-Host Relationships. p.184 (1985); B is from J Gen Virol 35:535-543 (1977); C-E are from Mol Cell 9(3):505-514 (2002).

1.2). This provides an obvious channel through which to import necessary factors such as free nucleotides and to export newly synthesized progeny viral RNA to the cytoplasm for packaging or translation. Measurements of FHV spherule size and the stoichiometry of replication components were consistent with models in which ~100 copies of the self-interacting, transmembrane FHV protein A coat the spherule interior (Fig. 1.2C). This model is similar to that originally proposed by Schwartz et al. for BMV spherules (Fig. 1.4F) [17]; similar models have since been considered for RCs of other viruses [32-34]. The organization and role of replication proteins in the spherule interior remains an important question for the understanding of all spherule-type RCs.

Other well-studied viruses with spherule-type RCs include the alphaviruses Semliki forest virus and Sindbis virus, which form spherules on the plasma membrane. These spherules are then internalized by endocytosis, forming larger vesicles, known as cytopathic vacuoles, harboring multiple spherules each [26, 35]. DENV, West Nile virus, and many plant viruses such as tomato bushy stunt virus (TBSV) also form spherule-type RCs [14, 36-38].

Double-membrane vesicle-type replication compartments

Early EM studies of PV infected cells revealed a variety of intracellular structures including single-membrane vesicle clusters [39] and double-membrane vesicles [40]. EM tomography of PV RCs revealed that structures previously characterized as vesicles actually represent a convoluted network of tubular structures 100-200 nm in diameter, derived from cis-Golgi membranes that change in morphology throughout infection [41] (Fig. 1.3D,E). Single-membrane tubules observed at early time points extend or collapse into double membrane structures that begin to enclose cytoplasmic material as they develop into DMVs late in infection. It is not definitively known where productive RNA replication is occurring within these structures. The majority of viral RNA is synthesized early in infection when the membrane is predominantly comprised of branching single-membrane tubes [41]. However, immuno-EM labeling indicated that BrUTP, which labels RNA synthesis products, and dsRNA replication intermediates were associated with both single- and double- membrane structures [41].

The formation of DMVs has been observed for several other viruses as well, including SARS-CoV, HCV, and equine arteritis virus [42, 43]. Tomography of SARS-CoV indicated that unlike in PV, ER-derived DMVs ~250 nm in diameter are present early in infection along with convoluted membrane (CM) (Fig. 1.3A) [13]. The DMVs and CMs merge into vesicle packets 1-5μm in diameter which contain multiple single membrane vesicles late in infection. The outer membranes of the DMVs remain continuous with other DMVs, CM, or rough ER, however there is no apparent connection between vesicle interiors and their surrounding environment in PV or SARS-CoV. The majority of SARS-CoV RNA replicase proteins localized to CM structures while dsRNA predominantly localized to the DMV interiors, highlighting the necessity of further work to pinpoint the location of RNA replication within these structures[13].

RC assembly requires viral and host contributions

The exact mechanisms of RC assembly are not fully understood, but in many cases it is known to involve oligomerization of viral membrane proteins, alteration of lipid composition, and interaction with host membrane proteins.

The essential self-interaction of viral membrane proteins has been reported for several viruses. Yeast two-hybrid and in vivo crosslinking studies have shown BMV 1a efficiently self-interacts in vivo through multiple domains [44, 45]. Identification of 1a fragments dominant negative to RC assembly and RNA replication provides evidence that these interactions are essential for 1a functions [45]. Expression of a single HCV protein, NS4B, is sufficient to induce formation of a membranous web, the predominant membrane-rearrangement of the HCV RC [46]. NS4B self-interaction is essential for membrane rearrangement and for supporting HCV RNA replication. Mutations that disrupted NS4B self-interaction abolished RNA replication and altered membrane rearrangements. Pseudoreversions that restored RNA replication also restored NS4B self-interaction and normal membrane rearrangements [47]. Expression of just PV 2BC protein induces extensive membrane rearrangement resembling that of full infection [48]. Mammalian two-hybrid studies showed that 2BC efficiently homo-oligomerizes [49].

FHV protein A self-interactions through multiple domains have been identified in vivo using fluorescence resonance energy transfer [50]. Unlike the above examples, protein A is not

sufficient to induce membrane rearrangements resembling those in full infection. FHV requires viral RNA replication for spherule assembly [51]. The Semliki forest and Sindbis alphaviruses have also been shown to require RNA replication for spherule assembly [35, 52]. The mechanism by which RNA synthesis contributes to spherule assembly remains unknown.

Modulation of host lipid composition is essential for (+)RNA virus replication. RC membrane rearrangements result in an obvious expansion of local membrane surface area. Consistent with this, BMV and many other viruses induce substantial de novo lipid synthesis upon infection [45, 53, 54]. A host mutation that causes significant proliferation of ER membranes correspondingly increased TBSV RNA replication and RC formation, indicating that available membrane surface area may be a limiting factor for some viruses [55].

There are several additional proposed roles of lipid synthesis and modification in RC assembly. Lipids have been shown to play a role in localizing RC assembly through preferential binding by viral proteins. HCV localizes host phosphatidylinositol 4-kinase III α to the RC during infection, increasing the local concentration of PI4P phospholipids [56]. Increased PI4P nucleates RC assembly by attracting additional cellular and viral proteins required for RC assembly. Lipids also play a role in membrane remodeling. The DENV NS3 protein recruits fatty acid synthase to the RC and stimulates its activity [57]. Increased fatty acid synthesis has been suggested to allow for membrane expansion and increased fluidity to facilitate RC formation for a number of different viruses [58-60]. Deletion of host Δ9 fatty acid desaturase inhibits BMV RNA replication at a step between spherule formation and (-)RNA synthesis [61]. Deletion of acyl-coA binding protein inhibits BMV RNA replication and significantly alters spherule morphology [62].

In addition to modulating lipid synthesis, viruses have been shown to recruit cellular membrane shaping proteins to assist in assembling the RC. The ESCRT proteins, required for the formation of multi-vesicular bodies, cell division, and other dynamic membrane processes, are essential for RNA replication and RC assembly in BMV and TBSV [63]. The reticulon homology domain containing proteins, which induce and stabilize positive curvature of the tubular ER, are essential for enterovirus 71 RNA replication [64] and RNA replication and RC

assembly in BMV [65]. PV RC assembly involves COPII proteins from the host anterograde transport pathway [66].

Potential for common underlying principles

Despite the diversity of RC topologies and membranes utilized for RCs, there is strong evidence that RNA replication and RC assembly in spherule- and DMV- type RCs rely on common principles. DENV, West Nile virus, and HCV are all members of the flaviviridae family of viruses and have largely parallel genomes. However, both DENV [14] and West Nile virus [36] form spherule-like RCs while HCV induces a membraneous web comprised largely of ~150 nm DMVs at the time of peak RNA production [67] that is more similar to the RCs of the unrelated SARS-CoV and PV. Thus, similar proteins from related viruses can induce markedly different membrane rearrangements.

In BMV, altering the levels of the viral polymerase in vivo alters the RC structure from 60-70 nm spherules in the perinuclear ER to stacks of double-membrane sheets surrounding the nucleus ~80 nm apart from one another [68]. Both structures support similar levels of RNA replication and assembly of both structures requires host reticulon proteins [69]. Thus, the same viral and host proteins can support RNA replication processes occurring in the interior of a vesicle and on the surface of a membrane sheet that is similar in topology to the exterior of a single-membrane tubule or DMV.

Assembly of both spherule- and DMV- type RCs share many requirements, such as dependence on membrane synthesis and rearrangement, viral protein multimerization, and utilization of host membrane shaping proteins. The broad conservation of these principles in (+)RNA RC assembly, and the role of the RC in multiple steps of the viral lifecycle, make RC assembly a valuable therapeutic target. Future treatments designed to disrupt RC assembly might target viral proteins or the host genes they depend upon. The recently approved HCV drug Daclatasvir targets HCV NS5A and disrupts RC formation [70]. Advances in our understanding of (+)RNA virus RCs should have broad impacts on our understanding of RNA replication and/or other forms of membrane rearrangements as well.

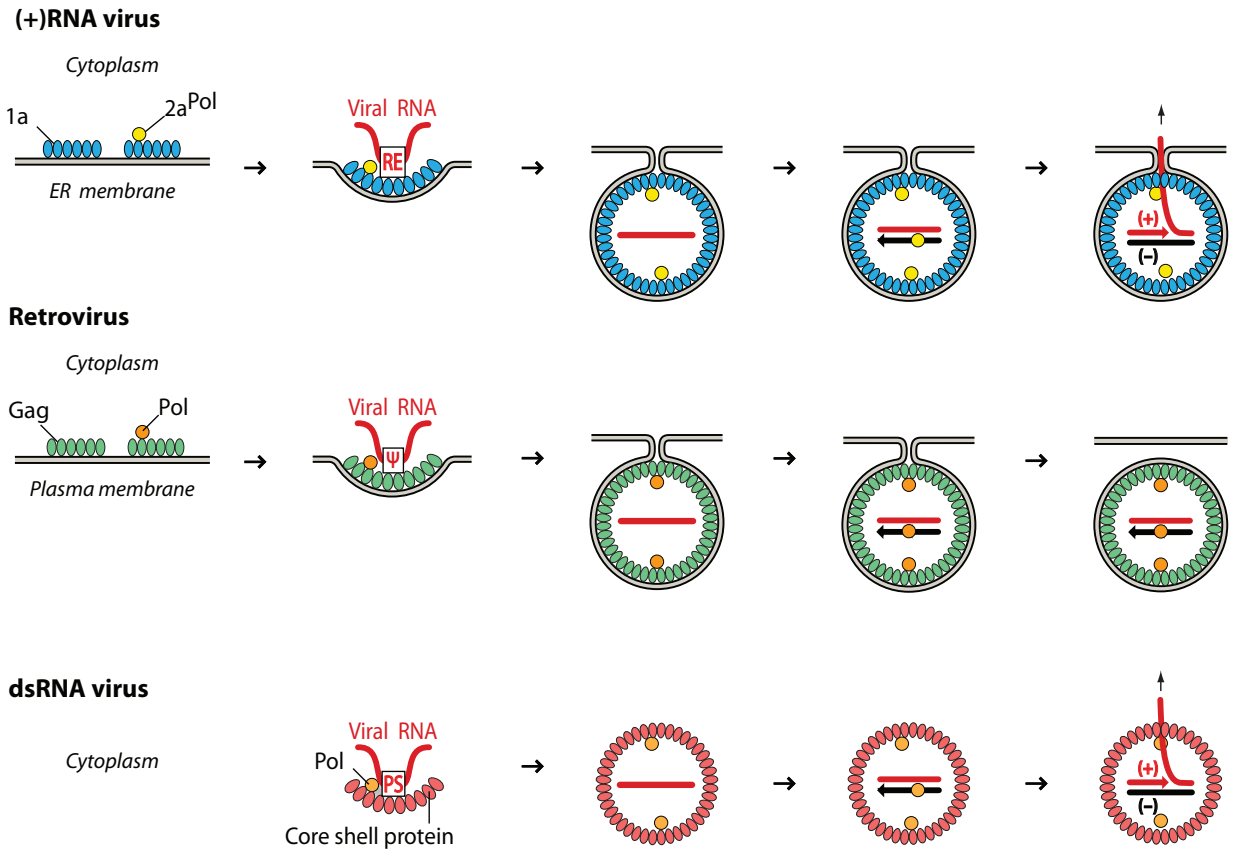

Figure 1.5. Parrallels between (+)RNA virus spherules and retrovirus and dsRNA virus capsids. Immature retrovirus capsids and (+)RNA spherules both induce membrane invaginations with negative membrane curvature (away from the cytoplasm) containing viral RNA and viral polymerase activity. Unlike retrovirus virions, there is no evidence that spherules ever bud from the membrane. dsRNA virus cores also carry out RNA replication in a viral protein shell, though they are not directly associated with host membrane. Image adapted from Ahlquist, P. Nature Reviews Microbiology, 4 p.371-382 (2006).

Functional and potential evolutionary links to other viruses

The structure and function of the (+)RNA RC has significant parallels in other viruses as well including dsRNA virus replicative cores and virion assembly in reverse transcribing viruses (Fig. 1.5) [17, 71]. All three structures provide a protected location for genomic replication using viral polymerases. dsRNA virus cores and (+)RNA virus RCs must both provide a mechanism to exchange nucleotides and other factors with the cytoplasm and allow for the import and export of viral RNAs while protecting the RNA from degradation and host recognition.

The membrane topology of an immature budding retroviral capsid is similar to the topology of spherule-type RCs. For example, FHV and HIV-Gag both induce formation of vesicles with negative membrane curvature containing hundreds of self-interacting membrane proteins [25, 72]. Though the topology of an HCV DMV and budding retrovirus are less similar, both HIV Gag and HCV NS5A rely on similar mechanisms of membrane targeting through phospholipids [56, 73]. Similar membrane remodeling host proteins are utilized for (+)RNA virus RC formation and retrovirus virion assembly as well. The ESCRT family of proteins are essential for BMV RC assembly and HIV budding [74, 75].

Brome Mosaic Virus

BMV is an extensively characterized and well studied model virus. BMV encodes four proteins from its tripartite genome and a subgenomic RNA (Fig. 1.6) (for review see [76]). The genomic RNAs have a standard 5' m7g cap, but are not polyadenylated. Bromovirus RNAs all contain a highly conserved tRNA like structure at their 3' end. RNA1 encodes the multifunctional BMV 1a protein which, in addition to its role in RC assembly, contains RNA capping/methyltransferase activities and an NTPase/helicase-like domain. RNA2 encodes the RNA-dependent RNA-polymerase. RNA3 directly encodes a cell-to-cell movement protein, 3a, and the BMV coat protein is translated from the subgenomic RNA4 transcribed from negative strand RNA3. The formation of a truncated positive strand RNA3 that contains the 5' UTR and 3a ORF, but terminates near the subgenomic promoter region has been reported to occur as a more efficient template for the translation of 3a than the genomic RNA3 (Fig. 1.6) [77].

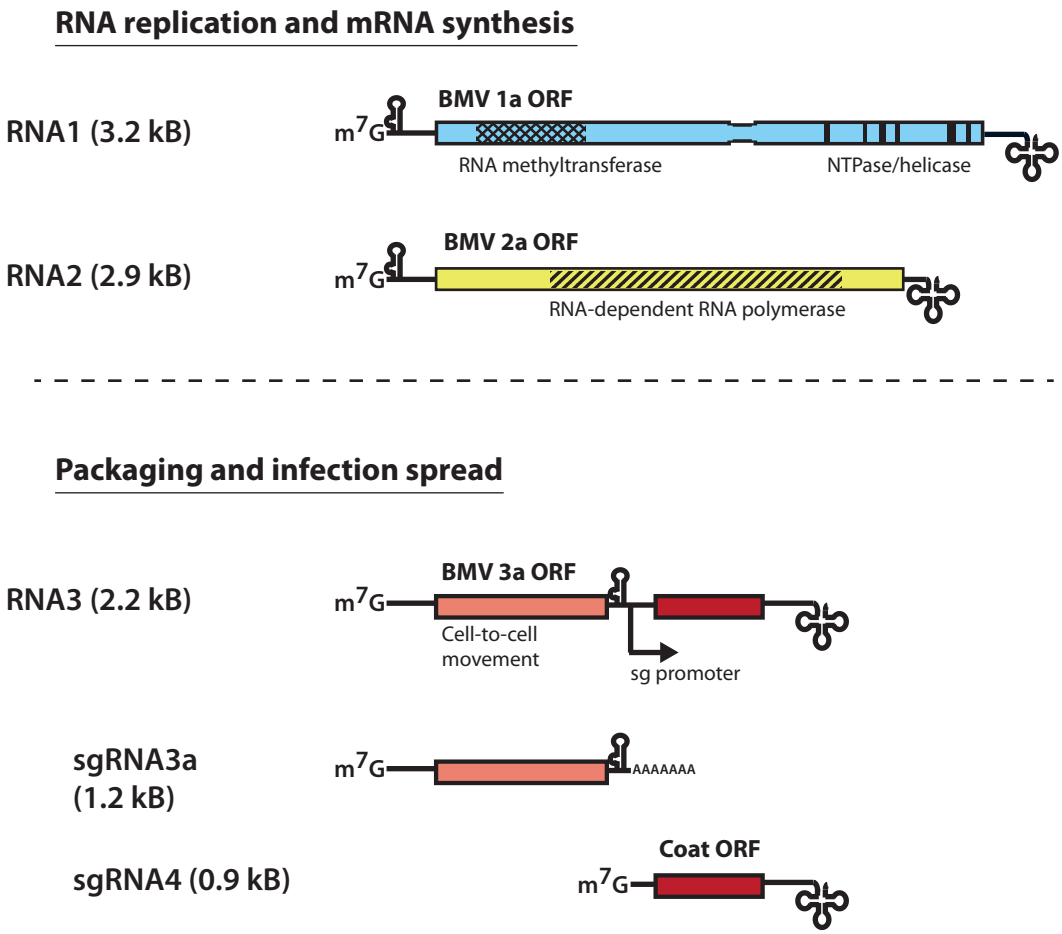

Figure 1.6. BMV genome. All BMV genomic RNAs are capped, have a conserved tRNA-like structure at the 3′ end, and a box B motif containing stemloop near the 5′ end (RNA 1,2) or the intergenic region (RNA3). RNA 1 encodes the multifunctional 1a methyltransferase/NTPase that also drives replication complex assembly. RNA2 encodes the RNA polymerase. RNA3 encodes the 3a protein essential for cell-to-cell movement in plants. Subgenomic RNA3a, formed by early termination of (+)RNA3 synthesis from (-)RNA3, has a 3′ variable length poly(A) and also encodes the 3a protein. Subgenomic RNA4 synthesis is initiated from an internal promoter in (-)RNA3 and encodes the coat protein for virion production.

BMV 1a is a 961 amino acid long peripheral membrane protein predicted to fold into two main domains separated by a proline-rich linker region. BMV 1a localizes to the perinuclear ER, induces spherule formation, and recruits the 2a polymerase, viral RNA, and essential host factors to the RC. There is evidence that 1a also interacts with coat protein during infection and colocalizes with the 3a movement protein [78, 79].

The N-terminal domain contains methyl- and guanylyl- transferase activity necessary for capping viral RNAs [80]. The RNA capping domain contains two regions that have been termed the core and iceberg regions. The core region has strong sequence conservation throughout the alphavirus-like superfamily. The 'iceberg' region is not as well conserved, but retains conservation of secondary structure throughout the alphavirus-like superfamily [81].

In addition to its enzymatic activities, the BMV N-terminal domain contains an amphipathic helix responsible for the majority of BMV 1a's membrane association [82]. Expression of the N-terminal domain (aa1-557, 1aN) alone is sufficient for membrane association and ER localization. The 1aN protein fragment assembles into membrane associated arrays of protein tubules suggesting the presence of multiple self-interactions within this domain [45].

The BMV C-terminal domain has NTPase activity and is predicted to contain helicase activity based upon homology with other viral helicases [83, 84]. When expressed alone, the BMV 1a C-terminal domain retains a small degree of membrane association, but does not localize to the perinuclear ER. Multimers of a C-terminal domain fragment were identified in crosslinking experiments indicating it contains self-interaction independent of those in the N-terminal domain [45].

Brome mosaic virus as a model system

In vitro transcribed, unpackaged BMV RNAs are infectious to plants after mechanical inoculation. The 1a+2a proteins expressed from non-replicatable cDNAs are fully competent for trans-replication of wildtype viral RNA templates [85]. This system allows for independent mutation of viral proteins or RNA. Additionally, when replication protein expression is

separated from the RNA replication templates, the effects of mutations that reduce RNA replication are not amplified by a corresponding reduction in viral protein expression.

As mentioned previously, the yeast *S. cerevisiae* supports BMV genomic RNA replication and encapsidation [86, 87]. Expression of 1a+2a from DNA plasmids supports replication of authentic BMV RNA2 and BMV RNA3 genomic RNAs also expressed from DNA. Replication of BMV in yeast generates ratios of positive- to negative- strand RNA synthesis and subgenomic RNA synthesis similar to that in plants. The 3a and/or coat proteins may be replaced with foreign genes for auxotrophic selection or other reporters such as luciferase. Translation from the coat protein ORF is dependent on RNA replication [31].

The ability to carry out RNA replication in yeast has enabled many studies of BMV that would not have been possible in plants. *S. cerevisiae* is a classical model organism with a sequenced and extremely well annotated genome. Homologous recombination in yeast allows for the targeted knockout or replacement of endogenous genes and the majority of yeast knockouts remain viable. In addition to commercially available knockout libraries of the non-essential genes, there are multiple libraries available that allow for reduced or controlled expression to study the function of individual essential genes (for review see [88]). The effects of over 5,000 yeast genes on BMV replication has been studied through use of these libraries, revealing many host pathways required by the virus [89, 90].

In addition to being able to manipulate the host, we can specifically assay many steps of BMV viral replication in yeast. These include: localization of 1a and 2a, membrane association of 1a, 2a, and viral RNA, accumulation and nuclease susceptibility of viral RNA, 1a induced membrane rearrangements, negative-strand RNA synthesis, positive-strand RNA synthesis, and subgenomic RNA synthesis. Furthermore, yeast support the selective packaging of viral RNAs into properly assembled BMV virions [87].

Recruitment of RNA to the replication complex

The mechanism of recruiting the viral genomic RNA from translation to the RC for (-)RNA synthesis is best understood for PV [23]. PV RNA is translated from an internal ribosome entry site that allows ribosomes to load at an internal site of the 5' UTR rather than scanning from the

5' end. At the immediate 5' end is another RNA structure known as the cloverleaf. Binding of the cellular poly(C)-binding proteins to the cloverleaf enhances translation of the RNA. The cloverleaf contains an overlapping binding site for PV 3CD that inhibits translation and promotes synthesis of (-)RNA. The nascent 3CD interacts in cis- to recruit the RNA to the RC for RNA synthesis, thus PV RNA recruitment requires translation [23].

The mechanism of BMV 1a recruiting RNA away from translation remains unknown. BMV 1a can inhibit translation of BMV RNA1 and 2 through a mechanism dependent on a 5' RNA element also essential for recruitment [91]. 1a is able to recruit RNA to the membrane in trans as shown by its ability to recruit RNA2 and RNA3 templates in the absence of 2a or coat protein expression. Translation is not required for the recruitment of RNA to the membrane by BMV 1a [19].

Recruiting BMV RNA3 to the RC results in increased half-life and accumulation in yeast. Recruited RNA is resistant to nuclease-treatment in cellular extracts, but rendered susceptible to digestion upon the addition of detergents [19, 92]. Mutations of the NTPase motifs in the 1a C-terminal domain, which do not disrupt 1a spherule formation, block recruitment of RNA3 to a nuclease resistant state and dramatically decrease the pool of membrane associated RNAs [84]. This data, combined with the viral RNA-independent assembly of spherules by 1a, suggests a model in which the RNA is recruited into a preformed spherule, though models of concurrent RNA recruitment and spherule formation cannot be ruled out.

All three BMV RNAs contain a motif corresponding to the box B element of RNA polymerase III promoters and the TΨC loop of tRNAs. This box B motif is present in the apical loop of extended, imperfect stemloops, known as the recruitment elements (REs), that are present near the 5' end of RNAs 1 and 2 and in an intercistronic region of RNA3 approximately 1 kb from the 5′ end (Fig. 1.6). The RNA3 RE is necessary and sufficient for recruiting RNA3 to the RC by 1a. Adding the RE to internal sites of non-viral RNA is sufficient to induce 1a recruitment of those RNAs [19]. The 5′ end of the RNA may contribute to template recognition and recruitment even in RNAs with an internal RE. Deleting the BMV RNA3 5′ UTR inhibits recruitment; however, function is completely restored by unrelated cellular 5′ UTRs, eliminating the possibility of sequence specific requirements in the UTR [19]. It has been

proposed that the requirement of Lsm1p, a snRNP-like host protein, for efficient recruitment of RNA3 may involve the m7G cap or 5′ end binding proteins [93].

The BMV RNA2 RE is also sufficient for recruiting non-viral RNAs by 1a, though additional RNA regions in the 2a ORF enhance RNA recruitment [94]. Actively translated BMV RNA2 can be recruited through an RE-independent mechanism by interaction of 1a with the nascent 2a polypeptide [95]. The BMV RNA1 RE has not been as extensively studied, but is highly similar to the RNA2 RE and is required for both cis- and trans- replication of RNA1 [96].

The presence of a box B element is highly conserved within viral RNAs in the bromoviridae family. However, not all bromovirus genomic RNAs have an identified box B element. Cowpea chlorotic mottle virus (CCMV) and broad bean mottle virus have box B elements at the 5' end of RNAs 1 and 2, but do not have a recognized box B element in RNA3. Unlike BMV, the intercistronic region of CCMV is dispensable for RNA replication. A minimum template comprised of a portion of the CCMV RNA3 5' UTR and 3' UTR is replicated to high levels by CCMV 1a+2a [97]. BMV and CCMV RNA3 can be replicated by the heterologous 1a+2a proteins, despite these differences in the requirement for the intercistronic region and presence of a box B motif. CCMV 1a+2a replication of BMV RNA3 is dependent on the presence of the RNA3 intercistronic RE [98]. This indicates the presence of a conserved mechanism for RNA recruitment within bromoviridae.

CHAPTER 2

Bromovirus 1a protein contains multiple determinants for membrane association and localization of the RNA replication complex

All experiments were designed and performed by Bryan Sibert. Ling Liu (Ahlquist lab) and Arturo Diaz (Ahlquist lab) provided DNA constructs and helpful discussions.

INTRODUCTION

(+)RNA viruses have no DNA stage and replicate their genomes through RNA intermediates in the host cytoplasm. Many hosts have robust innate immune defenses against the presence of dsRNA in the cytoplasm through RNAi and/or activation of interferon signaling . The assembly of a membrane-associated RNA replication complex, a feature conserved in all (+)RNA viruses, sequesters dsRNA replication intermediates from host recognition proteins. The replication complex serves many other functions as well, including coordinating transitions from RNA translation, replication, and encapsidation (for review see [12, 99]). The conservation and essential function of membrane rearrangement by (+)RNA viruses makes it a valuable target for the development of antivirals.

Brome mosaic virus, a member of the alphavirus-like superfamily, is a well-studied (+)RNA virus that can carry out genomic RNA replication and encapsidation in the yeast *Saccharomyces cerevisiae* in addition to its natural plant hosts [31, 86, 87]. BMV has a tripartite genome that encodes four proteins. BMV RNAs 1 and 2 encode the multifunctional methyltransferase/helicase-like 1a protein and the 2a polymerase, respectively. These are the only viral proteins required for BMV RNA replication. BMV RNA3 encodes the 3a movement protein and the viral coat protein from a subgenomic RNA4. These proteins are necessary for systemic infection of plants [100].

BMV RNA replication occurs in 60-80 nm spherule invaginations of the perinuclear endoplasmic reticulum (ER) [17]. BMV 1a is the only viral factor necessary to induce spherule membrane rearrangements in plants and yeast [17, 101]. BMV 1a is sufficient to localize to the

perinuclear ER and associate with membrane [102]. It is responsible for membrane association of the 2a polymerase and viral RNA by recruiting them to the replication complex.

Similar spherule invaginations are induced by a broad range of (+)RNA viruses [25, 103-105], including members of the alphavirus-like superfamily [35] that many plant, animal, and important human pathogens such as Chikungunya virus. Different viruses induce spherules on different cellular membranes and organelles including the ER, plasma membrane, mitochondria, tonoplasts and others [17, 25, 35, 106]. Viruses also utilize various strategies for localizing to and binding their target membrane. Many viruses, such as hepatitis C virus and Flock house virus, encode transmembrane proteins responsible for membrane rearrangement [107, 108]. Cucumber mosaic virus and tobacco mosaic virus interact with host transmembrane proteins thought to play a role in anchoring the replication complex to the membrane [106, 109]. Semliki Forest virus and other alphaviruses bind to the membrane through an amphipathic helix after which the protein is further anchored to the membrane through palmitoylation [110, 111].

BMV 1a is a peripheral membrane protein with no predicted transmembrane helices and no known sites of lipid acylation. No protected fragments were identified after protease digestion of membrane associated 1a indicating the absence of a transmembrane segment [112]. Though BMV 1a interacts with multiple host membrane proteins essential for replication complex assembly, expression of BMV 1a relocalizes these proteins to the ER suggesting that 1a's known host interaction partners are not essential for initial localization and membrane association of BMV 1a [69, 75].

An amphipathic helix, helix A (BMV 1a aa392-407), significantly contributes to 1a membrane association through insertion into the outer leaflet of the membrane bilayer [82]. BMV 1a remains associated with membranes even after high salt and pH treatments commonly used to strip peripheral membrane proteins [112]. Fusion of Helix A to the normally soluble GFP is sufficient to drive membrane association. Deletion of helix A abolishes 1a localization to the perinuclear ER and drastically decreases 1a membrane association. However, 30-50% of 1a is still membrane associated following deletion or mutation of helix A [82]. Other regions of 1a,

including the first 158 aa, are also able to induce membrane association of GFP-fusions, though to a lesser extent [112].

In order to better understand how BMV 1a associates with and rearranges the membrane, we investigated BMV 1a helix A independent membrane association.

Here, we show that 1a contains regions in addition to the previously identified helix A that contribute to its strong salt and pH resistant membrane association. Deletion of the N-terminal 18 amino acids abolishes 1a localization to the perinuclear ER and reduces the percentage of 1a associated with membrane in floatation assays from >90% to approximately 40%. A series of deletions throughout the first 158 aa of the protein had similar effects on localization and membrane association. Insertional mutations at several positions in the 1a N-terminal domain also disrupted localization and membrane association. Mutations that disrupted membrane association also disrupted interaction of 1a by yeast two-hybrid (Y2H) assays indicating the possibility of shared requirements for or interdependence of 1a-membrane and 1a-1a interactions. These preliminary results provide new foundations for future work and demonstrate that successful localization and membrane association of 1a has multiple requirements that may include proper folding and conformation of the entire N-terminal domain.

RESULTS

Multiple regions of BMV 1a contribute to its strong affinity for membrane

The ability of BMV 1a to remain associated with membranes treated with high salt or pH has been described previously. A fragment of BMV 1a consisting of aa367-480 is sufficient to confer salt and pH resistant membrane association to GFP in a fusion protein [112]. This fragment contains BMV helix A (aa389-407), which is responsible for the majority of 1a membrane association [82]. We set out to test if helix A was the sole factor conferring this strong membrane association to BMV 1a or if membrane association directed by other regions of 1a were similarly resistant to high salt and pH.

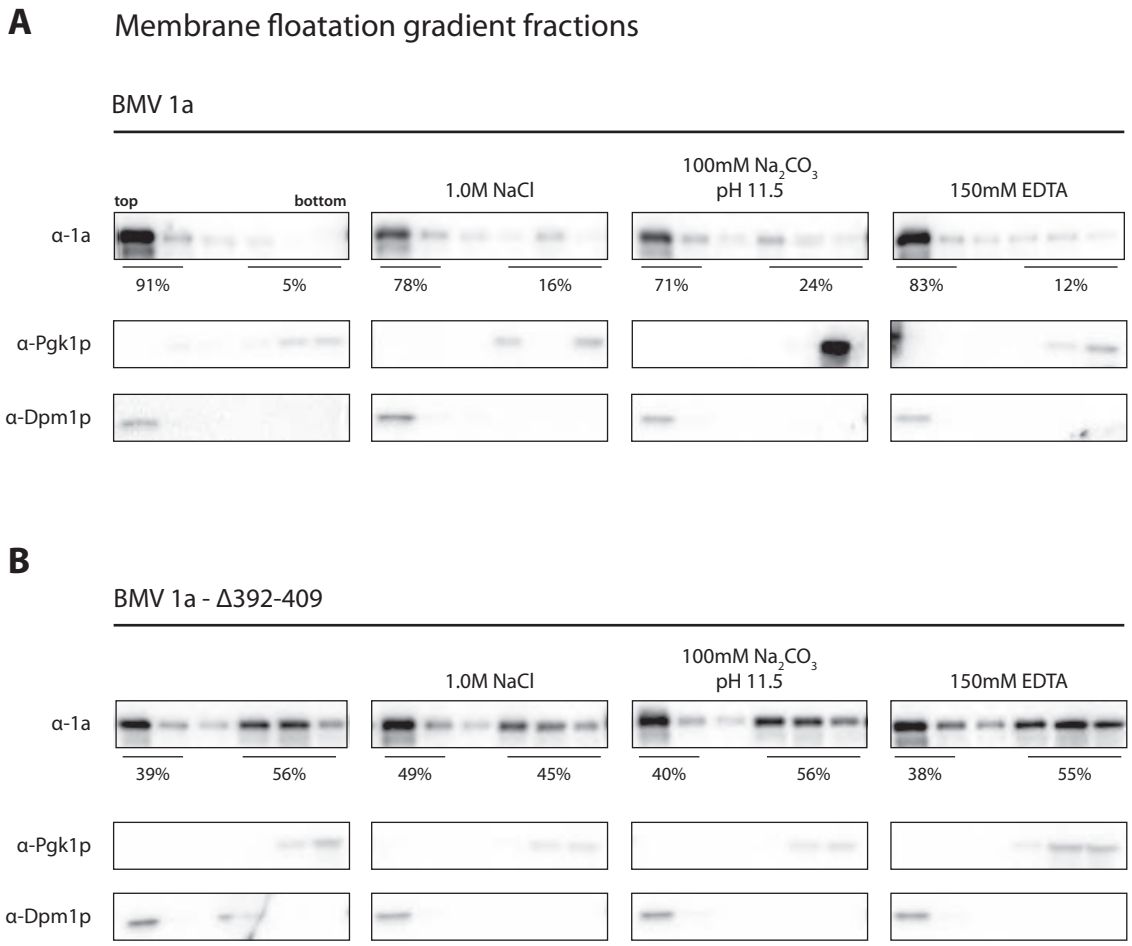

Figure 2.1. BMV 1a retains strong membrane association after deletion of helix A. Western blots of fractioned membrane floatation gradients from yeast expressing (A) BMV 1a or (B) BMV 1a with a deletion of helix A. Fractions were loaded top to bottom from left to right. 1a in the top two fractions was considered membrane associated. The lysates were treated with the indicated conditions prior to loading in the gradient. Blots for endogenous cytoplasmic Pgk1p and transmembrane Dpm1p are shown to indicate appropriate fractionation.

To do this we used membrane floatation assays to measure the percentage of BMV 1a associated with membrane. Membrane floatation is preferable to simpler sedimentation experiments because it discriminates between truly membrane associated 1a and aggregated or insoluble 1a, which both appear in the pellet after sedimentation. Cellular lysates were mixed with 60% OptiPrep gradient medium (45% final), overlayed with 30% OptiPrep, and subjected to ultracentrifugation (see Methods for details). Membranes and their associated proteins float up to the top fractions of the gradient, while cytosolic proteins remain in the bottom fractions. The gradients are fractionated and analyzed by western blotting. In addition to 1a, we used antibodies to detect the endogenous transmembrane Dpm1p and the cytosolic Pgk1p to confirm appropriate fractionation.

Cellular lysates were incubated in lysis buffer or the indicated conditions prior to being subjected to floatation. High salt, pH, and EDTA have all been described elsewhere as useful in stripping peripheral membrane proteins from the membrane [113]. We found that the majority of wildtype 1a was still membrane associated following these treatments, as determined by its presence in the top two fractions of the gradient (Fig. 2.1A). Interestingly, we found that though deletion of helix A significantly decreased the percentage of 1a associated with membrane, none of the peripheral membrane protein stripping treatments further reduced 1a membrane association (Fig. 2.1B). Thus, additional regions of 1a outside of helix A also strongly associate with membrane.

Deletions near the BMV 1a N-terminus substantially disrupt membrane association

Fusion of BMV 1a aa1-158 to GFP resulted in membrane association of approximately 20% of the fusion protein, whereas GFP alone only had 5% membrane association [112]. For this reason, we decided to look for an additional membrane associating region within this N-terminal region of the protein. We divided the 1a aa1-158 region into seven sections based upon predicted secondary structure (Fig. 2.2A) [114]. We then individually deleted each of these regions and assayed the effect on 1a membrane association. We found that deleting any of the seven regions reduced 1a membrane association to approximately 50% (Fig. 2.2B). Possible mechanisms of this reduction are discussed in more detail later.

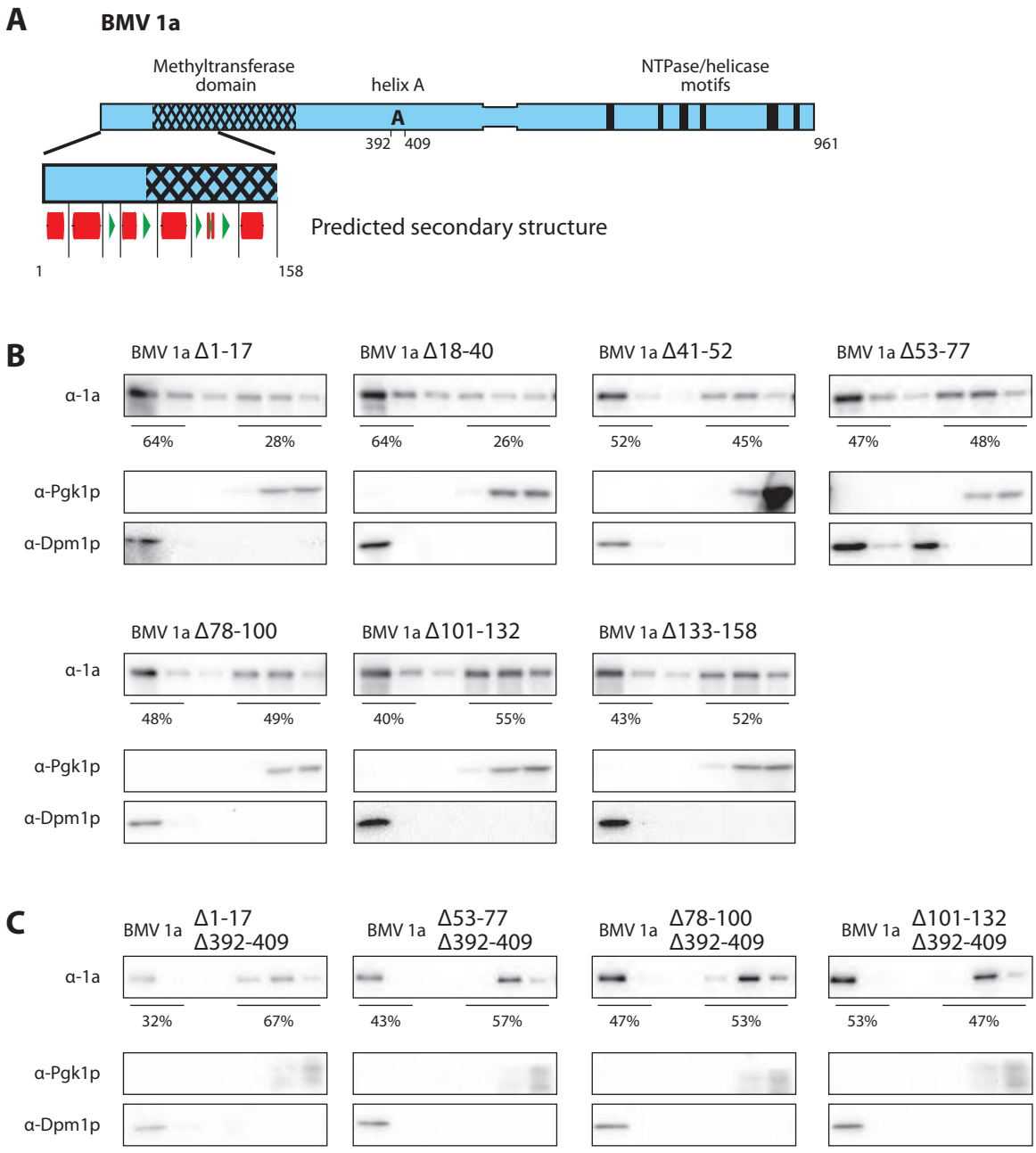

Figure 2.2. Deletions near the N-terminus of BMV 1a reduce 1a membrane association. (A) Diagram of BMV 1a. Methyltransferase core domain and helicase motifs are marked by the hatch pattern and black bars. The 'A' denotes the position of helix A. The boundaries of the deletions used in B and C are indicated by the lines dividing the predicted secondary structure. Helices are red and beta sheets are green. (B) Western blots to detect BMV 1a containing the indicated deletions in fractions from membrane floatation gradients. Proteins in the top two fractions are considered membrane associated. Endogenous Dpm1p and Pgk1p were probed for as controls. (C) As in B, with BMV 1a containing deletions of two regions as indicated.

We chose four of the N-proximal deletions to delete in conjunction with helix A, generating double deletions. All of the double deletions remained 30-50% membrane associated (Fig. 2.2C), within the range we generally see for deletion of helix A alone. Thus, we cannot definitively conclude whether the N-proximal deletions are indirectly disrupting helix A mediated membrane association or disrupt local contributions to membrane association.

Decreased 1a membrane association correlates with aberrant localization

In addition to decreased membrane association, deletion of helix A also results in the loss of localization of 1a to the perinuclear ER, yielding a diffuse cytoplasmic distribution (Fig. 2.3) [82]. We examined all of our N-terminal deletions by immunofluorescence confocal microscopy to test whether their reduced membrane association was associated with a similarly disrupted 1a localization. Wildtype 1a significantly colocalized with our Sec63-GFP endoplasmic reticulum marker. All of our 1a deletion mutants had an aberrant localization, most commonly diffuse throughout the cytoplasm. Notably, BMV 1a Δ53-77 formed a large punctae in most cells, with significant diffuse cytoplasmic signal as well (Fig. 2.3).

Mutations throughout the 1a N-terminal domain disrupt 1a localization

Given that all of our deletion mutants disrupted 1a membrane association and localization, we decided to examine additional regions of 1a with potentially less disruptive mutations. To do this we tested several insertion mutants throughout 1a that have been previously characterized in multiple studies [44, 115, 116] (Fig. 2.4A,B). We selected mutants that failed to support significant levels of RNA replication in plants to examine by immunofluorescence microscopy. We selected a greater number of mutants within the N-terminal domain (1aN, aa1-557) since it is known to be sufficient for membrane association and co-localization with ER markers [45]. We found a variety of localization phenotypes among these mutations. The C-terminal mutants, pk18, pk19, and pk 20, plus one mutant in 1a's N-proximal half, pk4, co-localized with ER markers as for wildtype 1a (Fig. 2.4C). Unlike the other N-terminal mutants which had no detectable replication in plants, pk4 is a temperature sensitive mutant that supports low levels of RNA replication (<0.5%) at permissive

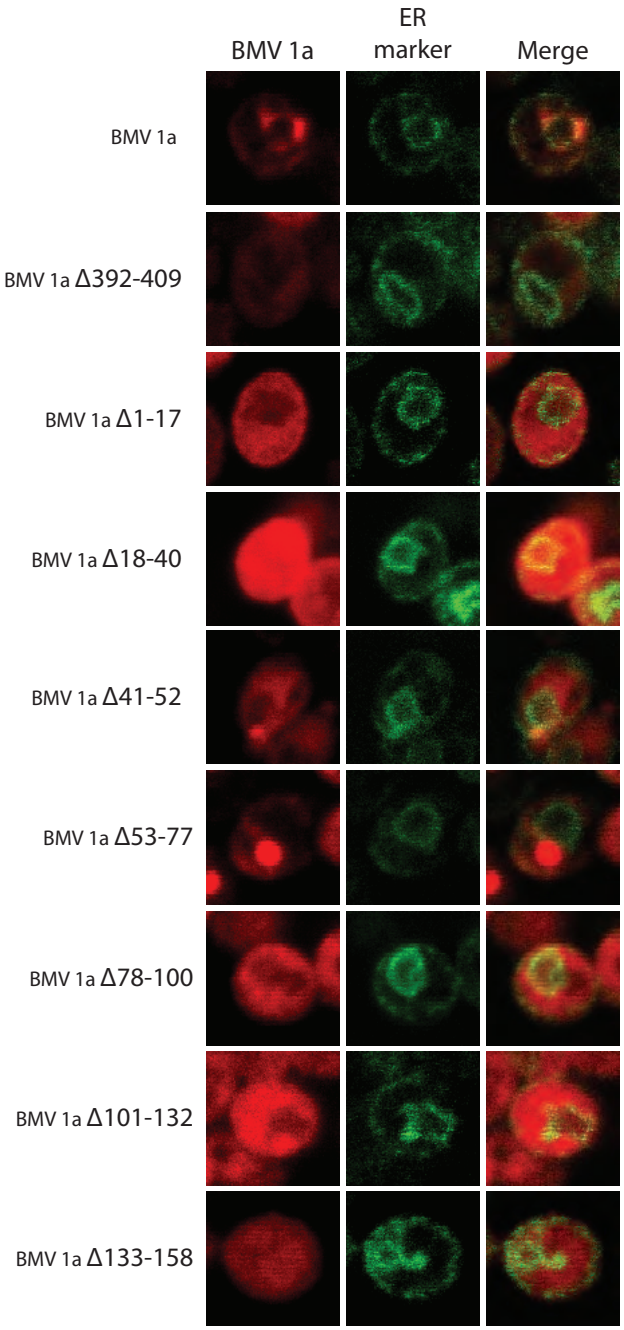

Figure 2.3. BMV 1a perinuclear localization is disrupted by deletions near the N-terminus. Confocal microscopy was used to detect the localization of BMV 1a with deletion of the indicated amino acids. BMV 1a was visualized using an antibody raised against the N-terminal domain. Sec63-GFP was co-expressed as a marker of the ER membrane.

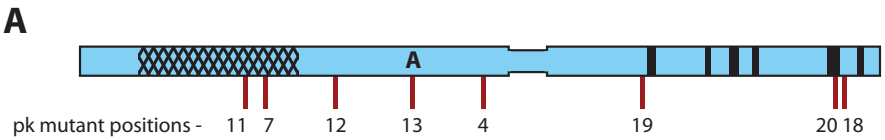

B

	Amino acid insertion (Kroner et al. 1990)	RNA replication in protoplasts (Kroner et al. 1990)	Co-IP with 2a (O'Reilly et al. 1997)	Y2H interaction with 1a (bkg = 1.0) (O'Reilly et al. 1998)
WT 1a	–	+	+	5.2
pk4	F492-GS-D493	TS	+	10.6
pk7	F239-GS-D240	–	+	1.2
pk11	G203-GP-T204	–	+	1.1
pk12	K311-WAH-V313	–	+	n.d.
pk13	K403-WAH-E405	–	+	1.1
pk18	N912-GS-V913	–	–	0.8
pk19	S670-GS-A671	TS	TS	6.3
pk20	A905-DP-Q906	–	–	1.2

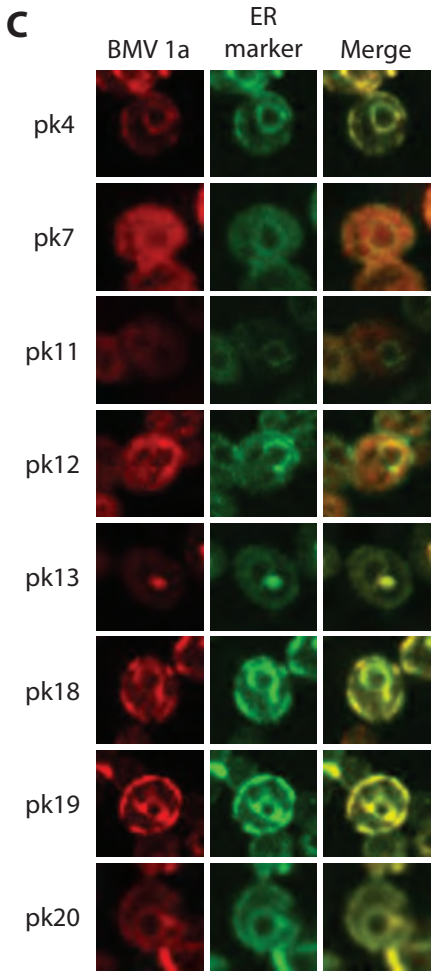

Figure 2.4. Mutations at several positions in 1a disrupt ER localization. (A) Diagram of 1a indicating the position of selected insertional mutations previously generated by Kroner et al. (B) Chart indicating the nature of each insertional mutation and its ability to support replication in barley protoplasts, Co-IP with 2a from in vitro translation assays, or interact with wildtype 1a by Y2H as previously tested in the indicated references. (C) Localization of the 1a mutants by confocal microscopy. 1a was visualized using antibodies and cells were co-transformed with Sec63-GFP as a marker for the ER.

temperatures in plants [116]. Pk13 also co-localized well with ER markers, but was much more punctate in appearance than the 'halo' localization of wildtype 1a. Pk12 localized partially to the perinuclear ER, but also had diffuse cytoplasmic localization more prevalent than for wildtype 1a or other ER-localizing mutations in many cells. pk7 and 11 had diffuse localization similar to our N-proximal deletions and deletion of helix A (Fig. 2.4C).

Yeast two-hybrid reveals correlation between 1a localization and 1a intermolecular interaction

Since all of the deletions that we tested and found to have decreased membrane association (Fig. 2.1B,2.2B) also had aberrant localization (Fig. 2.3), we checked the four pk mutants with aberrant localization for their ability to associate with membrane. Consistent with our prior results, all of the mutants had decreased membrane association compared to wildtype 1a. We found that only about 50% of pk7, pk11, and pk12 were membrane associated and 71% of pk13 was associated with membrane by floatation assay (Fig. 2.5A).

All of these 1a mutants have been previously shown to have low to no interaction with wildtype 1a in Y2H assays (Fig. 2.4B) [115]. We tested all of the pk mutants analyzed here by Y2H, including pk12 which was not included in the previous study. We also tested a triple point mutation within helix A (L396/400/407A, 3xLA) that results in decreased membrane association, similar to helix A deletion [82]. We used the interaction trap system [117] which directs β-galactosidase expression upon interaction of the 'bait' and 'prey' fusion proteins. Our results were largely similar to the prior data (Fig. 2.5B, 2.4B) [115], with the exception pk13, which had significant interaction with wildtype 1a in our assay despite almost no interaction in the previous study [115]. One potential explanation for this discrepancy is the use of different fusion proteins. Co-immunoprecipitation or other interaction assays may be useful in resolving this in future studies. We did not detect any interaction between 1a and 1a with the pk12 or 3xLA mutation.

The BMV 1a fragment aa1-515 is sufficient for interaction in Y2H [115]. BMV aa1-557 (1aN), is sufficient for ER localization and membrane association [45]. Given this, and since the three pk mutants in the C-terminal domain that we tested significantly colocalized with the ER,

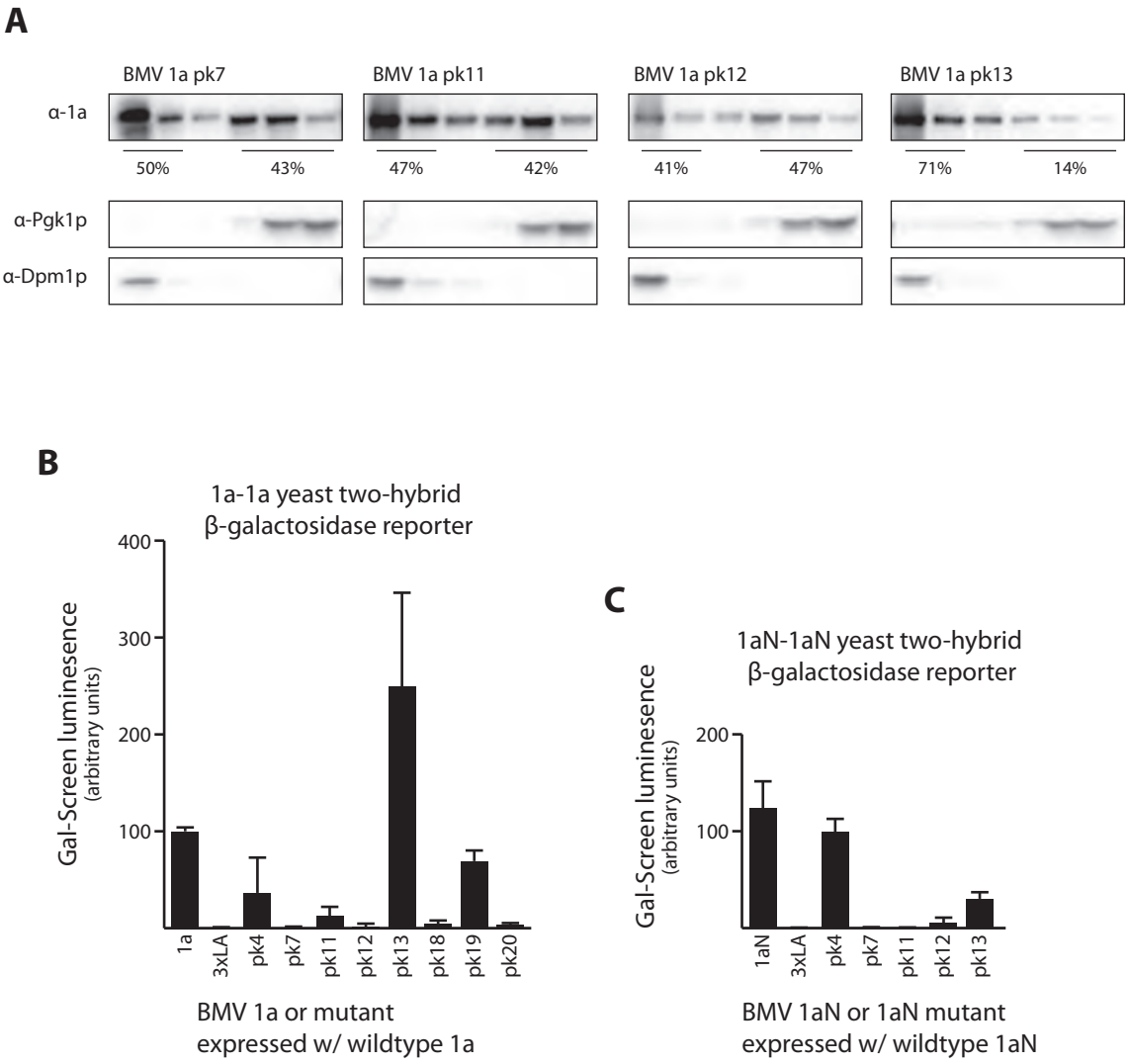

Figure 2.5. Decreased membrane association and aberrant localization are correlated with decreased 1aN interaction by Y2H. (A) Western blots of membrane floatation of BMV 1a with the indicated mutations. Endogenous Pgk1p and Dpm1p were probed as controls for fractionation. (B,C) β-galactosidase was expressed under control of yeast two-hybrid interaction (see Methods) and its resultant activity was assayed with a luminescent substrate.
(B) Interactions between wildtype BMV 1a and BMV 1a with the indicated mutations.
(C) Interactions between wildtype BMV 1aN (aa1-557) and BMV 1aN with the indicated mutations.

we also tested the ability of 1aN fragments bearing the selected helix A or pk mutations to interact with wildtype 1aN by Y2H. We found that the three mutants with completely diffuse localization, 3xLA, pk7, and pk11, had no detectable 1aN-1aN interaction by Y2H (Fig. 2.5C). Pk12 and pk13, which respectively displayed partial and significant, but punctate colocalization with Sec63-GFP, had interaction above background, but substantially lower than wildtype 1a or pk4.

DISCUSSION

Despite their broad diversity, all (+)RNA viruses thus far have been found to replicate their genomes in association with host membrane. Recent studies taking advantage of advances in light and electron microscopy have revealed the 3D membrane ultrastructure of the replication complexes of many viruses. However, the mechanisms by which the viruses induce these membrane rearrangements remains poorly understood. To better understand the initial steps of replication complex assembly, we investigated the membrane association of BMV 1a, the only viral factor necessary to induce replication compartment membrane rearrangements in the model virus BMV.

BMV 1a membrane association requires contributions from multiple 1a regions

There are many known mechanisms utilized by proteins to contribute to membrane curvature. Some mechanisms require multiple membrane interactions within a single protein, while for others a single anchor or interaction is sufficient. Our results, combined with previous studies [82, 112], show that 1a attains strong membrane association through multiple regions of the protein. The similar loss of membrane association by deletions and insertions throughout 1a suggests that proper conformation may be essential for at least some 1a membrane interactions. This data is consistent with models of membrane bending where 1a may be acting as a direct scaffold to bend the membrane around it as originally proposed by Schwartz et al. [17]. Additionally or alternatively, the presence of multiple membrane interactions could represent that 1a interacts with membranes in multiple distinct conformations. Different regions of the protein may interact with membrane in different 1a conformations.

It is interesting that deleting helix A decreases the total percentage of 1a associated with membrane, but the fraction of 1a that remains membrane bound is strongly anchored. One might have expected that the decreased percentage of membrane associated 1a reflected the combined effect of weaker or more transient binding by all 1a proteins, but our data seem to indicate that this is not the case. It is possible that not all 1a is directly associated with the membrane and that a percentage of 1a is associated with membrane through a 1a-1a interaction or 1a conformation that is disfavored by deleting helix A. Alternatively, the strength of 1a membrane association may be effected by the lipid composition of the membrane. If the helix A deletion associates with membrane non-specifically, consistent with its localization by immunofluorescence microscopy, it may be able to bind some membranes more strongly than others.

Though the mechanism of BMV 1a localization to the perinuclear ER remains unknown, it has been hypothesized for other viruses that lipid composition plays an important role in localization of the replication complex [56, 118]. The pk12 and pk13 mutants retained at least partial colocalization with the ER despite decreased membrane association. The seven N-terminal deletions plus pk7 and pk11 did not show any ER specific localization. Future analysis of the specific membranes and lipids associated with wildtype 1a and these mutants may provide important insight into the role of lipid composition in 1a localization and membrane affinity.

Mutation of 1a revealed a correlation between loss of membrane association, localization, and 1a interaction

All of the 1a mutations analyzed in this paper with aberrant 1a localization also had decreased membrane association. These two functions are both essential for the earliest steps of replication complex assembly. Membrane association and localization are potentially interdependent, for example, if 1a localized through interaction with lipids specific to the ER. If 1a localization were largely dependent upon direct interaction with a host factor, such as a resident ER protein, these two functions may be separable. Our results here do not exhaustively rule out either possibility as a single mutation could disrupt both functions, especially if the mutation grossly altered the

protein conformation. All of the N-terminal pk mutants have been previously shown to interact with 2a, demonstrating that at least some other 1a functions are retained (Fig. 2.4B) [44]. Analysis of additional 1a mutants in combination with assays to examine 1a-lipid and 1a-host protein interactions should be useful for investigating the association between 1a localization and membrane association.

In addition to the correlation between membrane association and localization, we also observed a correlation between these functions and 1aN-1aN interaction. The pk7 and pk11 1a mutants had decreased membrane association, diffuse cytoplasmic localization, and no detectable interaction within the 1aN fragment by Y2H. A weak interaction between full-length pk11 and 1a was detected by Y2H, but it is possible that interactions in the C-terminal domain contributed to this. The 3xLA mutation in helix A also showed no 1a-1a or 1aN-1aN interaction by Y2H. Notably, the 3xLA mutation also induces both decreased membrane association and diffuse localization of 1a, similar to helix A deletion [82]. Further supporting the correlation between localization, membrane affinity, and 1aN-1aN interaction is that pk12 and pk13, which partially localized to the ER, had detectable 1aN-1aN Y2H interaction. Pk4, with near wildtype levels of 1aN-1aN interaction, and all of the C-terminal mutants, which are wildtype for the 1aN domain, colocalized with the ER similar to wildtype 1a. Cooperative binding of 1a multimers to the membrane could contribute to its high membrane affinity.

The HIV Gag protein binds to the plasma membrane and is responsible for the formation of the immature retroviral virion [72]. Prior to budding from the plasma membrane the morphology of the immature virion is similar to that of the BMV spherule. Both are vesicular with predominantly negative membrane and contain viral RNA in their interiors that are connected with the cytoplasm [17]. Multimerization of the Gag matrix domain is essential for its localization to and association with the plasma membrane [119]. Critical experiments to demonstrate this took advantage of being able to separate the membrane binding matrix domain from the self-interacting capsid domain of Gag [119]. Though it is known that BMV 1a contains multiple interactions through multiple domains, these interactions have not been mapped. Further mapping of 1a-1a interactions will be necessary to determine their role in 1a membrane association, localization, and replication compartment assembly.

MATERIALS AND METHODS

DNA plasmids & yeast culture

Yeast strain YPH500 was grown as described previously [31, 120]. All yeast were subcultured twice in selective galactose media for a total of 36 hours prior to harvesting during mid-log phase. Yeast were transformed using the Frozen-EZ Yeast Transformation II kit (Zymo Research). BMV 1a was expressed from pB1YT3 [121]. All BMV 1a deletion and mutant derivatives were constructed using standard molecular biology techniques in the pB1YT3 backbone; BMV 1a Δ392-408 and the 3xLA mutant were generated previously [82]. pWSECG [84] was used to express Sec63-GFP as an endoplasmic reticulum marker.

Membrane floatation

Membrane floatation assays were done as described previously [82]. Ten OD600 units of yeast were spheroplasted and subsequently lysed in 200 μl of 1x TNE with protease inhibitors (50 mM Tris pH 7.4, 150 mM NaCl, 5 mM EDTA, 1 mM phenylmethylsulfonyl fluoride, 10 mM benzamidine, 5 μg of pepstatin, 10 μg of leupeptin, and 10 μg of aprotinin per ml). The lysate was diluted to 400 μl with 1x TNE or the appropriate buffer to bring the final concentration to 1.0 M NaCl, 100mM Na_2CO_3 pH 11.5, or 150 mM EDTA as indicated and incubated on ice for 30 minutes. 250 μl of lysate was mixed with 500 μl 60% OptiPrep (Sigma-Aldrich) and overlayed with 1.4 ml 30% OptiPrep and 100 μl 1x TNE. Samples were centrifuged at 55,000 rpm in a Beckman TLS55 rotor for two hours. Six fractions were collected from top to bottom and boiled in laemmli buffer prior to SDS-PAGE and western blotting. The polyclonal anti-BMV 1a antibody has been described previously [122]. Mouse monoclonal antibodies for detection of yeast Dpm1p and Pgk1p were purchased from Molecular Probes.

Confocal microscopy

Yeast were prepared for confocal microscopy essentially as described previously [45]. Two OD600 units of yeast were fixed in 4% formaldehyde in 0.1M potassium phosphate buffer pH 6.5. Cells were partially spheroplasted with 200U lyticase (Sigma-Aldrich) for 40 minutes at

30°C in spheroplast buffer (1.0 M sorbitol, 0.1 M KPO_4 pH 7.5) with 0.2% β-mercaptoethanol. Yeast were further permeabilized by incubation in spheroplast buffer with 0.1% Triton X-100 for 15 minutes. Immunostaining for BMV 1a was done at 1:100 with anti-BMV 1a antisera [122] followed by incubation with 1:100 goat anti-rabbit conjugated to Alexa 568 (Molecular Probes). Images were acquired using confocal microscopy on a BioRad Radiance 2100 MP Rainbow.

Yeast two-hybrid assay

BMV 1a and the 1aN (aa1-557) fragment were cloned into the pJK202 [123] Y2H 'bait' plasmid containing a LexA DNA binding domain and a nuclear localization signal. Wildtype 1a, 1aN and the mutant derivatives were cloned into the Y2H 'prey' plasmid pJG4-5 [123] containing a nuclear localization signal and the B42 transcription activation domain. Yeast were transformed with a single bait and prey plasmid as indicated in addition to the pSH18-34 reporter plasmid [123] that expresses β-galactosidase under control of eight LexA operators. pJK202, pJG4-5, and pSH18-34 were a gift from the Roger Brent lab. β-galactosidase activity was measured as luminescence using the Gal-Screen System (Applied Biosystems) according to the manufactures instructions. Luminescence from yeast expressing pJK202-1a, pSH18-34, and pJG4-5 with no fusion protein was considered background and subtracted from all samples; samples with signal less than background are reported as zero. The average and standard error of five replicates is shown.

CHAPTER 3

Bromovirus hybrids reveal host-specific effects in viral RNA template recruitment and replication

Electron microscopy was done in collaboration between Janice Pennington (Ahlquist lab) and Bryan Sibert. All other experiments were designed and performed by Bryan Sibert. Xiaofeng Wang (Ahlquist lab) provided DNA constructs and helpful discussions. Further guidance with electron microscopy was provided by Ben August and Marisa Otegui. The lab of Aurelie Rakotondrafara provided guidance for using the *A. sativa* cell culture.

INTRODUCTION

Positive-strand RNA ((+)RNA) viruses comprise most plant viruses as well as many important human pathogens such as Middle East respiratory system and severe acute respiratory syndrome coronaviruses, dengue virus and chikungunya virus. A universal feature of (+)RNA viruses is the assembly of cytoplasmic membrane-associated RNA replication complexes [124, 125]. The membrane utilized and morphology of replication complexes varies among viruses. Data from many viruses suggests conserved functions of these replication complexes including acting as a scaffold for host and viral replication factors and protecting viral RNA from host innate immune recognition and degradation (for review see [124]). Despite the central importance of membrane-associated replication complexes to (+)RNA virus replication, their mechanism of assembly remains poorly understood.

Brome mosaic virus (BMV) is a well-studied (+)RNA virus that naturally infects barley and other monocots and whose RNA replication can be reconstituted in the yeast *Saccharomyces cerevisiae* [31, 86, 87]. The ability of BMV to assemble replication complexes and carry out full RNA replication in yeast has allowed for many advances in understanding these processes. Infection with BMV induces remodeling of the endoplasmic reticulum (ER) membranes in plants and yeast [17, 28, 29]. BMV RNA replication complexes, known as spherules, consist of membrane invaginations of the endoplasmic reticulum (ER), ~70 nm in diameter, whose

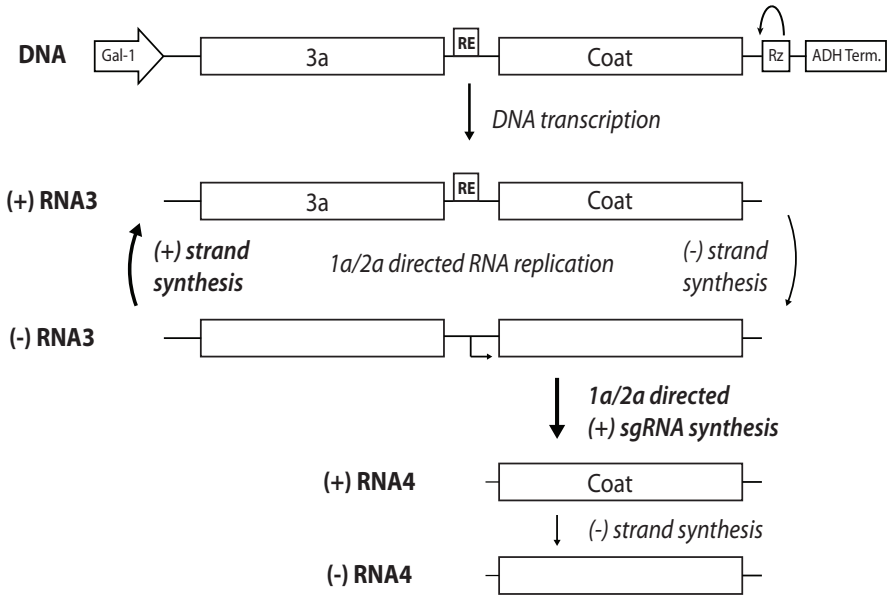

Figure 3.1. DNA based BMV RNA3 expression and replication. A BMV RNA3 cDNA is expressed from the yeast *GAL1* promoter with a yeast terminator. A ribozyme (Rz) derived from hepatitis delta virus inserted after the viral 3′ UTR cleaves itself from the RNA leaving the natural viral 3′ end. Recruitment of the RNA to the replication complex is dependent on the presence of a box B containing structural element in the intercistronic region (RE). BMV 1a and 2a proteins direct negative-strand synthesis, which then serves as a template for additional positive strand replication. Expression of the coat protein depends on synthesis of (+)RNA4 from the (-)RNA3 template.

interiors remain connected with the cytoplasm through a thin neck [17, 26]. Cowpea chlorotic mottle virus (CCMV), the closest known relative to BMV, forms similar vesicles along the plant ER during infection[27, 29]. This spherule morphology is conserved throughout the alpha-like virus superfamily. Alphaviruses, such as Semliki Forest virus and Sindbis virus, form spherules on the plasma membrane that are internalized onto structures known as cytopathic vesicles, retaining the spherule morphology and connection to the cytoplasm [35, 126].

BMV and CCMV both have a tri-partite genome. RNA1 from both viruses encodes a multifunctional 1a protein that has methyltransferase and helicase domains and is also primarily responsible for replication complex assembly. RNA2 encodes the RNA-dependent RNA polymerase (2a). RNA3 encodes a cell-to-cell movement protein (3a) and the coat protein,` which is translated from a subgenomic RNA4 (Fig. 3.1). RNA3/4 and their products are dispensable for RNA replication [76]. BMV and CCMV share few natural systemic hosts, however both viruses can replicate their RNAs in a wide range of cultured plant cells including those from barley and cowpeas. Determinants for systemic infection of various hosts have been mapped to all three viral RNAs [127, 128]. Both viruses support replication of the heterologous RNA3/4, although heterologous 1a/2a pairings do not support full RNA replication [129].

The BMV 1a protein is necessary and sufficient among viral proteins to induce spherule membrane rearrangements in yeast [17]. Each spherule contains hundreds of self-interacting [45, 115], membrane-associated [82, 112] 1a proteins and approximately twelve 2a polymerase proteins [17]. A number of host factors essential for spherule assembly and function have been identified [62, 69, 75]. 1a is sufficient to recruit viral RNA and the 2a polymerase to the replication complex [17]. Expression of BMV 1a, 2a, and a replication competent BMV RNA3 template supports negative- and positive- strand RNA3 synthesis of at ratios similar to those observed in plants, with positive strand RNA3 in far excess. As in plants, expression of RNA4 from the RNA3 subgenomic promoter and subsequent translation of its product, coat protein, depends upon active RNA replication in yeast [31].

Recruitment of BMV RNA3 to the RNA replication complex is dependent on an intercistronic, cis-acting RNA recruiting element, the RE, that contains a tRNA-like box B element[19]. Inserting the RE in exogenous RNAs is sufficient to induce their recruitment by the

BMV 1a protein. RNAs recruited to the replication complex are membrane-associated and nuclease resistant. BMV 1a dramatically increases the half-life of RNA3 and increases total RNA3 accumulation even in the absence of 2a [19]. RNAs 1 and 2 of BMV and CCMV have similar box B containing hairpins at their immediate 5' ends [130]. This region has been shown to be essential for 1a induced recruitment of BMV RNA2 [94]. Unlike BMV, the intercistronic region of CCMV RNA3 is dispensable for RNA replication and the RNA elements involved in recruitment to the replication complex are unknown [97].

Here we show that many functions of the BMV 1a protein that are required for RNA replication complex assembly, including perinuclear localization, membrane association and rearrangements, self-interaction, and recruitment of 2a polymerase, are conserved in the related CCMV 1a in yeast. CCMV 1a and 2a supported replication of BMV RNA2 to levels similar to those of BMV 1a and 2a. CCMV 1a and 2a also supported negative- and positive- strand synthesis from BMV RNA3 templates, although to levels significantly lower than BMV 1a and 2a. No replication of CCMV RNA3 was detected in yeast despite the ability of both viruses to replicate CCMV RNA3 in plants. These data indicate different template-dependent host requirements for the replication of bromovirus RNAs. CCMV 1a only slightly increased BMV RNA3 accumulation and recruited less RNA to a membrane-associated state than BMV 1a. This data indicates 1a dependent host contributions to RNA recruitment. Mutation of the BMV RNA3 RE reduced RNA replication and recruitment by CCMV 1a, demonstrating that CCMV 1a is responsive to the BMV RE.

RESULTS

CCMV RNA3 replication template activity is restricted in yeast relative to plant cells

Protoplasts from many plant species support bromovirus RNA replication[131], allowing for focused analysis of single cycles of RNA replication in newly infected cells, without complications from cell-to-cell spread and other factors that significantly affect viral RNA levels in whole plants [131]. We transfected in vitro transcripts from cDNA clones of BMV and/or CCMV RNAs into protoplasts isolated from suspension cultures of oat (*A. sativa*) cells [132].

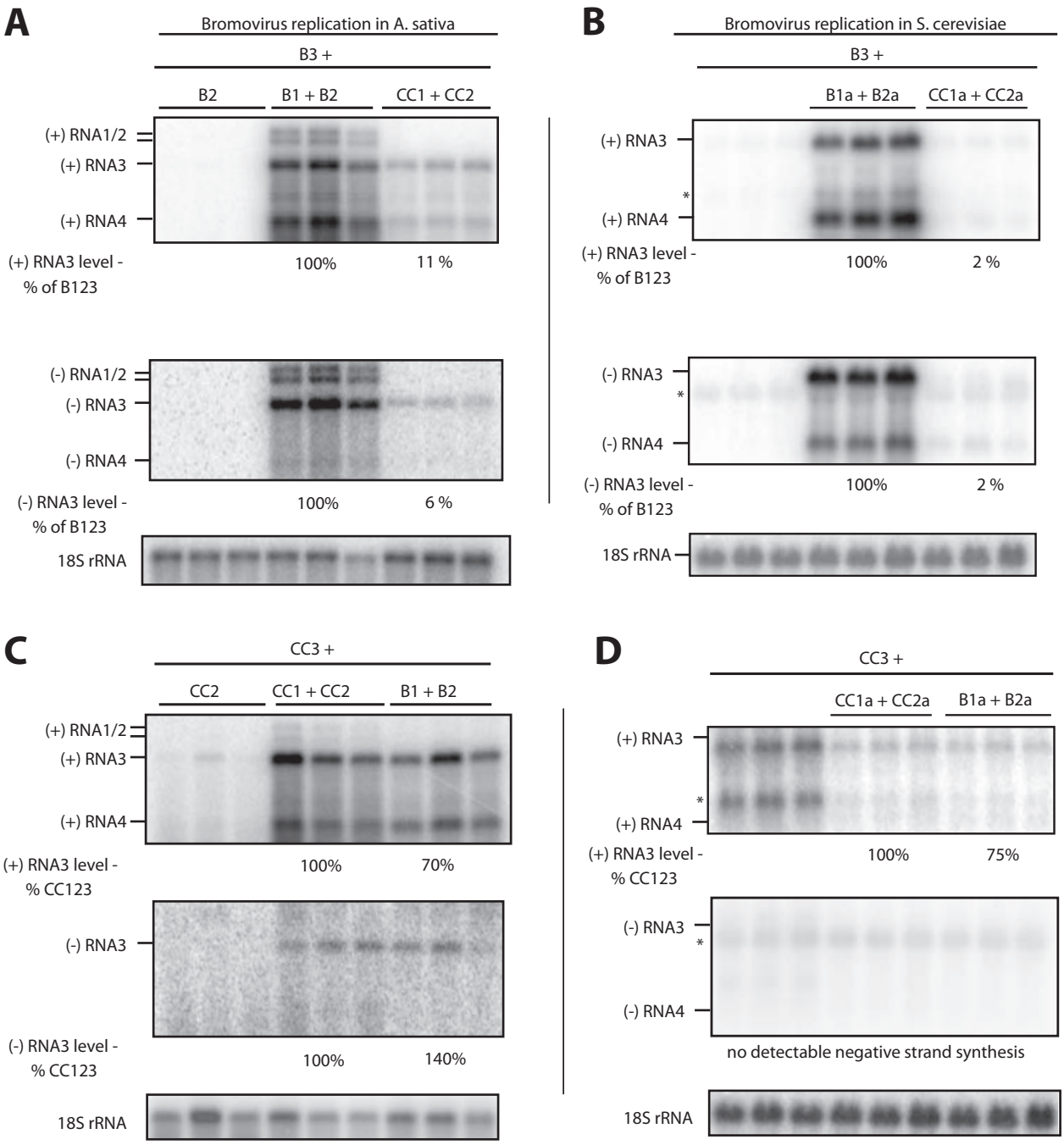

Figure 3.2. RNA template specific differences in the ability of BMV and CCMV to support RNA replication in plants and yeast. (A,C) Positive (+) and negative (-) strand RNA from BMV or CCMV were detected by northern blotting as indicated using a probe which hybridizes RNA3 and RNA4. (A) RNA was isolated from oat protoplasts transfected with the indicated RNAs from BMV or CCMV. (B,D) RNA was isolated from yeast expressing BMV RNA3 or CCMV RNA3 and mRNAs expressing BMV or CCMV 1a and 2a proteins as indicated. Bands present in the absence of RNA replication are marked with a an asterisk.

RNAs 1+2 from both viruses supported readily measurable replication of their own and the heterologous RNA3 (Fig. 3.2A,C), consistent with previous reports in barley and cowpea protoplasts [98]. BMV RNA3 replication was markedly stronger by cognate BMV RNAs 1+2 (Fig. 3.2A), while CCMV RNA3 was replicated to similar levels by both BMV or CCMV RNAs 1+2 (Fig. 3.2C).

In yeast, plasmid-directed expression of multifunctional BMV 1a protein and 2a polymerase directs robust replication of BMV RNA3 (Fig. 3.2B). To test the ability of CCMV 1a and 2a proteins to direct RNA replication in yeast, we generated plasmids expressing CCMV 1a and 2a mRNAs and full-length RNA3 (see methods). BMV and CCMV 1a+2a were then tested for their ability to replicate both RNA3 templates. As in plant cells, CCMV 1a+2a directed negative-strand RNA synthesis and positive-strand RNA amplification from BMV RNA3 templates, although CCMV 1a+2a replication of BMV RNA3 in yeast averaged ~20- to 30-fold lower than that by BMV 1a+2a, compared to ~10-fold lower in plant cells (Fig. 3.1A).

Notably, no replication of CCMV RNA3 was detectable in yeast with either 1a+2a pair (Fig. 3.2D), revealing a marked difference in host requirements between BMV and CCMV RNA replication. This must include yeast-specific restrictions on CCMV RNA3's activity as an RNA replication template, since BMV 1a+2a are clearly functional in yeast (Fig. 3.2B), and in plant cells replicated CCMV RNA3 to fully 70% of the level produced by the cognate CCMV RNAs 1 and 2 (Fig. 3.2C).

CCMV 2a polymerase is competent for negative-strand RNA synthesis in yeast

Bromovirus RNA replication requires functional compatibility between the RNA replication proteins 1a and 2a: CCMV 1a and BMV 2a do not support detectable RNA synthesis in plant protoplasts, while BMV 1a/CCMV 2a support negative-strand, but not positive-strand, RNA synthesis[85]. To determine if these compatibility requirements were conserved in yeast, and to separately test CCMV 1a and 2a function, we tested the ability of heterotypic 1a/2a pairs to direct replication of BMV RNA3. Paralleling function in plant cells, BMV1a and CCMV 2a supported negative-strand synthesis of BMV RNA3 (Fig. 3.3B), while no replication products were detected from yeast expressing CCMV1a/BMV2a (Fig. 3.3A). Intriguingly,

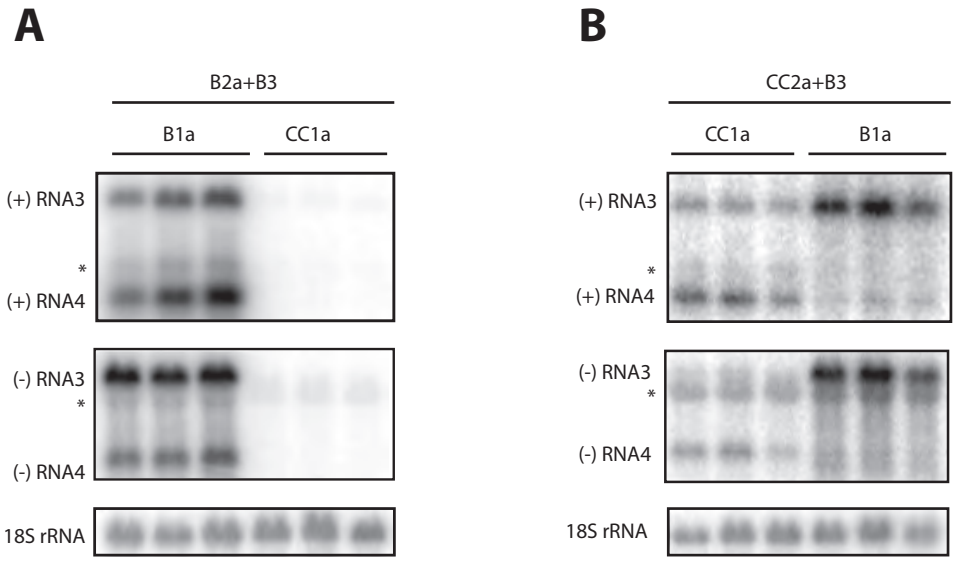

Figure 3.3. CCMV 2a polymerase is competent for negative-strand RNA synthesis in yeast. Northern blotting was used to detect viral RNA from yeast expressing BMV RNA3 with (A) BMV 2a or (B) CCMV 2a and BMV or CCMV 1a as indicated. Bands detected in the absence of RNA replication are indicated with an asterisk.

BMV1a/CCMV2a directed significantly higher levels of negative-strand RNA synthesis than the homologous CCMV 1a+2a pair (Fig. 3.3B). This collective competence of BMV1a/CCMV 2a and BMV RNA3 for negative-strand RNA synthesis demonstrates that CCMV 2a polymerase is at least partially functional in yeast. Moreover, when combined with these results, the severe inhibition of negative-stand RNA synthesis by CCMV 1a+2a in yeast implies a host-dependent restriction of CCMV 1a function at an early step or steps in RNA replication, prior to initiation of negative-strand RNA synthesis.

CCMV 1a is defective relative to BMV 1a in recruiting RNA templates in yeast

For BMV, 1a is the only viral protein required to selectively recruit viral RNA templates to the RNA replication complex, resulting in 1a-induced partitioning of BMV genomic RNA into a membrane-associated, nuclease-resistant state that is well correlated with RNA replication [92]. In yeast, recruiting BMV RNA3 to such membrane-associated RNA replication complexes stabilizes the RNA, and thus increases its total accumulation [19]. Since the results from figures 2-3 indicated a CCMV 1a defect prior to negative-strand RNA synthesis, we compared the abilities of BMV and CCMV 1a to stimulate BMV or CCMV RNA3 accumulation and membrane association as signatures of RNA template recruitment.

For BMV RNA3, BMV 1a stimulated accumulation ~10-fold over that in the absence of 1a, consistent with prior findings [19], while CCMV 1a only stimulated accumulation by ~2-fold (Fig. 3.4A). To test RNA recruitment even more directly, we fractionated yeast lysates to determine the levels of soluble and membrane associated RNA. In the absence of 1a, BMV RNA was distributed 97% in the soluble fraction and 3% in the membrane fraction (Fig. 3.4B). Consistent with prior findings [17], BMV 1a preferentially and strongly stimulated the level of membrane-associated BMV RNA3, boosting the membrane fraction to over 4-fold higher than the soluble fraction. By contrast, and consistent with its ~5-fold lesser stimulation of total BMV RNA3 accumulation, CCMV 1a only weakly increased membrane-associated BMV RNA3, raising this level to only slightly above that in the soluble fraction (Fig. 3.4B).

Neither BMV nor CCMV 1a protein detectably stimulated the accumulation of total CCMV RNA3 (Fig. 3.4A). Nevertheless, the more discriminating fractionation assay showed

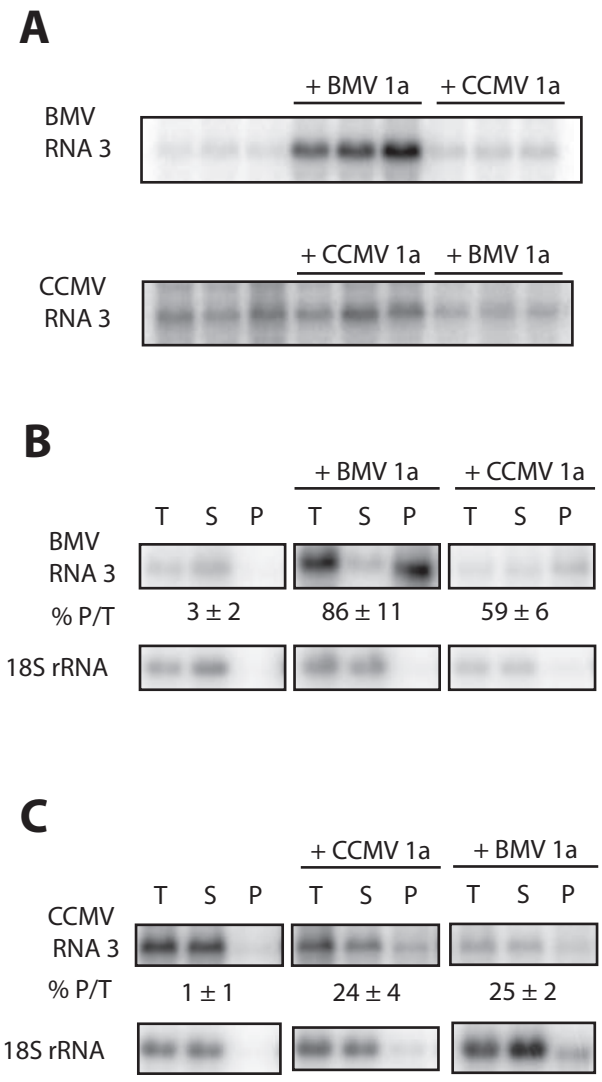

Figure 3.4. CCMV 1a is defective relative to BMV 1a in recruiting RNA templates to membranes. (A) Positive-strand BMV or CCMV RNA3 accumulation was detected by northern blotting from cells expressing RNA3 alone or with BMV or CCMV 1a as indicated. (B,C) As in (A) except yeast were lysed and centrifuged to pellet cellular membranes prior to RNA isolation. Accumulation of positive-strand RNA3 was assayed from total lysate (T), supernatant (S), and pellet (P) fractions.

that both 1a proteins recruited modest amounts of CCMV RNA3 to the membrane, boosting the fraction of membrane-associated CCMV RNA3 from ~2% in the absence of 1a to ~25% (Fig. 3.4C).

CCMV 1a localizes to the perinuclear ER and recruits CCMV 2a

One possible explanation for the limited RNA3 template recruitment and replication by CCMV 1a in yeast would be a reduced ability to assemble ER membrane-linked RNA replication complexes. Accordingly, we used confocal microscopy to check for proper localization of 1a and 2a proteins in yeast as a pre-requisite for RNA replication complex assembly. BMV and CCMV 1a were detected with a polyclonal antibody against an N-terminal BMV 1a fragment [122]. To visualize 2a protein localization, we used N-terminal GFP fusions. GFP-BMV2a showed equivalent function to wildtype BMV 2a in replicating BMV RNA3 (Fig. 3.5A), as in a previous report [120]. Similarly, GFP-CCMV 2a was as functional as wildtype, untagged CCMV 2a in replicating BMV RNA3.

When expressed in the absence of 2a, BMV and CCMV 1a proteins each localized to the perinuclear ER membranes, colocalizing strongly with a Sec63-GFP ER marker (Fig. 3.5B,C, top panels). When expressed in the absence of 1a, BMV and CCMV 2a each showed a diffuse distribution throughout the cytoplasm (Fig. 3.5B,C). When co-expressed with BMV 1a, the majority of BMV 2a was recruited to the perinuclear ER, as in prior reports [102, 120]. Similarly, CCMV 1a recruited a substantial fraction of CCMV 2a to the perinuclear ER (Fig. 3.5C). Thus the ability to localize to the perinuclear ER and to recruit 2a polymerase to these membranes, including in yeast cells, is conserved between BMV and CCMV 1a.

CCMV 1a induces spherule membrane invaginations along the ER

BMV 1a protein induces spherule membrane invaginations of the ER membrane in the absence of other viral factors [17]. To determine if ER membrane-localized CCMV 1a induces any membrane rearrangements in yeast, we performed transmission electron microscopy (EM) using traditional chemical fixation and embedding. With yeast cells expressing BMV 1a, we observed typical spherular vesicles in the lumen of the perinuclear ER membrane ~70 nm in

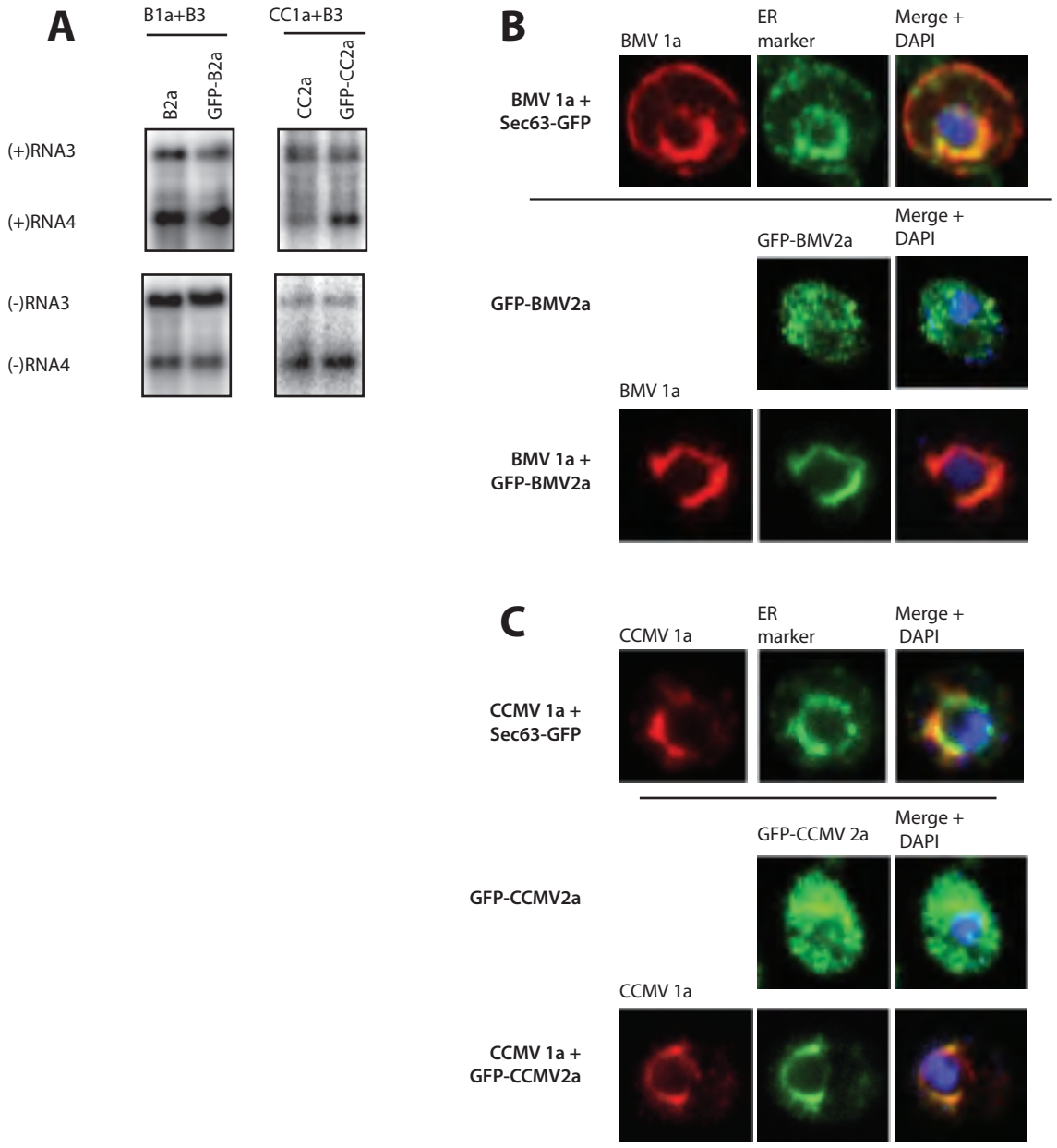

Figure 3.5. CCMV 1a localizes to the perinuclear ER and recruits CCMV 2a. (A) Replication of BMV RNA3 by BMV and CCMV with untagged 2a and GFP-2a was detected by northern blotting. (B) BMV 1a (red) and Sec63-GFP (ER marker) or GFP-2a (green) localization was detected by immunofluoresence. DNA was stained with DAPI as a nuclear marker. (C) Localization of CCMV 1a and GFP-2a. Images are a mean projection of 5 images covering 0.8 μm in the z-axis. BMV and CCMV 1a were detected with a polyclonal antibody raised against BMV 1a.

diameter (Fig. 3.6A). We observed similar vesicular structures in the perinuclear ER in cells expressing CCMV 1a (Fig. 3.6B).

We then prepared cells expressing BMV 1a or CCMV 1a for electron microscopy using high pressure freezing and freeze substitution (HPF-FS). HPF uses extremely rapid cryo-fixation followed by freeze-substitution and embedding to greatly reduce fixation and dehydration artifacts associated with traditional chemical fixation [133].

Notably, for these HPF samples, both the fraction of cell sections showing spherules and the average number of spherules visible per cell section were higher than for previous observations of chemically fixed cells in our laboratory. Moreover, while chemical fixation revealed spherule diameters primarily between 60-80 nm [17, 82, 84], these HPF samples showed a greater range of vesicle diameters from ~20-100 nm in cells expressing BMV 1a (Fig. 3.6C). The implication that HPF may preserve some 1a-induced membrane rearrangements lost in chemical fixation, and related points, are considered further in the Discussion.

To better visualize the membrane rearrangements induced by BMV 1a, we performed EM tomography [134]. This allows us to reconstruct thin z-sections throughout a tomographic volume, in contrast to thin section transmission EM which provides a only a single projection image of the entire section. Consistent with findings from chemical fixation [17], the spherules were clearly vesicular in nature and remained connected to the perinuclear ER by a thin neck (Fig. 3.7).

HPF -FS of cells expressing CCMV 1a induced highly similar spherular vesicles in the ER lumen at a frequency similar to or even greater than BMV 1a (Fig. 3.6D). CCMV 1a-induced spherules ranged in size from ~40-100 nm, but most CCMV 1a-induced spherules were in the range of 50-70 nm and smaller spherules were considerably more rare than for BMV 1a. For both BMV and CCMV 1a, occasional cells displayed a greater frequency of smaller diameter spherules, and these cells generally also displayed larger numbers of spherules.

1aN multimerization is conserved between BMV and CCMV

An N-terminal fragment of BMV 1a (1aN, aa 1-557), which contains the methyltransferase domain and is homologous to the alphavirus RNA replication protein nsP1, is sufficient for ER

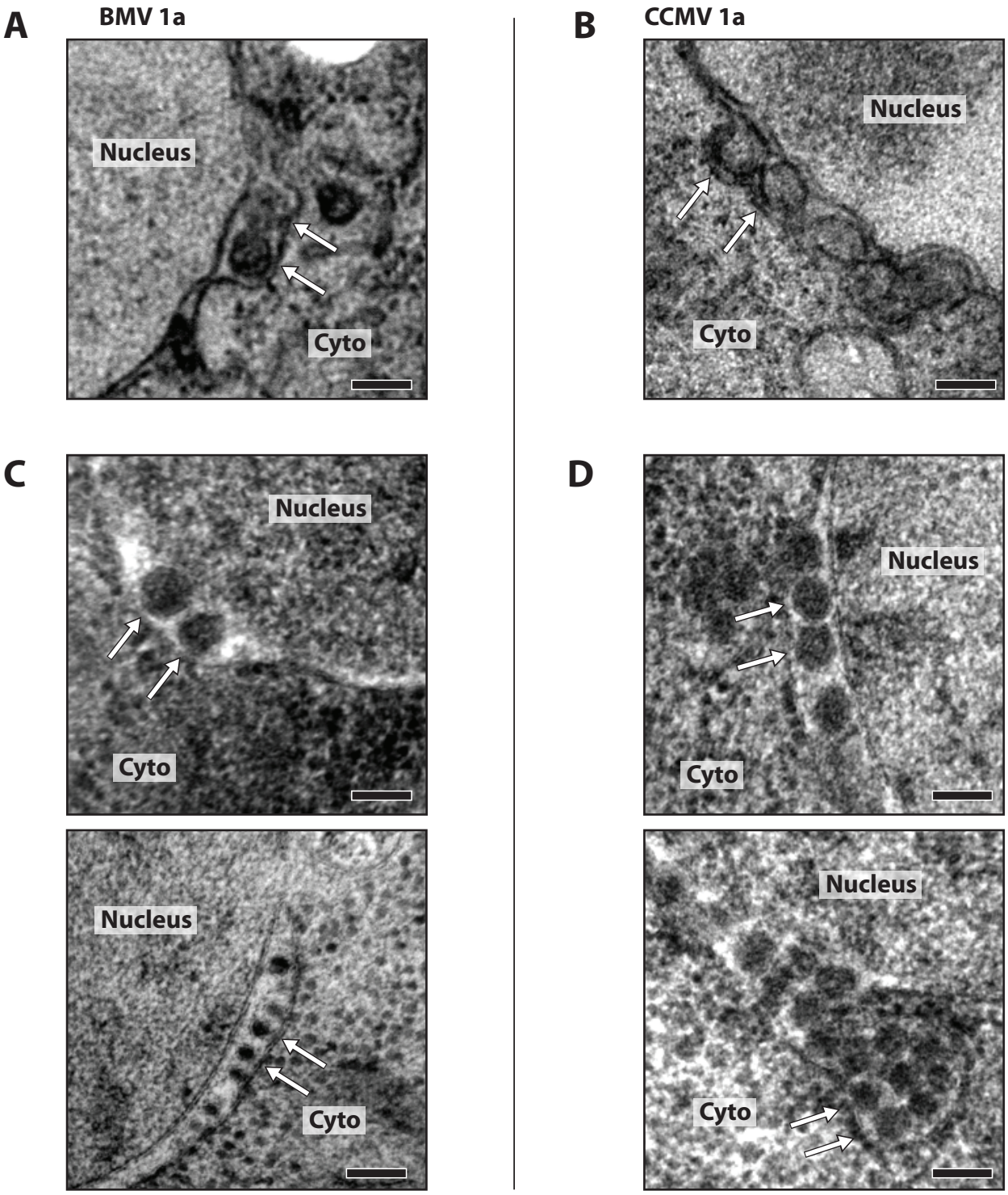

Figure 3.6. CCMV 1a is sufficient to induces spherule membrane rearrangements along the ER. Yeast expressing BMV 1a (A) or CCMV 1a (B) were prepared for EM using conventional chemical fixation and embedding (see Methods for details). Arrows identify 1a protein induced invaginations along the perinuclear ER. (C,D) Representative images of yeast expressing BMV or CCMV 1a prepared be high-pressure freezing and freeze substitution. All scale bars are 100 nm.

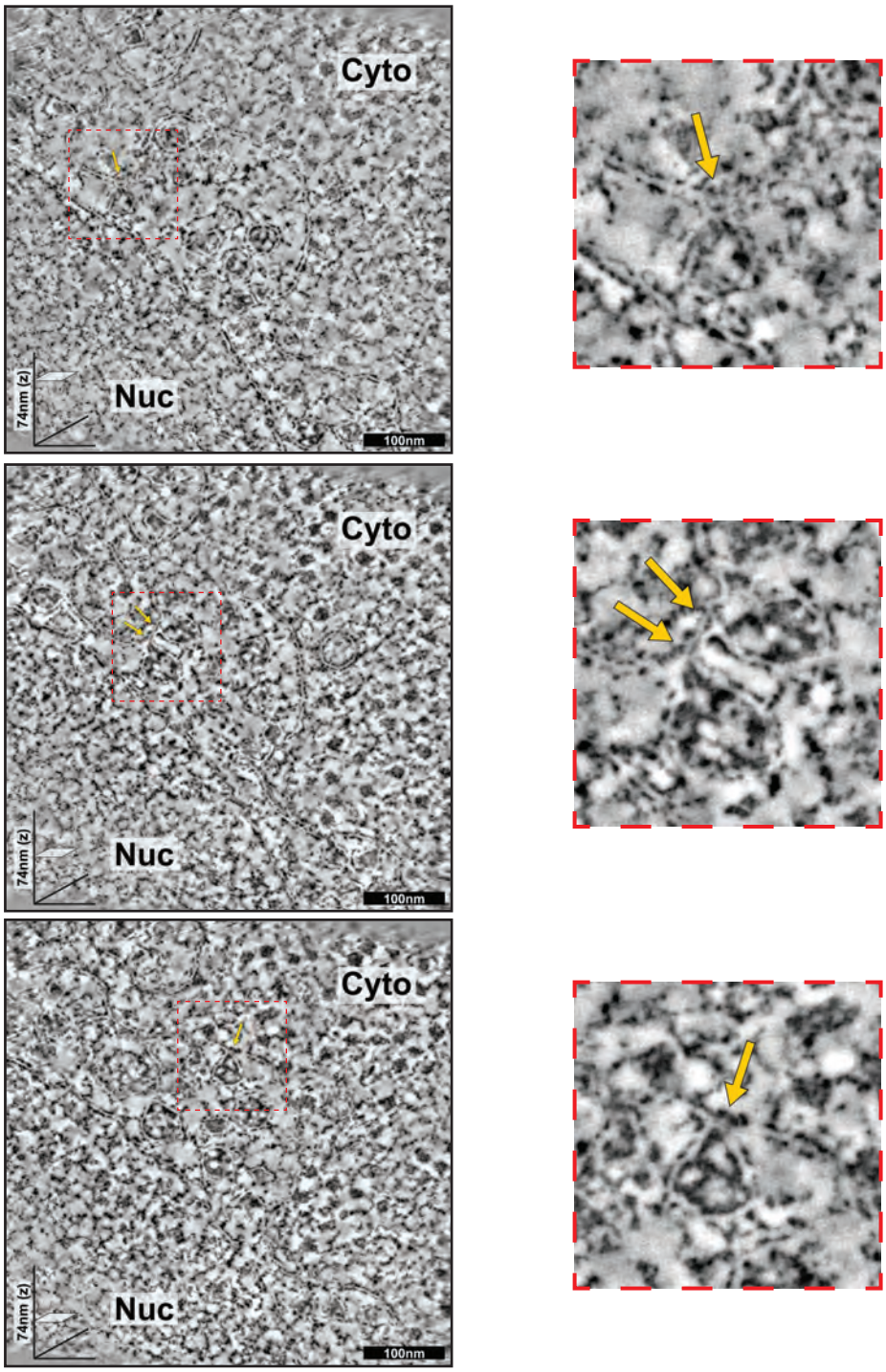

Figure 3.7. Tomography of BMV 1a membrane rearrangements. Three slices from a 3D tomographic reconstruction of BMV 1a induced membrane rearrangements are shown. The position of each slice within the 74 nm thick volume is indicated in the lower left of each image. Selected connections between spherules and the perinuclear ER are indicated by arrows. The area within the red box is shown enlarged to the right of each image for enhanced clarity. Nuc = nucleus; Cyto = cytoplasm. Scale bar = 100 nm.

membrane localization (Fig. 3.8A) [45]. While full-length BMV 1a localizes predominantly to the perinuclear ER membrane, 1aN accumulates not only on perinuclear ER, but also in μm-long filamentous structures that extend from along the nuclear envelope into the cytoplasm [45]. Electron microscopy reveals that these 1aN filamentous structures consist of ~18 nm diameter protein tubules often interlinked in parallel rows along the perinuclear ER membrane and occasionally extending from such ER association into large hexameric lattices [45]. Multiple results imply that the 1aN-1aN interactions forming these tubules and lattices are critical for formation of RNA replication vesicles by full length, wt BMV 1a [45].

Since the involvement of BMV 1aN tubule- and lattice-forming interactions in RNA replication could have important implications, we further tested the potential significance of these behaviors by asking if similar interactions might be conserved in the analogous fragment of CCMV 1a. To this end, we generated a similar CCMV 1aN fragment containing CCMV 1a amino acids 1-557 and a C-terminal FLAG-tag for detection. Our confocal and electron microscopy confirmed the prior observations of nuclear-flanking, ER-associated BMV 1aN tubules (Fig. 3.8A,C). More importantly, they revealed that CCMV 1aN formed ~18 nm diameter, μm-long tubules whose appearance, localization and spacing (Fig. 3.8B,D) were indistinguishable from those induced by BMV 1aN.

CCMV 1aN fragment dominant negatively inhibits CCMV 1a+2a -directed RNA replication

The conservation of tubule-forming interactions between BMV and CCMV 1aN further supports emerging evidence [45] that these interactions are functionally important in full-length 1a. In keeping with this, BMV 1aN is dominant negative to full-length 1a in BMV RNA replication [45]. Accordingly, we tested for possible trans effects of CCMV 1aN on RNA replication by CCMV 1a+2a. Since BMV RNA3 is replicated by both BMV 1a+2a and CCMV 1a+2a (Fig. 3.1), as a replication template we used a BMV RNA3 derivative, B3Rluc. In this derivative, the capsid ORF was replaced by the *Renilla* luciferase ORF (Fig. 3.1). In plant or yeast cells, genes so substituted for the capsid ORF in full length RNA3 are not directly translatable, and are only expressed if viral RNA-dependent RNA synthesis produces negative-strand RNA3 and, from this negative-strand, the subgenomic mRNA, RNA4 (Fig. 3.1) [86, 135]. By assaying

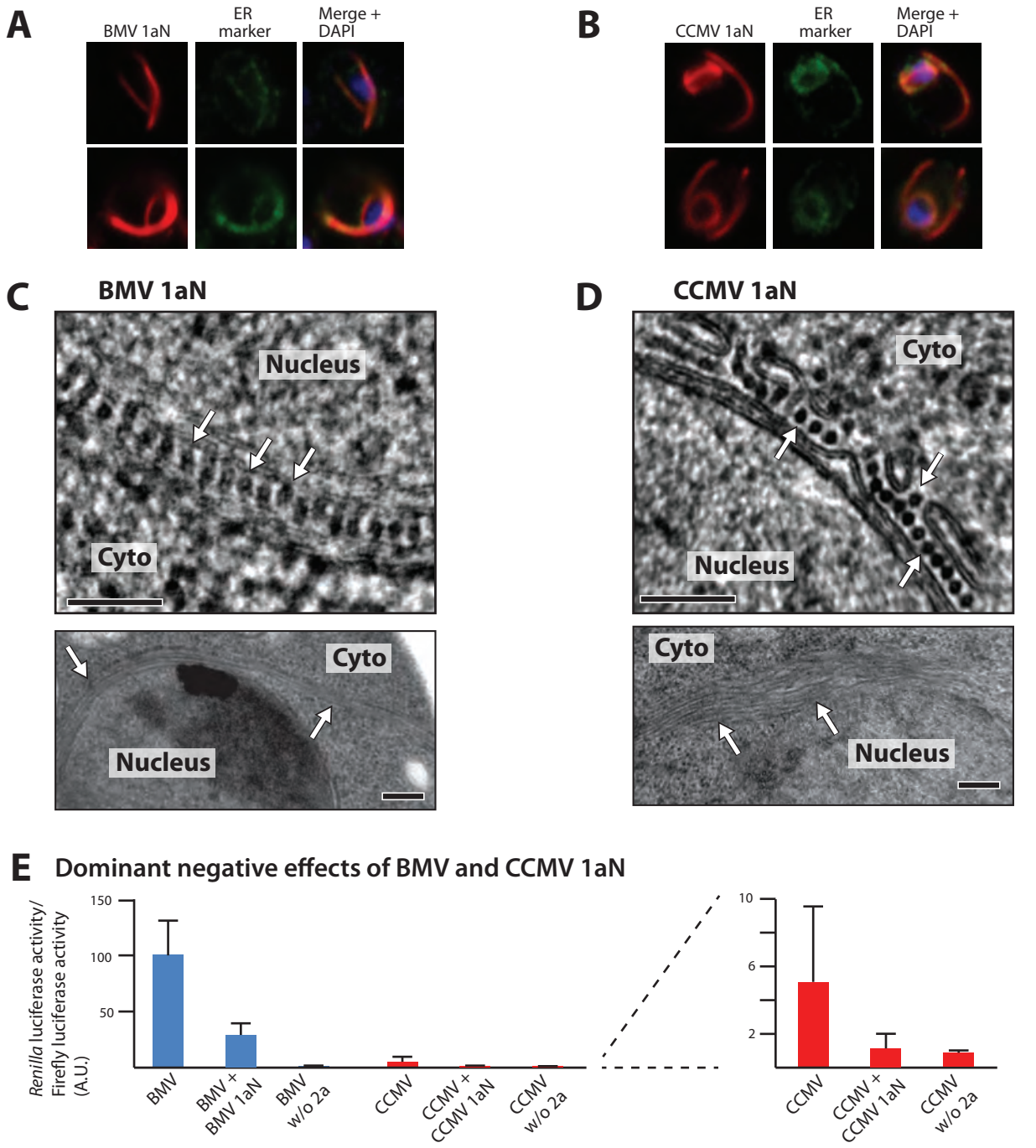

Figure 3.8. Essential multimerization of the 1a N-terminal domain is conserved between BMV and CCMV. Immunofluoresence of (A) BMV 1aN-FLAG and (B) CCMV 1aN-FLAG (red). Sec63-GFP (green) was expressed to label ER membranes. DAPI was used to stain DNA as a nuclear marker (blue). Images are a mean projection of 5 images across 0.8 μm of the z-axis. (C) HPF-FS EM images of BMV 1aN and (D) CCMV 1aN tubules. The tubules (indicated by arrows) appear as protein rings (top image) or long filaments (bottom image) depending upon their orientation within the section. Scale bar = 100 nm. (E) RNA replication dependent *Renilla* luciferase (R-luc) activity normalized to constitutively expressed firefly luciferase (arbitrary units). Cells for all lanes expressed the BMV RNA3 derived R-luc reporter. Cells also expressed BMV or CCMV 1a/2a, 1a/2a/1aN, or 1a only as indicated.

for *Renilla* luciferase activity, we thus could quantitatively assess any trans effects of BMV or CCMV 1aN fragments on RNA replication by their corresponding wt 1a+2a (Fig. 3.8E).

In parallel to the ~20-fold lower replication of wt BMV RNA3 in yeast by CCMV (Fig. 3.1), CCMV 1a+2a replicated and expressed B3Rluc to ~20-fold lower levels than BMV 1a+2a (Fig. 3.8E). Nevertheless, co-expressing the CCMV 1aN fragment with wt CCMV 1a+2a further suppressed *Renilla* luciferase activity by 5-fold, which was even greater than the dominant negative effect of BMV 1aN on *Renilla* luciferase expression by BMV 1a+2a from the same B3Rluc template (Fig. 3.8E). Thus, CCMV as well as BMV 1aN conserved both the ability to assemble long membrane-interacting and self-interacting tubules, and a strong dominant negative effect on RNA replication by the corresponding wt 1a. The mechanistic implications of these results are considered further in the Discussion.

CCMV 1a and 2a support replication of BMV RNA2 in yeast

In BMV RNA3, the cis-acting RE is located in the central intercistronic region, ~1 kb from either end (Fig. 3.1). In BMV genomic RNA2, an equivalent cis-acting recruiting signal is provided by a 5′ terminal sequence that is similarly essential for BMV 1a-mediated RNA2 recruitment and replication [94]. The essential core of this signal is a 5′-terminal stemloop that, like a similar stemloop in the BMV RNA3 RE and related 5′ stemloops in BMV RNA1 and CCMV RNAs 1 and RNA2, contains essential conserved sequences matching the invariant residues of host tRNA TΨC loops [94].

Given this similarity in template recruiting signals and our finding above that CCMV 1a+2a replicate BMV RNA3 in yeast, we tested whether CCMV 1a+2a also replicate BMV RNA2 in yeast. To avoid any interference from BMV 2a polymerase or its translation in cis from the intended RNA2 replication template, we used a BMV RNA2 derivative, RNA2-fs2, that fails to express 2a protein due to a frameshift mutation, but is replicated by BMV 1a+2a expressed in trans [94] (and Fig. 3.9A). In particular, co-expressing BMV 1a+2a markedly induced accumulation of negative-strand RNA2-fs (Fig. 3.9A). BMV 1a alone stimulated positive-strand RNA2-fs2 accumulation by ~3 fold (Fig. 3.9A), as expected for RNA template recruitment, although BMV 1a+2a did not increase positive-strand RNA2-fs accumulation significantly

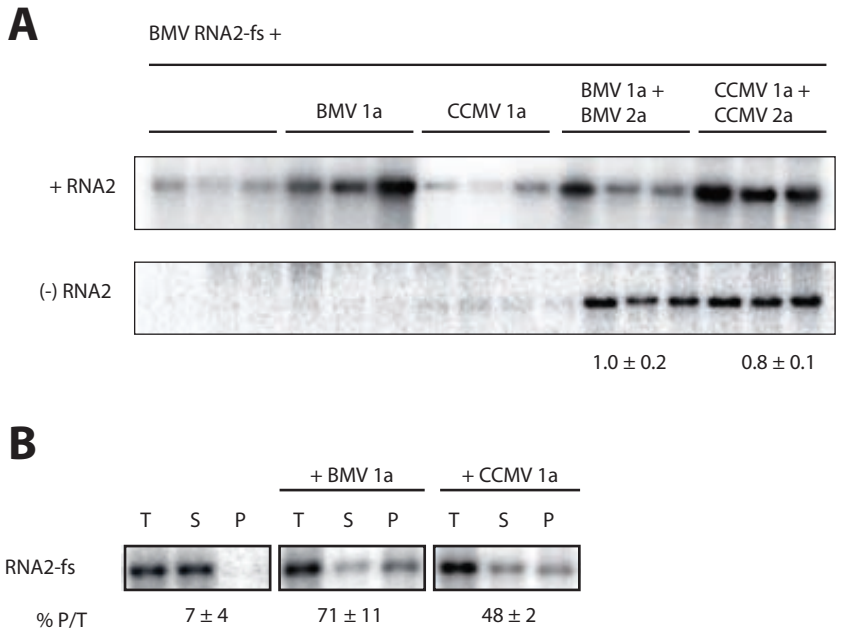

Figure 3.9. CCMV 1a and 2a supports replication of BMV RNA2 in yeast. (A) Accumulation of positive and negative strand frame-shifted BMV RNA2 was assayed by northern blotting from cells expressing RNA2-fs alone, with BMV or CCMV 1a, or 1a and 2a as indicated. (B) Cellular lysate from yeast expressing BMV RNA2-fs with or without BMV or CCMV 1a was centrifuged to pellet cellular membranes prior to RNA isolation. Accumulation of positive-strand RNA2-fs was assayed from total lysate (T), supernatant (S) and pellet (P) fractions.

beyond this level (Fig. 3.9A). Prior results show, however, that excess positive-strand RNA2 replication products are synthesized by BMV 1a+2a, but are turned over in the absence of capsid protein and RNA stabilization by encapsidation [94].

Interestingly, CCMV 1a+2a also replicated BMV RNA2-fs in yeast (Fig. 3.9A). Negative-strand RNA2 accumulation was equivalent to that directed by BMV 1a+2a. Moreover, while CCMV 1a alone did not detectably stimulate positive-strand BMV RNA2 accumulation, positive-strand RNA2 levels substantially increased in the presence of CCMV 1a+2a, to levels similar to or even greater than those with BMV 1a+2a (Fig. 3.9A).

Although CCMV 1a alone did not detectably stimulate BMV RNA2 accumulation, the ability of CCMV 1a+2a to replicate BMV RNA2 implies some level of recruitment to the replication complex. To further test this we used membrane fractionation to determine if CCMV 1a recruited BMV RNA2 to a membrane-associated state. We found that BMV 1a recruited approximately 70% of RNA2 to the membrane, and that CCMV 1a recruited approximately 50% of RNA2 to the membrane, consistent with the ability of RNA2 to be replicated (Fig. 3.8B). Prior results also suggest that BMV or CCMV 2a protein might enhance recruitment of RNA2 templates [94] .

DISCUSSION

Despite on-going advances in understanding the membrane-associated replication complexes of positive-strand RNA viruses, many questions remain relating to the mechanisms of assembly and the roles of these complexes in RNA replication. Some important insights have been gained previously through the study of BMV replication complexes in the model organism *S. cerevisiae*. We examined the RNA replication and replication complex assembly of another bromovirus, CCMV, in yeast to better identify and understand conserved features of BMV and to develop further tools to study replication complex assembly and function. Our results show that, as for BMV, expression of CCMV 1a is sufficient to induce spherule membrane rearrangements along the perinuclear ER. Further, CCMV 1a recruits CCMV 2a and BMV RNA templates to these replication complexes and supports both negative- and positive- strand RNA synthesis. Multimerization of the 1a N-terminal domain, previously shown to involve interactions

essential for spherule formation in BMV [45], is also conserved in CCMV 1a. Despite this significant conservation of function, relative levels of replication supported by BMV and CCMV 1a+2a varied significantly depending on the RNA replication template. CCMV RNA3, for example, failed to function detectably as a template for either virus.

CCMV 1a directs assembly of functional membrane-associated RNA replication complexes in yeast

BMV 1a is the only viral factor required to induce membrane rearrangements in plants and yeast [17, 101]. The RNA capping methyltransferase/guanylyltransferase and NTPase/helicase enzymatic activities of 1a are not required for spherule assembly [84]. Moreover, 1a induced membrane rearrangement can be studied independently of other essential 1a functions, such as recruiting the viral 2a polymerase to the replication complex and stimulating RNA synthesis. By contrast, some other positive-strand RNA viruses including Flock house virus and the alphavirus, Semliki Forest virus, have been shown to require viral RNA synthesis for spherule membrane rearrangement [51, 52].

While BMV has supported advanced studies of RNA replication, it is important to be able to distinguish between those results which identify well-conserved, essential mechanisms for general viral replication from those which are highly specific to BMV. To this end, we show here that the 1a protein from the related CCMV preserves many activities that have previously been observed only for BMV. For example, CCMV 1a is also able to induce spherule membrane rearrangements in yeast in the absence of other viral factors, recruit CCMV 2a to the perinuclear ER, recruit viral RNA templates to a membrane associated state, and support synthesis of negative- and positive- strand viral RNAs. Though CCMV is closely related to BMV, their 1a proteins share only 68% identity at the amino acid level and their respective dicot (CCMV) and monocot (BMV) host ranges are almost non-overlapping. Since there is no evolutionary pressure for either virus to function in yeast, common phenotypes between these two proteins likely reflect 1a properties that have been conserved due to an essential role in natural infection.

Previous studies using chemical fixation and plastic embedding of yeast for electron microscopy have shown BMV spherules to have diameters of 60-80 nm [82, 84, 133]. Our results

with chemical fixation matched these prior results for BMV 1a and showed that CCMV 1a induces similar structures. Based upon its demonstrated ability to provide better preservation of fine structures and cellular morphology [133] we chose to use HPF-FS to examine BMV and CCMV 1a-induced membrane rearrangements. We consistently observed well-preserved membranes surrounding the ER-associated replication complexes and throughout the cell. We also observed enhanced preservation of the dense yeast cytoplasm, which resulted in a decreased apparent contrast of the membrane relative to its surroundings when compared to traditional osmium fixation. Interestingly, though the overall morphology of the spherules was maintained between HPF-FS and chemical fixation reported previously, the majority of BMV spherules observed in HPF-FS samples had diameters from 30~50 nm, though 60~80 nm spherules were also present (Fig. 3.6C, top vs. bottom). One possible explanation is that a variety of spherule sizes are present in the yeast and smaller spherules are not well preserved during the prolonged chemical fixation and dehydration process. Future studies using cryo-electron microscopy, in which samples undergo no fixation or embedding, should allow observing spherules in a near native state to resolve this issue. The 30-50 nm spherules observed in HPF-FS should still be sufficient to contain all of the necessary proteins and RNA templates for replication.

Spherules smaller than 50 nm were rare in cells expressing CCMV 1a and CCMV-induced spherules were larger on average than for BMV. Previous studies have shown that the size of BMV spherules can be altered by mutation of 1a itself or through the deletion of host proteins that contribute to replication complex assembly [62, 65, 82, 136]. Whether the difference in size range observed between BMV and CCMV spherules is due varied interaction with yeast host factors or other differences between the 1a proteins will require further investigation.

CCMV 1aN assembles into membrane-associated multimers

BMV 1aN is sufficient for ER targeting, membrane association, and assembly into high-order multimers, but not spherule formation [45]. 1aN multimers occur in the form of membrane associated protein tubules that associate via short filaments with bounding ER membranes and with each other in rows or hexameric lattices [45]. CCMV 1a and an N-terminal fragment

derived from it have each been shown to self-interact in yeast two-hybrid studies [44]. We found that, in vivo, the corresponding CCMV 1aN fragment assembles into protein tubules indistinguishable from those of BMV 1aN (Fig. 3.8C,D). Moreover, as for BMV 1aN, the expression of CCMV 1aN was dominant negative to RNA replication. This suggests that 1aN tubule-forming interactions are essential for formation of the spherule replication compartments and for RNA replication in BMV and CCMV and imply that BMV and CCMV depend on similar mechanisms of 1a-1a multimerization for replication complex assembly.

Unlike their counterparts, the BMV 1a and 2a proteins, alphavirus non-structural proteins are translated as a polyprotein cleaved by a viral protease. Thus, while BMV 1a contains both methyltransferase and NTPase activity, these functions are ultimately separated into two smaller proteins, nsP1 and nsP2 respectively, in alphavirus infections. Interestingly, alphavirus (Sindbis and Semliki forest virus) nsP1, homologous to BMV 1aN, has been shown to induce filopodia-like extensions of the plasma membrane when expressed alone, or in the context of infection [137]. These filopodia may be induced by assembly of membrane-wrapped nsP1 filaments, much like BMV 1aN filaments that can be observed interacting with multiple ER membranes simultaneously (Fig. 3.6C). In support of this, the nsP1 induced plasma membrane extensions have been shown to contain nsP1, but not actin or microtubules [137]. As with bromovirus 1aN, exogenous nsP1 expression is dominant negative to alphavirus RNA replication [138]. Though the bromovirus 1aN is a protein fragment, its shared ability with the homologous, naturally occurring, alphavirus nsP1 to make membrane-associated extended protein filaments is striking. Further investigation into the mechanisms of 1aN filament and nsP1 filopodia assembly may reveal essential, broadly conserved, multimerizing interactions among alphavirus-like replicase proteins.

Template dependent RNA replication by CCMV 1a/2a

Previous studies of RNA replication by BMV/CCMV hybrids in plant protoplasts, and our results here (Fig. 3.2A,C), show that the BMV and CCMV 1a+2a pairs each support replication of the heterologous RNA3 [98, 129]. RNA3 is a useful template for studying bromovirus RNA replication as its products are not required for RNA replication, alleviating the need to

distinguish between potential cis- and trans- activity of the template. Additionally, RNA3 is the most abundant template during natural infection and directs sub-genomic mRNA synthesis, absent from genomic RNAs 1 and 2, thus allowing for a more complete analysis of 1a/2a function.

In previously published results with plant cells, CCMV and BMV 1a+2a supported similar levels of BMV RNA3 replication [85, 98, 129]. In yeast, CCMV replication of BMV RNA3 was significantly lower than levels generated by BMV (Fig. 3.2B). Our data suggests this is primarily due to a decreased efficiency in the recruitment of RNA3 to the replication complex. We also found that unlike BMV RNA3 in plants or yeast, or CCMV RNA3 in plants, CCMV RNA3 was not functional as a replication template for BMV or CCMV 1a+2a in yeast. Though both 1a proteins recruited CCMV RNA3 to a membrane-associated state, the level of recruitment, ~25% vs >80% for BMV 1a/RNA3, suggests a major defect at or before this early step. Consistent with these data that the defect for CCMV RNA3 replication in yeast occurs prior to negative-strand synthesis, CCMV RNA3 is replicated in vitro by RNA-dependent RNA polymerase activity isolated from yeast expressing BMV 1a, 2a, and RNA3 [139]. Notably, this in vitro system is able to replicate exogenous BMV RNA3 templates with deletions of the essential RE element, required for RNA recruitment in vivo [139]. Thus, the in vitro system that supports CCMV RNA3 replication by BMV 1a+2a is insensitive to the normal in vivo template recruitment step.

Given that BMV RNA3 and RNA2 were functional templates in yeast for CCMV as well as BMV 1a+2a and have been previously characterized for BMV replication, we focused primarily on the replication of these templates in this manuscript. Replication of CCMV RNA3 may require a yet unidentified plant specific host factor or its function may be inhibited by factors unique to yeast or to DNA based expression. A minimal template required for CCMV RNA3 replication in plant cells, consisting of portions of the 5' and 3' UTRs, has been identified [140]. However, CCMV RNA3 lacks an identified tRNA-like box B motif present in all other BMV and CCMV RNAs, suggesting its recruitment may depend on unique factors. The mechanisms box B dependent recruitment of BMV RNAs 2 and 3 and the apparently box B independent recruitment of CCMV RNA3 remain important avenues for future research.

BMV RNA2 was replicated by both BMV 1a+2a and CCMV 1a+2a in yeast. Even under replicating conditions, positive strand RNA2 accumulation was only ~3-5 fold over the plasmid expressed template. Chen et al. have suggested this may be due to rapid turnover of the positive-strand product in yeast based upon an observed increase of the signal in the presence of BMV capsid protein [94]. Though BMV RNA2 levels are less than that of RNA3 in natural infection, it remains possible that the low levels of RNA2 replication in yeast represent a template-specific host restriction. One model consistent with our data would be a single host-restriction of recruiting BMV RNA templates that BMV1a/RNA3 are able to circumvent that CCMV 1a and BMV RNA2 are not.

Here we establish a CCMV RNA replication system in yeast. Overall, our data shows that the functions of BMV 1a and CCMV 1a are largely conserved and that, just as for BMV, many CCMV 1a functions can be reconstituted and studied in yeast. Comparative analysis of the replication complexes of these two systems should prove a valuable tool as we learn more about replication complex structure and assembly. The primary defect of CCMV RNA3 replication in yeast was mapped to poor recruitment of RNA to the replication complex, with independent contributions to this defect from CCMV RNA3 and CCMV 1a. We identified significant differences in the function of three viral templates: BMV RNA3, RNA2, and CCMV RNA3. Models and future studies of bromovirus RNA replication should therefore account for these multiple template- and 1a- specific variations in host dependencies for recruiting RNA to the replication complex.

MATERIALS AND METHODS

Protoplasts growth and transfection

Avena sativa cell suspension culture was a gift from Dr. Aurelie Rakotondrafara. Cell growth and protoplast generation were performed as described [132] with minor modifications. The growth media contained Murashige and Skoog modified vitamin solution (MP Biomedicals) and 0.05% plant preservative mixture (Plant Cell Technology). Viral RNAs were transcribed from the previously described plasmids pB1TP3, pB2TP5, pB3TP8, pCC1TP1, pCC2TP2, and

pCC3TP4 [129, 141]. 1x10^6 protoplasts were electroporated with 5μg of each indicated RNA in a BTX 600 for approximately 6 ms (325 V/350 μF/48 Ω). RNA was extracted with hot phenol after 24 hours [142].

Yeast and plasmids

S. cerevisiae strain YPH500 and culture conditions were as described previously [31, 93]. BMV 1a, 2a, and RNA3 were expressed from pB1YT3, pB2YT5, and pB3MS82 [17, 120, 121] unless otherwise noted. Standard molecular cloning techniques were used to replace the BMV derived sequences in these plasmids with the corresponding CCMV sequences from pCC1TP1, pCC2TP2, and pCC3TP4 to generate pCC1GCU, pCC2GCL, and pCC3GCW respectively. In experiments containing frame-shifted RNA2 (pB2NR3-M1 [94]), BMV 1a and 2a were expressed from pB1YT3H [121] and pB2YT3 (Ura^+ derivative of pB2YT5). Corresponding CCMV 1a and 2a plasmids pCC1GCH and pCC2GCU were generated as described above. In experiments containing RNA3 with an RE mutation (pB3VG104 [143]), pB3VG103 [143] was used to express wildtype RNA3. GFP from GFP-BMV2a (pB2YT5-G2 [120]) was cloned into pCC2GCL to generate GFP-CCMV2a (pCC2GCL-G). Plasmids expressing amino acids 1-557 of BMV or CCMV 1a followed by the FLAG peptide (DYKDDDDK) were generated by replacing the full-length 1a sequence (PacI-BamHI fragment) in pB1YT3 and pCC1GCU respectively. Plasmid pDKBG is a Trp^+ derivative of pB3BG29 [90] containing a bidirectional Gal 1/10 promoter expressing firefly luciferase and a BMV RNA3 template in which coat protein has been replaced with *Renilla* luciferase. BMV and CCMV 1a and 2a were expressed from pB1YT3H, pB2YT5, pCC1GCH, and pCC2GCL in luciferase experiments. Total yeast RNA was harvested using hot phenol [142].

Cell fractionation

Cell fraction as done as described elsewhere [94]. Briefly, yeast were spheroplasted and osmotically lysed. Half of the lysate was set aside for total RNA. The remaining lysate was centrifuged at 20,000 xg for 5 minutes at 4°C. The supernatant was saved as the soluble fraction and the pellet was washed once more with lysis buffer. All three fractions were adjusted to

equal volume with lysis buffer and an equal volume of each fraction was used for analysis, equivalent to 2.0 μg of total RNA.

RNA analysis

RNA electrophoresis and northern blotting was done as described previously [120]. Briefly, 2.0 μg of total RNA from yeast or oat protoplast was electrophoresed a 1% denaturing agarose gel and transferred onto nylon membrane. The membranes were probed with ^{32}P-labelled probes and radioactivity was measured using storage phosphor screens imaged on a Typhoon scanner (GE Healthcare). Viral RNA from protoplasts was detected using probes complementary to the conserved 3' end of RNAs 1,2,3, and 4 of BMV or CCMV generated as described [98] from pB3HE1 [144] or pCC3RA518 [100], respectively. Viral RNA from yeast was detected using strand-specific probes complementary to BMV RNA3/4 nt 1250-1755 [121] or the homologous region of CCMV RNA3/4, nt 1355-1868. BMV RNA2 was detected by strand-specific probes complementary to nt 1441-1685 [94]. The 18s rRNA probe was transcribed from pTRI RNA 18S Antisense Control Template (Ambion).

Luciferase assay

Yeast luciferase assays were performed using the Promega Luciferase and *Renilla* Luciferase Assay Systems as described elsewhere [90] and according to the manufactures instructions. The RNA replication-dependent *Renilla* luciferase activity was normalized to the constitutively expressed firefly luciferase activity to adjust for differences in cell number or lysis efficiency.

Electron microscopy

Chemical fixation, dehydration, and embedding of yeast was done as described previously [17]. To prepare sections for tomography, yeast were harvested by centrifugation (6000 xg, 2 min) and washed in 1% type IX-A ultra-low gelling temperature agarose (Sigma). The yeast were then centrifuged again and the supernatant was removed leaving a thick yeast paste. The paste was loaded into the 0.1 mm side of two type A planchettes pre-treated with hexadecene (0.2 mm total sample thickness) and frozen in an HPM 010 high pressure freezer. Freeze substitution

and embedding in HM20 were done as described by Giddings [133], using 0.25% glutaraldehyde, 0.05% uranyl acetate in dry acetone in a Leica AFS. Tomograms were collected on a Tecnai TF-30 using 250 nm thick sections. The IMOD software suite was used for tomogram processing [145]. High pressure frozen yeast for thin section transmission EM were prepared in essentially the same manner except with 2% osmium, 5% water in acetone for freeze-substitution media followed by embedding in Eponate 12 (Ted Pella) at room temperature. Thin section imaging was done on a Phillips CM120.

Immunofluorescence

Yeast were prepared for confocal microscopy as in Chapter Two. The polyclonal rabbit antibody raised against an N-terminal fragment of BMV 1a [122] was used to detect both BMV and CCMV 1a proteins. Polyclonal rabbit-*α*-FLAG (Sigma, F7425) was used to detect the tagged 1aN constructs. Goat-*α*-rabbit antibody conjugated to Alexa Fluor 568 (Life technologies) was used as a secondary antibody for 1a antisera and F7425. DNA was stained with DAPI (4′,6-diamidino-2-phenylindole, Life technologies) as a nuclear marker. Images were collected on a Nikon A1R confocal system. Images shown are an average intensity projection of five images taken across 0.8μm in the z-axis, processed in Fiji [146].

CHAPTER 4

Analysis of bromovirus 1a protein hybrids reveals 1a-1a interactions essential for RNA replication complex assembly

All experiments were designed and performed by Bryan Sibert. Arturo Diaz (Ahlquist lab) and Xiaofeng Wang (Ahlquist lab) provided helpful discussions.

INTRODUCTION

All positive-strand RNA ((+)RNA) viruses assemble membrane-associated replication complexes that serve as a scaffold for RNA replication factors, protect viral components from host defenses, and coordinate RNA replication, translation, and packaging [124]. The critical involvement of these replication complexes in multiple stages of infection makes them a potentially valuable therapeutic target. The three-dimensional membrane ultra-structures of many replication complexes have been determined by electron microscopy (EM) tomography [125]. However, little is known about how the viral proteins localize to the correct membranes, induce replication complex membrane rearrangements, or how these proteins are organized within the complex.

Brome mosaic virus (BMV) is a plant virus whose RNA replication is also supported in the yeast *Saccharomyces cerevisiae*. Only a single viral factor, the multifunctional BMV 1a protein, is necessary to induce replication compartment membrane rearrangements in plants or yeast [17, 101]. BMV 1a recruits the 2a RNA-dependent RNA polymerase, viral RNA templates, and essential host factors to the replication complex. In addition to its role in replication complex assembly, BMV 1a contains RNA-capping activity in its N-terminal domain and NTPase/helicase activity in its C-terminal domain [80, 147]. BMV 1a and 2a are translated from genomic RNAs 1 and 2 respectively and are the only viral proteins necessary for BMV RNA replication. The BMV genome additionally contains a genomic RNA3 that directly encodes the 3a movement protein essential for cell-to-cell movement in plants and a subgenomic RNA4, transcribed from negative-strand RNA3, that encodes the coat protein for virion assembly [76].

In yeast, BMV 1a induces invaginations of the perinuclear ER approximately 60-80 nm in diameter that remain connected to the cytoplasm by a neck-like structure, similar to the vesicles induced on the endoplasmic reticulum in bromovirus infected plants [17]. Other members of the alphavirus-like superfamily, such as Semliki forest virus (SFV), flavivirues, such as Dengue virus, and many other (+)RNA viruses form structurally similar vesicular replication complexes, although on different host membranes [25, 26, 36, 67, 148]. The host and viral factors essential for localizing replication complex assembly to the appropriate membranes remain largely unknown.

Immuno-EM and other studies imply that each BMV spherule contains up to hundreds of strongly membrane associated 1a multimers [17]. The proteins responsible for RNA replication complex assembly in other viruses have also been shown to multimerize on host membranes [47, 50]. Disruption of viral replication complex protein multimerization has often been observed to occur in conjunction with loss of multiple protein functions [149-151], highlighting the importance of these interactions, while simultaneously complicating determination of the specific contributions of the interactions to RNA replication and replication complex assembly.

An N-terminal fragment of BMV 1a, BMV 1aN (aa1-557), is sufficient to localize to the ER and contains an amphipathic helix responsible for the majority of 1a's membrane association [45, 82]. When expressed in vivo, 1aN assembles into rows of ER-associated protein tubules, occasionally observed in large hexameric arrays [45]. In vivo crosslinking of tagged 1aN fragments indicated the tubules were likely comprised of directly self-interacting 1aN. Expression of the 1aN fragment is dominant negative to RNA replication and spherule formation, and recruits full-length 1a to the protein tubules indicating that these 1aN-1aN interactions are important in the context of full-length 1a as well [45].

Cowpea chlorotic mottle virus (CCMV) is closely related to BMV and its 1a protein shares 69% amino acid identity with BMV 1a. BMV and CCMV 1a also share many functional similarities including the ability of CCMV 1a to support RNA replication and induce perinuclear membrane rearrangements in yeast. BMV 1a and 1aN interactions are conserved in

CCMV 1a and 1aN [44][Chapter 3, this work] further supporting the role of these interactions in important and evolutionary conserved 1a functions.

The BMV 1a N- and C- terminal domains are independently capable of intermolecular self-interaction and can also interact with each other [45, 115]. Identifying and characterizing 1a-1a interacting regions in more detail is essential to understanding RNA replication complex assembly and functions. In this study, we used co-immunoprecipitation of 1a fragments to indentify two independent regions within the N-terminal domain of BMV 1a capable of self-interaction. These regions also interact with each other, suggesting a potential role in 1a conformational changes.

To indentify and map contributions of the 1a N-terminal domain to essential steps of RNA replication including RNA replication complex assembly we generated a series of hybrid 1a proteins replacing successive segments of BMV 1a with the corresponding sequence from CCMV 1a. The hybrids displayed a range of phenotypes including various levels of disruption of RNA replication,1a localization, and 1a stimulation of viral RNA accumulation, a signature of recruiting RNA to the replication complex [92]. One hybrid substituting a highly conserved motif in the core methyltransferase domain abolished 1a and 1aN localization, membrane rearrangement, and RNA replication. Simultaneously substituting a distal region, containing the membrane targeting helix, restored 1aN localization, but not RNA replication. Thus, the two regions require compatibility for 1a localization, but likely play other roles in RNA replication as well. Our co-immunoprecipitation results identify specific regions of the 1aN domain with essential contributions to 1a-1a interactions. Highly conserved motifs in these interacting regions require genetic compatibility for 1a localization and membrane rearrangement, essential first steps of replication complex assembly.

RESULTS

BMV 1aN contains at least two separate regions capable of multimerization

To test for 1a self-interactions we used co-immunoprecipitation (co-IP) assays. One advantage of co-IP assays is that they allow testing the interaction of minimally tagged proteins expressed

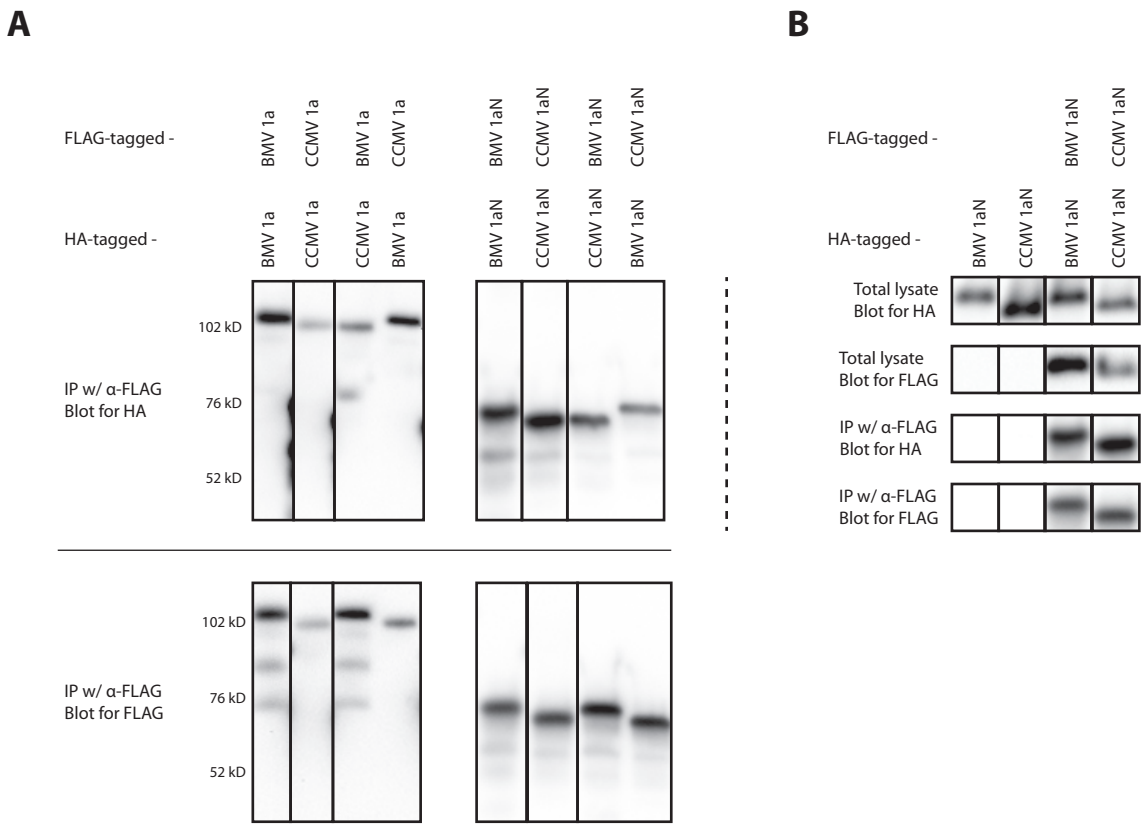

Figure 4.1. BMV and CCMV 1a proteins and their 1aN domains interact homo- and heterotypically. (A) Yeast were transformed to express BMV 1a, CCMV 1a, or N-terminal 1a fragments (BMV 1aN = aa1-557, CCMV 1aN = aa1-554) with a C-terminal FLAG or HA tag as indicated. Lysates were immunoprecipitated with an anti-Flag antibody and the precipitated proteins were analyzed by SDS-Page and western blotting using an anti-FLAG or anti-HA antibody as indicated. (B) The total lysate and IP elution from yeast expressing the indicated proteins were probed with antibodies against HA and FLAG to test for the specificity of immunoprecipitation. All lanes presented immediately adjacent to one another were cropped from the same image of a single blot and are presented at an equivalent exposure.

in vivo, in the cytoplasm, where 1a would normally be expressed and interact during RNA replication. We generated HA- and FLAG- tagged versions of BMV and CCMV 1a and their respective N-terminal domains (1aN, BMV aa1-557, CCMV aa1-554). This allows us to detect homotypic interactions by co-IP using antibodies against the unique epitopes of the differentially tagged 1a proteins or fragments.

Consistent with previous results using other assays [45, 115], we saw a robust co-IP of differentially tagged BMV 1a proteins as well as of 1aN (Fig. 4.1A). We also observed co-IP of CCMV 1a and CCMV 1aN and heterotypic interactions between BMV and CCMV as well (Fig. 4.1A). There was no drastic difference in the strength of the precipitated bands between the homologous and heterologous pairs, though it should be noted that co-IP band intensity does not directly correlate with the kinetics or stoichiometry of any given interaction.

The ability of the 1aN fragment to form extended protein tubules, with observed filamentous interactions between tubules, suggests there are multiple sites of intermolecular interaction in this region [45]. We chose to focus on interactions within this domain as an initial step to understanding all of the essential interactions in 1a. We generated a series of epitope-tagged N-terminal truncations of BMV 1aN and tested their ability to interact with BMV 1aN by co-IP in attempt to map regions involved in 1aN intermolecular interaction. The expression level of the N-terminally truncated fragments of 1aN were all significantly lower than the highly accumulated BMV 1aN. Nonetheless, we were able to determine that all of the fragments tested, including the smallest aa367-557, immunoprecipitated with 1aN (Fig. 4.2A). In this and other co-IP experiments in this work, strong precipitated bands generally correlated with higher levels in the total lysate blot as well. It is possible that multimerization or interaction with 1aN stabilizes the truncated fragments, resulting in higher levels of accumulation.

To determine if aa367-557 was interacting with the same or other sequences within 1aN, we tested the ability of our N-terminal deletion series to co-IP with BMV aa367-557. All of the fragments co-IPed with aa367-557 (Fig. 4.2B), indicating that this region is capable of homotypic, intermolecular, 1aN-1aN interactions.

To test for additional sites of interaction, we performed a similar co-IP experiment with C-terminal truncations of 1aN. We detected interaction of 1aN with aa1-480, but not with aa1-

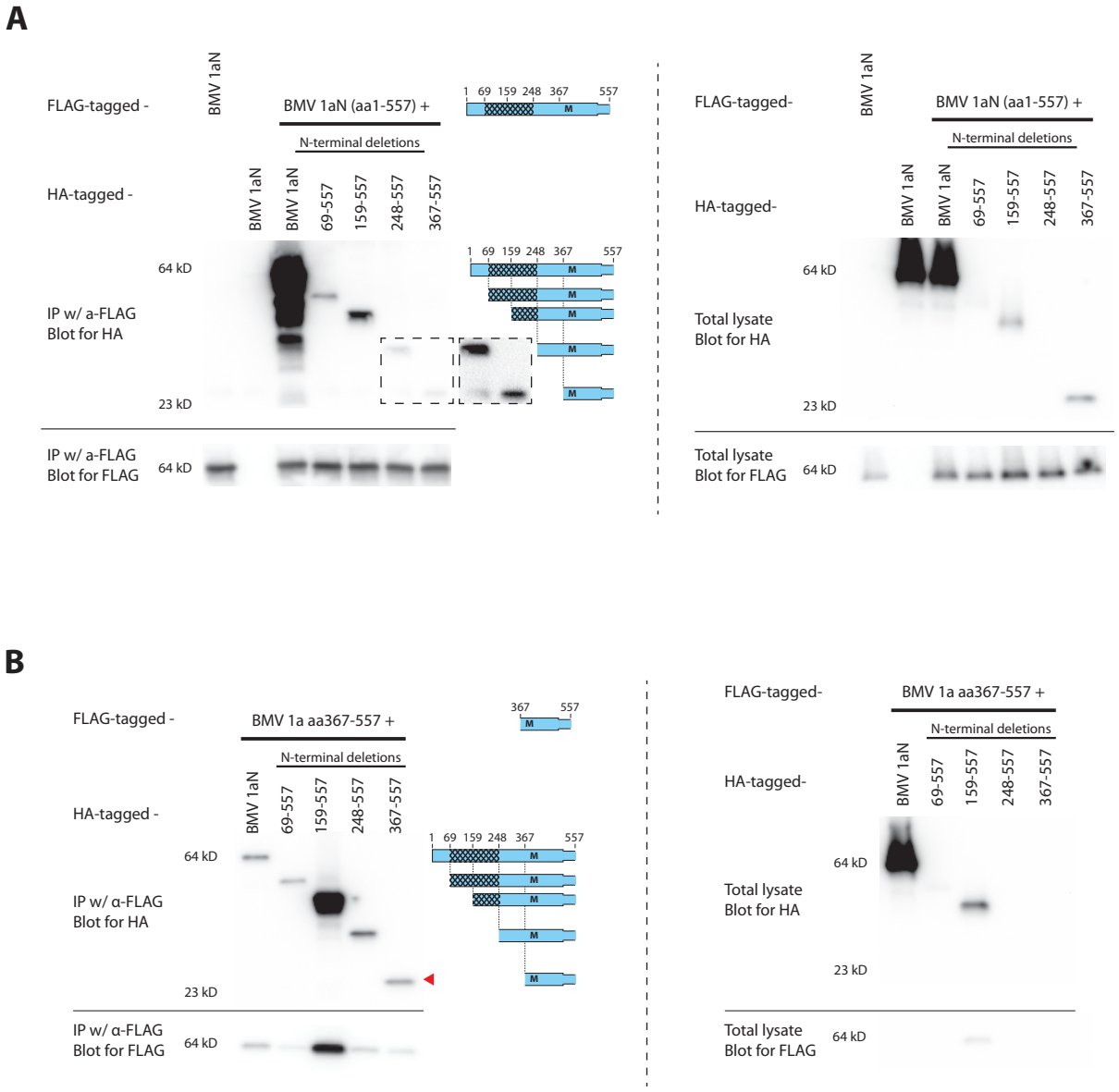

Figure 4.2. BMV 1aN contains a self-interaction within aa367-557. BMV 1aN or further truncated fragments of BMV 1aN were expressed with C-terminal HA or FLAG epitope tags as indicated above each lane. Total protein lysates were harvested and immunoprecipated using anti-FLAG antibodies and the resulting immunoprecipitates were analyzed by SDS-PAGE and western blotting using antibodies recognizing the FLAG or HA tag as indicated. Western blotting of the total lysate is shown on the right for comparison; some fragments were not detectable at the concentrations present in the total lysate. Blots are shown overexposed to visualize faint bands, the area in the dashed box is shown duplicated with even greater contrast. The band next to the red arrow indicates co-immunoprecipitation of fragment 367-557 with itself.

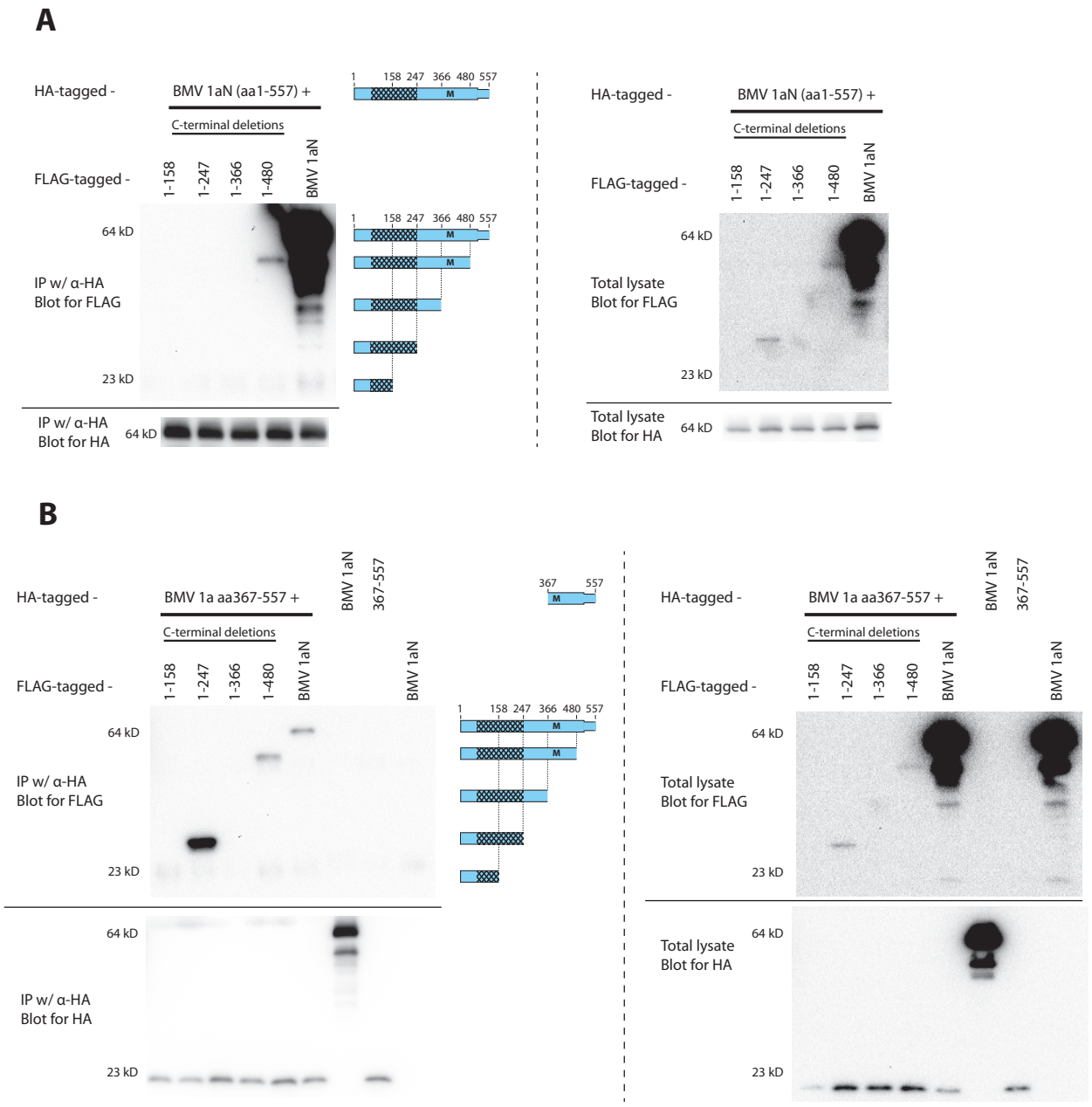

Figure 4.3. BMV 1aN aa367-557 co-immunoprecipates with aa1-247. Lysates from yeast expressing BMV 1aN-HA (A) or BMV aa367-557-HA (B) and C-terminally tagged truncations of 1aN were immunopreciptated with an anti-HA antibody and analyzed by SDS-PAGE/western blotting for FLAG and HA. Blots of total lysate are shown on the right. Blots are shown overexposed to visualize faint bands.

366 or smaller fragments (Fig. 4.3A), consistent with our earlier result identifying an interaction in the region of aa367-557 (Fig. 4.2B). We then tested the ability of the aa367-557 fragment to precipitate our C-terminal 1aN truncations and found that aa1-247 precipitated with aa367-557. Thus, BMV aa367-557 is capable of both homotypic multimerization and interaction with the distal region aa1-247 (Fig. 4.3B).

To investigate why we did not detect interaction between full-length 1aN and aa1-247, we reversed the co-IP and used aa1-247 as the bait. We also tested for homotypic interaction of aa1-247. We found that aa1-247 was able to interact homotypically and with full-length 1aN (Fig. 4.4A). As is explored further in the Discussion, the discrepancy in detection of this interaction depending on which fragment is immunoprecipitated may be explained by the differences in total abundance of the two proteins and the fact that smaller fragments must compete with intra- and inter- molecular 1aN-1aN interactions. Combined, we were able to identify three interactions through two distal regions. BMV aa1-247 and aa367-557 each multimerize homotypically and together interact heterotypically. Figure 4B shows a diagram of these newly identified interactions.

The conservation of any single 1aN-1aN interaction could result in the co-IP of BMV 1aN with CCMV 1aN. We were able to detect an interaction between CCMV 1aN and BMV aa159-557, but not BMV aa367-557 (Fig. 4.4C) which does interact with BMV 1aN. Thus although the two domains interact, the interaction may not occur in a complete and functional manner compared to the homotypic interactions.

Substitution of BMV 1a sequences with the corresponding sequence from CCMV 1a abolishes RNA replication in several regions

To further investigate the nature and roles of these 1aN interactions, we made a series of BMV 1a derivatives in which successive segments of 1aN bore the amino acid changes from the closely related CCMV 1a protein (Fig. 4.5A). The boundaries of the regions were selected to not split predicted helices or beta sheets. We first tested the ability of these hybrids to support replication of BMV RNA3 when coexpressed with BMV 2a in yeast. Four of the nine hybrid proteins, B/CC 2, B/CC 4, B/CC 8, and B/CC 9, retained the ability to support reduced, but

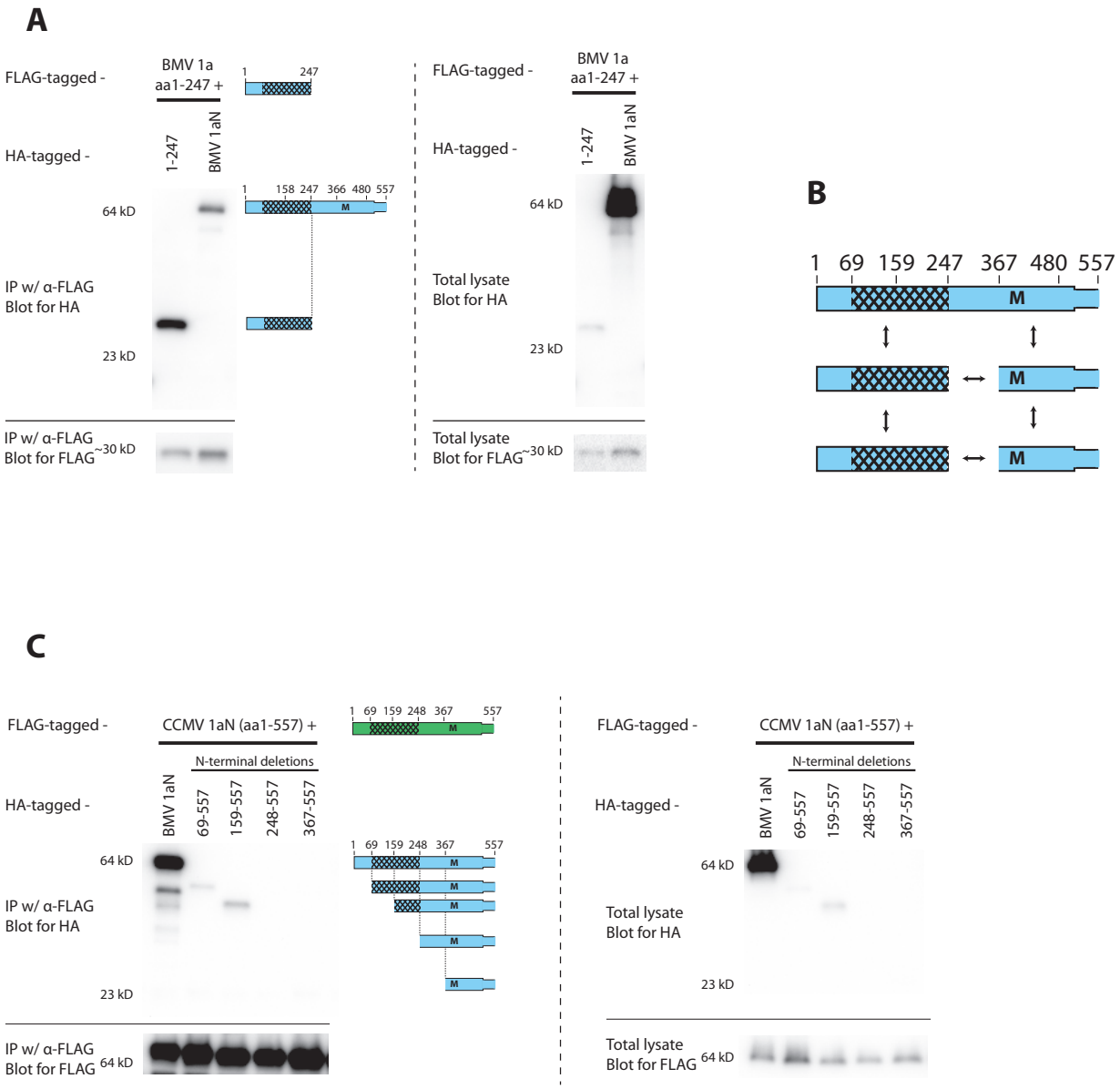

Figure 4.4. BMV 1aN contains at least two self-interacting regions. (A) C-terminally FLAG-tagged BMV aa1-247 co-immunoprecipitates HA-tagged aa1-247 and BMV 1aN. (B) A schematic of BMV 1aN and the aa1-247 and aa367-557 fragments with arrows indicating interactions detected by co-immunoprecipitation assays (this figure and figures 2 and 3). (C) The ability of HA-tagged BMV 1aN and fragments of BMV 1aN to interact with FLAG-tagged CCMV 1aN was tested by co-immunoprecipitation.

readily detectable positive- and negative- strand RNA synthesis (Fig. 4.5B). B/CC 2 and B/CC 4 both contain substitutions in the highly conserved core of the methyltransferase domain and retained the highest levels of RNA replication. B/CC 8 and B/CC 9 both supported low, but detectable levels of RNA replication despite a high number of introduced mutations due to their presence in a region of low primary sequence conservation at the end of the N-terminal domain. No RNA replication was detected for the other five hybrids.

To investigate at which steps of RNA replication the hybrids failed, we examined BMV RNA3 accumulation in the presence of the hybrids. Recruitment of the RNA to the replication complex is an essential early step of RNA replication. In yeast, BMV 1a recruits BMV RNA3 to a membrane-associated, nuclease-resistant state that increases RNA3 accumulation even in the absence of 2a polymerase. As expected, all of the hybrids that supported RNA replication (Fig. 4.5B) increased accumulation of RNA3 (Fig. 4.5C). Notably, B/CC 4 induced more RNA3 accumulation than B/CC 2 despite supporting lower levels of RNA replication, suggesting that B/CC 4 has a defect in 1a function after RNA recruitment and at or before negative-strand RNA synthesis. B/CC 7 also significantly increased RNA accumulation despite the absence of any negative strand synthesis indicating at defect at a similar stage (Fig. 4.5B,C).

Hybrid 1a proteins B/CC 3 and B/CC 7 have aberrant localization

Failure to properly assemble the membrane-associated RNA replication compartment would be one possible explanation for the failure of the non-functional BMV/CCMV 1a hybrids to recruit and stimulate accumulation of BMV RNA3. To investigate this possibility, we examined the localization of the 1a hybrids, as an essential first step of replication complex assembly, by immunofluorescence and confocal microscopy (Fig. 4.6A). Wildtype BMV 1a localizes to the perinuclear ER, as determined by colocalization with the endogenous luminal ER protein Pdi1p. With the exception of B/CC 3 and B/CC 7, the remaining hybrids all localized to the perinuclear ER in a manner similar to wildtype 1a. B/CC 3 formed a punctate structure that was perinuclear, but not significantly colocalized with Pdi1p. A significant portion of B/CC 7 was localized to the perinuclear ER, coincident with Pdi1p. However, a significant portion of B/CC 7 also localized to clusters in the cytoplasm not observed in wildtype 1a or any of the other hybrids.

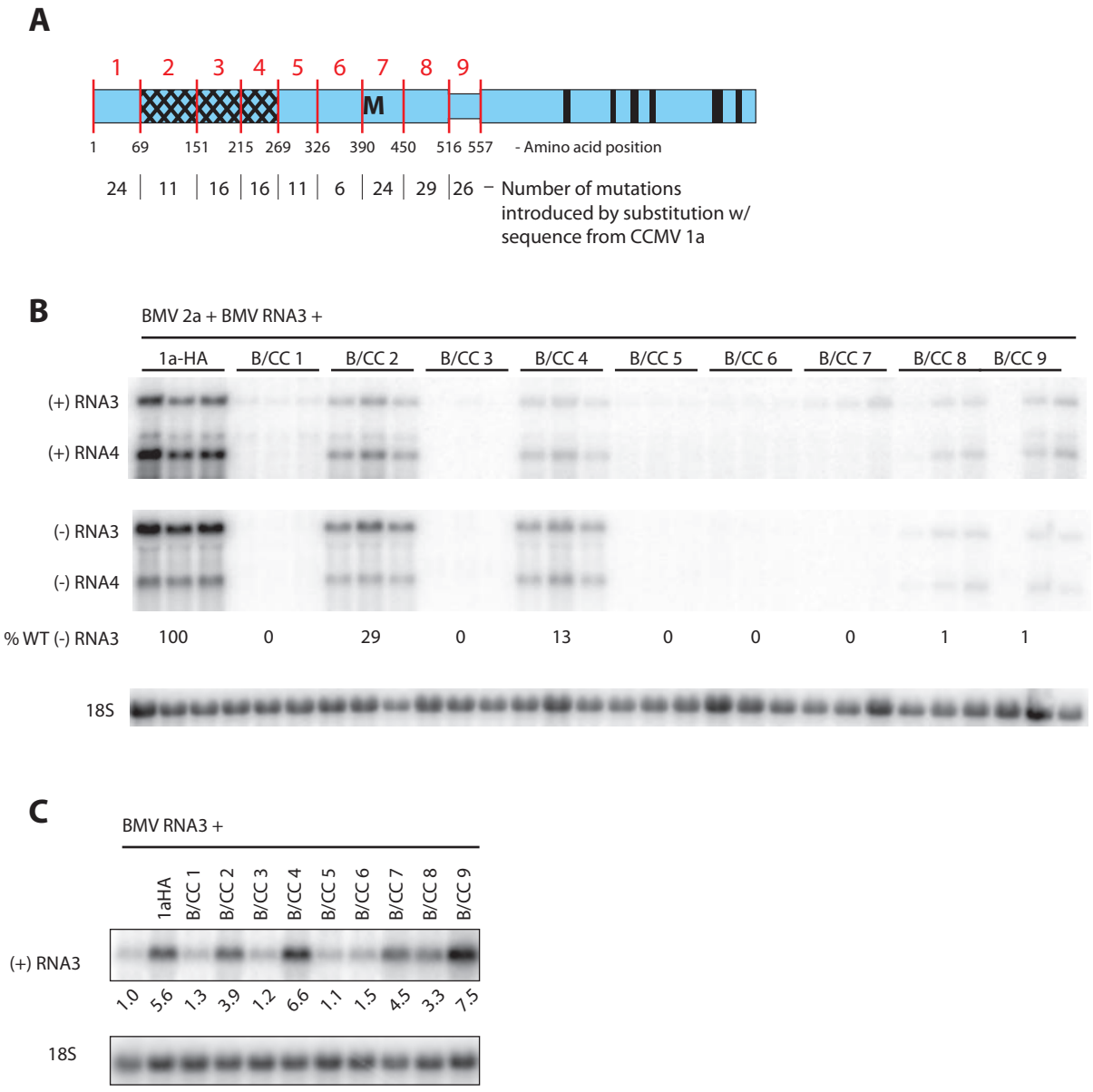

Figure 4.5. Substitution of BMV 1a sequences in several regions with the corresponding sequence from CCMV 1a abolishes RNA replication . (A) Schematic of BMV 1a. BMV 1aN was divided into 9 segments based upon predicted secondary structure and homology to CCMV. The boundaries of each region are indicated beneath the diagram using aa positions from BMV 1a. Each segment was individually replaced within BMV 1a by the corresponding sequence from CCMV. These constructs are referred to as 'B/CC #' with # indicating the substituted region. (B) BMV 1a-HA or HA-tagged B/CC hybrids were expressed in yeast along with BMV 2a and a replicatable BMV RNA3 template. Total RNA was isolated and analyzed by northen blotting. The presence of (+)RNA4 and (-)RNA3/4 requires 1a/2a dependent RNA replication. 18S RNA was probed for as a loading control. (C) Northern blotting analysis of BMV RNA3 accumulation in yeast expressing BMV 1a-HA or the B/CC chimeric proteins.

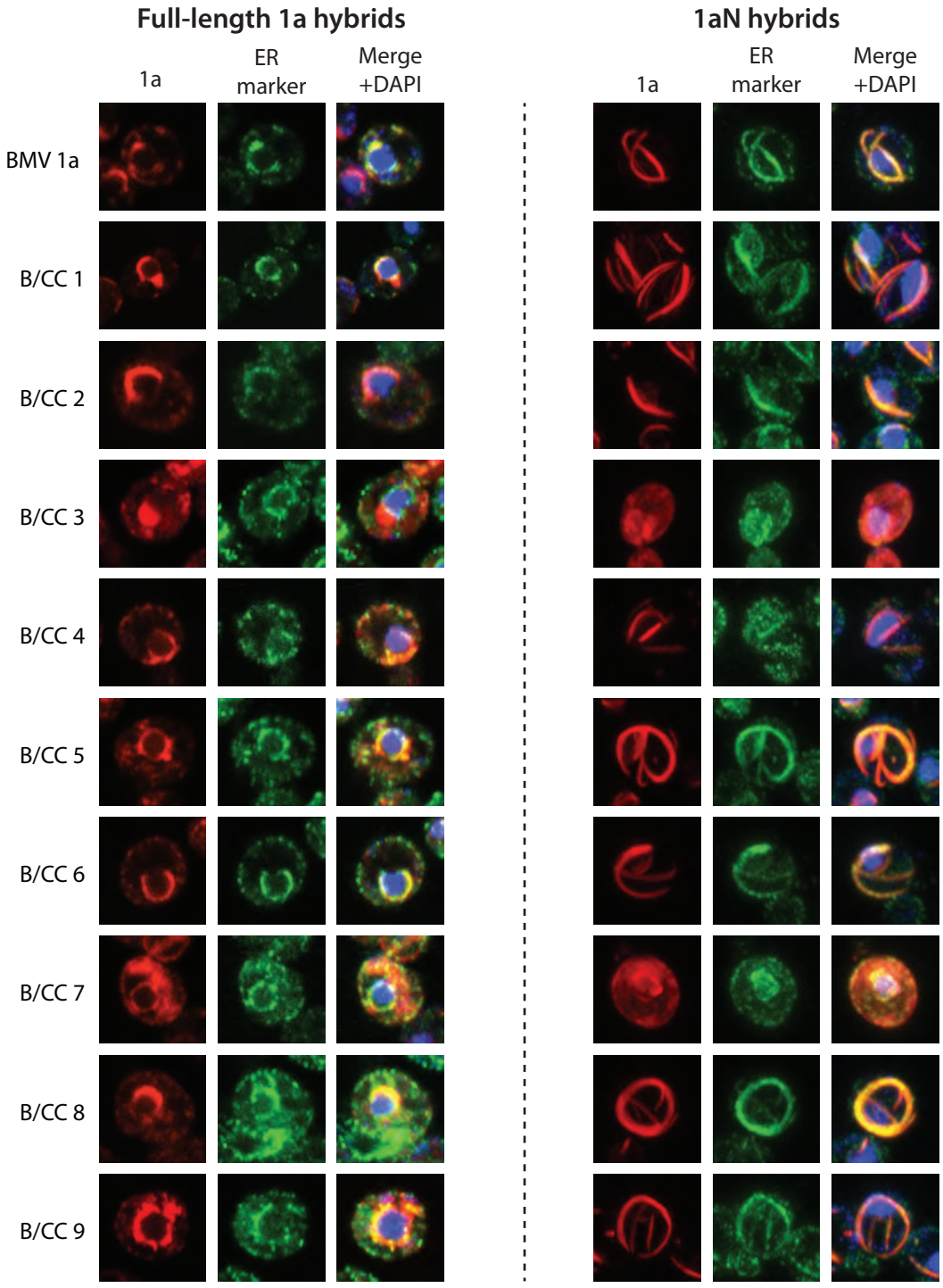

Figure 4.6. Substitution of BMV 1a regions 3 & 7 with corresponding CCMV sequence disrupts 1a and 1aN localization. Confocal microscopy was used to determine the localization of the B/CC hybrid 1a proteins and B/CC hybrid 1aN fragments. BMV 1a and fragments (red) were detected using an antibody raised against the BMV 1a N-terminal region. An antibody detecting endogenous yeast Pdi1p was used as a marker for the endoplasmic reticulum (green). DAPI was used to stain DNA as a nuclear marker (blue).

As mentioned previously, when BMV 1aN is expressed in cells, it assembles into long protein tubules whose underlying assembly interactions appear critical for RNA replication [45]. By immunofluorescence the tubules appear as well defined filaments, colocalized with ER makers, that often extend from the perinuclear region into the cytoplasm (Fig. 4.6B). To determine if any of the hybrids disrupted interactions essential for 1aN tubule assembly we checked the localization of the corresponding hybrid 1aN fragments. As with full-length 1a, only B/CC 7 and B/CC 3 had aberrant localization relative to wildtype. The other hybrids all displayed an ER-associated filament-like localization. B/CC 3 and 7 hybrids localized at least partially to the perinuclear ER, however there was a significant diffuse cytoplasmic localization and they lacked the hallmark sharp filament appearance of wildtype 1aN.

Hybrid 1a B/CC 3 fails to induce membrane rearrangements

In plants and yeast, BMV 1a induces spherules along the endoplasmic reticulum. When the 2a polymerase is expressed to high levels in yeast, BMV 1a induces an alternate replication complex ultrastructure consisting of a single or multiple layers of ER membrane evenly spaced approximately 70-80 nm from the perinuclear ER. These membrane layers support RNA replication to levels equivalent to that supported by spherules and are more easily visualized by electron microscopy [68]. Therefore, to initially test for the ability to induce membrane rearrangement, we checked the 1a hybrids for their ability to induce these membrane layers. Formation of membrane layers, as opposed to spherules, when 2a is overexpressed also indicates interaction between 1a and the 2a polymerase. Appressed ER membrane layering was induced by all of the hybrids except for B/CC 3 (Fig. 4.7), for which we saw no 1a-dependent membrane rearrangements. This indicates that hybrids 1,5, and 6 are able to induce RNA replication-linked membrane rearrangements, but fail to support RNA replication at or before the step of recruiting RNA. The BMV N-terminal domain has no known direct role in RNA recruitment, although the exact mechanism of RNA recognition and recruitment remains unknown. Potential mechanisms of failure for these hybrids are discussed later in this paper.

Consistent with its ability to stimulate RNA3 accumulation (Fig. 4.5C), we observed membrane layer formation by B/CC 7 (Fig. 4.7) though B/CC 7 1aN did not induce extended

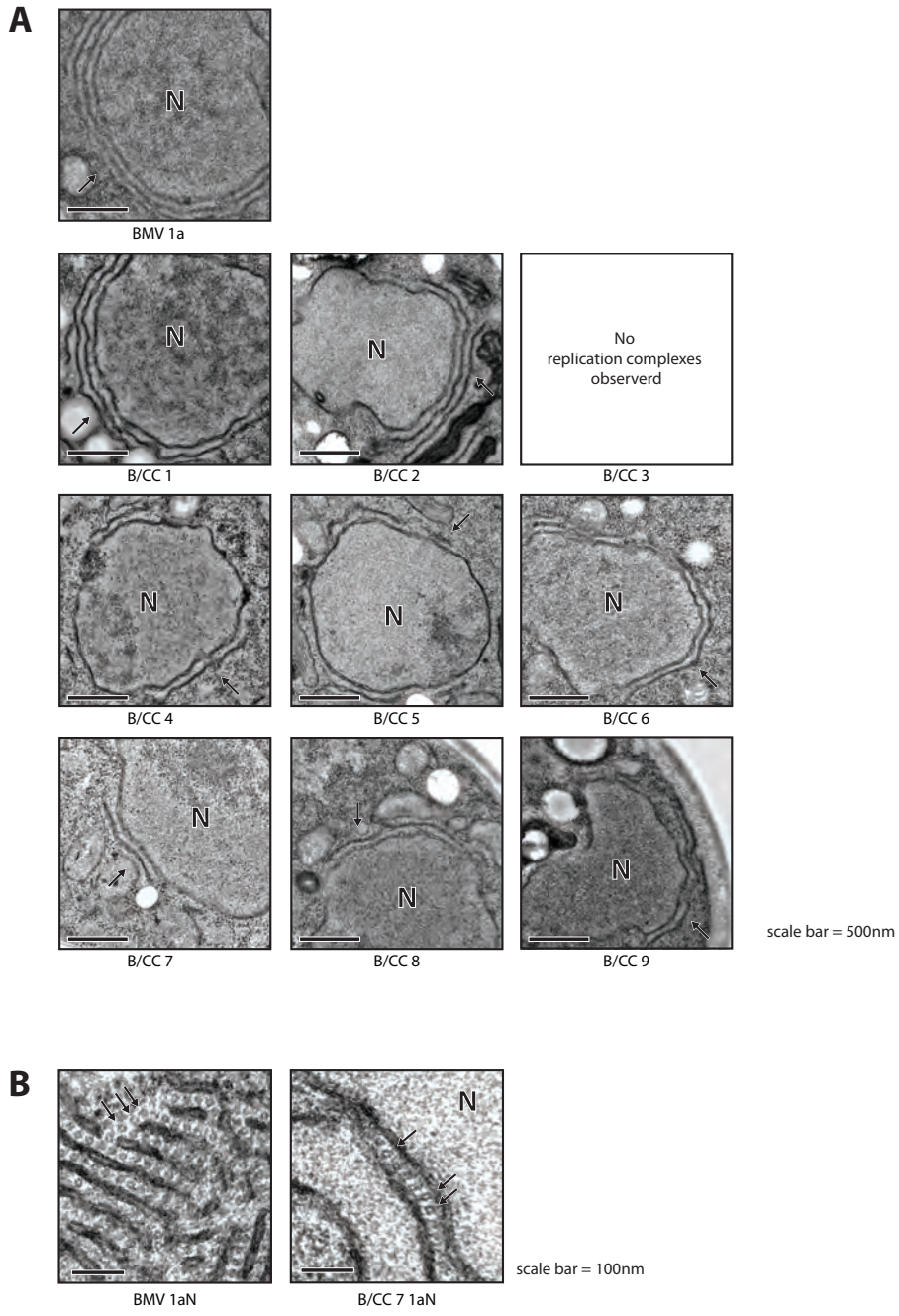

Figure 4.7. Hybrid 1a protein B/CC 3 does not induce membrane layer replication complexes along the yeast endoplasmic reticulum. (A) Yeast expressing BMV 2a, BMV RNA3, and BMV 1a or the indicated B/CC hybrid 1a protein were chemically fixed and embedded for electron microscopy. Representative electron micrographs are shown. Wildtype BMV 1a and all of the hybrid proteins except B/CC 3 induced membrane layers along the endoplasmic reticulum that are known to be 1a dependent and the site of RNA replication. In each image the nucleus is marked with 'N', an arrow points to the 1a-dependent membrane layers, and a 500 nm scale bar is shown in the lower left corner. (B) Electron micrographs of yeast expressing BMV 1aN and B/CC 7 1aN. Arrows indicate 1aN protein tubules. A 100 nm scale bar is shown in the corner.

detectable filaments by immunofluorescence (Fig. 4.6). To better understand the relation between the self-interactions responsible for 1aN filament formation and the self-interactions required for replication compartment assembly and RNA replication by full-length 1a, we used electron microscopy to determine more stringently if B/CC 7 induced any 1aN protein tubules. By this approach, we were able to find protein tubules in yeast expressing B/CC 7 1aN (Fig. 4.7B), although at a significantly lower frequency than wildtype 1aN. Consistent with the immunofluorescence (Fig. 4.6) for the B/CC7 1a hybrid, we did not observe any protein tubules extending away from the nucleus or large arrays of tubules as we routinely do for wildtype 1aN. In contrast, we were not able to identify any tubules or membrane rearrangements in yeast expressing B/CC 3 1aN (data not shown).

Localization of B/CC 3 1aN can be restored by additional substitution with CCMV 1a sequence in a distal region

We have previously shown that CCMV 1a and 1aN localize to the yeast ER in the same manner as BMV 1a and 1aN and that CCMV 1a+2a can support RNA replication in yeast [Chapter 3, this work]. Thus, all segments of CCMV 1a are functionally competent for localization and function in yeast if presented in a compatible sequence context. Therefore, we hypothesized that we may be able to restore B/CC 3 and B/CC 7 1aN localization by substitution of additional regions with CCMV 1a sequence. To this end, we first expanded the region of substitution around B/CC 3 and B/CC 7 to include adjacent regions. A 1aN hybrid with simultaneous substitution of regions 1-5 colocalized with Pdi1p, but did not appear to form the characteristic filaments of wildtype 1aN. Such ER-associated filaments were formed by a 1aN hybrid with simultaneous substitution of regions 5-9 (Fig. 4.8B, data not shown). Expansion of the B/CC 7 substitution (aa390-449) to include aa385-474 (B/CC 7+) 'rescued' the 1aN localization defect induced by substitution of B/CC 7 alone, resulting in wildtype-like 1aN localization (Fig. 4.8A).

We generated a hybrid substituting both B/CC 3 and B/CC 7 simultaneously to test if they could complement each other, however they did not (Fig. 4.8B, data not shown). Interestingly, the expanded substitution of region B/CC 7+, did complement substitution of B/CC 3 and restored wildtype-like 1aN localization (B/CC 3,7+ , Fig. 4.8A). A diagram of several

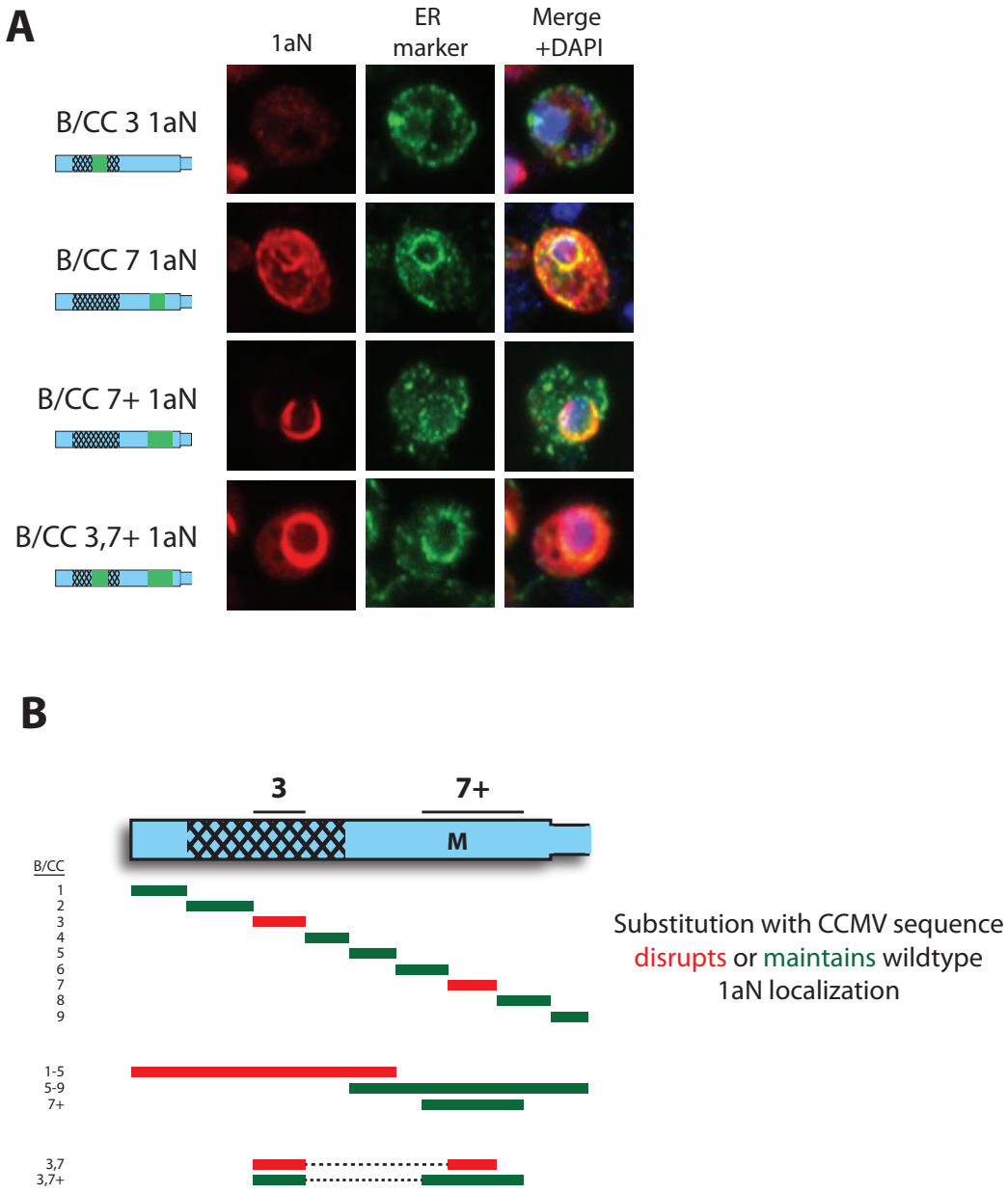

Figure 4.8. Co-substitution of region 3 and 7+ in BMV 1aN with sequence from CCMV restores 1aN localization. (A) Immunofluorescence (IF) of BMV 1aN containing regions substituted with the corresponding sequence of CCMV 1aN. (B) Diagram of 1aN hybrids whose localization has been determined by IF. The position and length of the bar represents the sequence replaced with CCMV sequence. Green bars indicate a sharp, filament-like ER associated signal similar to wildtype BMV 1aN (as in B/CC 7+ and 3,7+ in (A)); red bars indicate the absence of this phenotype (as in B/CC 3 or 7 in (A)). See figure 6 for more images.

1aN hybrids that we tested by immunofluorescence microscopy and their results is shown in figure 8B.

Restoration of 1aN localization for B/CC 3 and 7 is not sufficient to restore RNA replication

We are ultimately interested in how 1a interactions contribute to RNA replication in the context of full length 1a, so we generated full-length 1a expression constructs with substitution of B/CC 7+ and B/CC 3,7+ to test for their ability to recruit and replicate BMV RNA3. To test RNA replication we used an RNA3 construct in which the coat protein translated from the subgenomic RNA4 is replaced with a *Renilla* luciferase reporter. The resulting luciferase activity is a sensitive reporter for the amount of (+)RNA4 generated by RNA replication.

B/CC 7+ did induce slightly increased RNA3 accumulation compared to B/CC 7 (Fig. 4.9A), however it did not significantly increase RNA replication (Fig. 4.10B). B/CC 3,7+ retained the same level of RNA3 accumulation as B/CC 3, significantly lower than wildtype 1a or B/CC 7+ (Fig. 4.9A) and only 9% of wildtype replication (Fig. 4.9B). This indicates the both regions have functions for RNA replication other than the required compatibility for 1aN localization.

Mutation of BMV 1a near a highly conserved motif in the methyltransferase domain abolishes 1aN localization and RNA replication

Hybrid B/CC 3 contains sixteen mutations from wildtype BMV 1a. Since expanding the local region of substitution surrounding B/CC 3 did not restore 1aN localization, we split the region into three smaller sub-regions, 3a, 3b, and 3c (Fig. 4.10A) in an attempt to indentify the specific amino acid changes responsible for the loss of 1a function. Substituting either 3a or 3c did not disrupt 1aN localization, mapping this phenotype to the five amino acids mutated in 3b. We also generated the smaller hybrids in the context of full-length 1a to test their ability to support RNA replication. Although 3a and 3c 1aN localized as wildtype, neither 1a hybrid supported wildtype levels of RNA replication. Thus, while for sub-region B/CC 3c in particular, restoring 1aN localization correlated with restoring RNA replication, additional functions or interactions required for wildtype levels of RNA replication must be inhibited by mutations in region 3a and 3c.

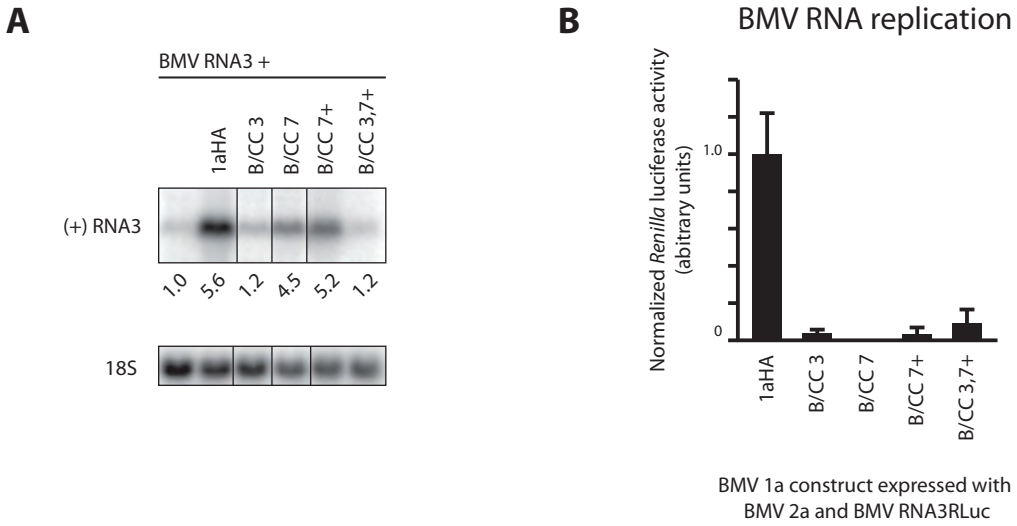

Figure 4.9. Substitution of region 7+ with CCMV sequence in B/CC 3 and B/CC 7 fails to restore RNA replication. (A) Northern blotting analysis of BMV RNA3 accumulation in yeast expressing BMV RNA3 alone, BMV 1a-HA or the B/CC chimeric proteins indicated. (B) Yeast were transfected with the 1a construct shown, BMV 2a, and a BMV RNA3 template that expresses *Renilla* luciferase from the subgenomic RNA4. The *Renilla* luciferase activity is normalized to constitutively expressed firefly luciferase activity to account for any differences introduced during cell harvesting or lysing.

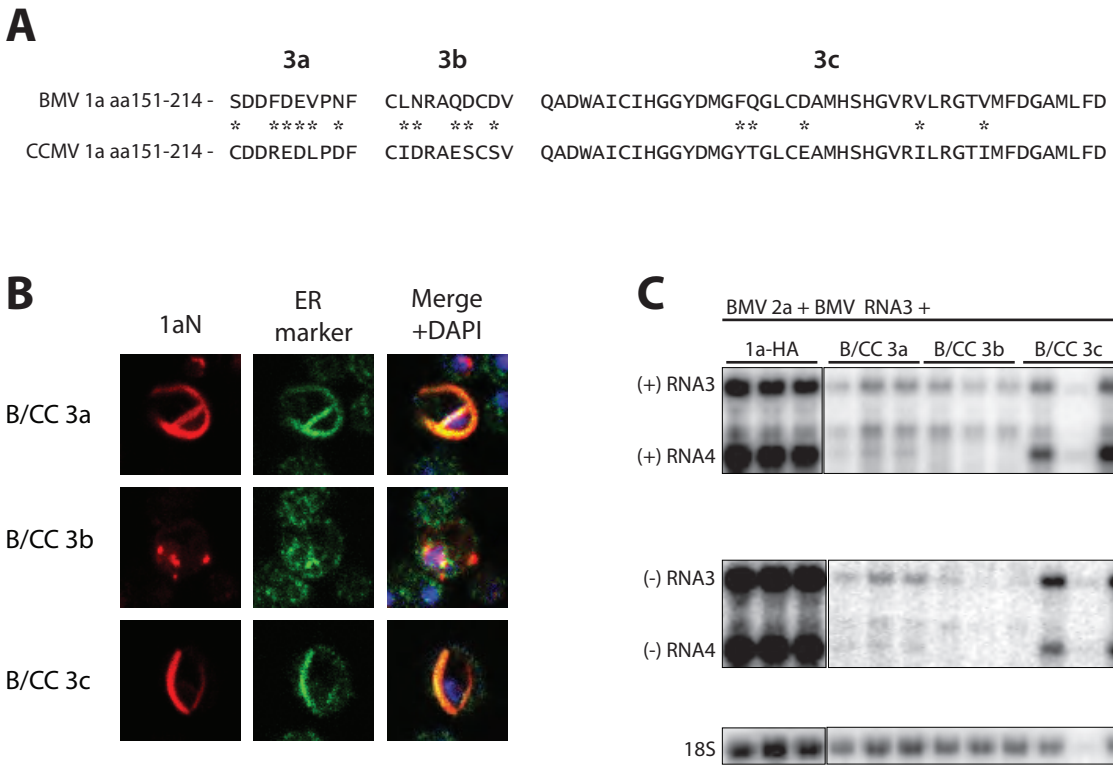

Figure 4.10. Mutation of five amino acids in BMV 1a abolishes 1aN filament formation and inhibits RNA replication. (A) Amino acid sequence of BMV and CCMV 1a in B/CC region 3. Mutations introduced by substitution of CCMV sequence into BMV 1a are indicated with asterisks. Region 3 was subdivided into three sections as shown and hybrid 1a and 1aN proteins with substitutions in these regions were constructed. (B) Localization of hybrid BMV 1aN fragments was determined by confocal microscopy. (C) Northern blots to test the level of RNA replication supported by BMV 1a and the hybrid 1a proteins indicated. Gel has been cropped for presentation;1a-HA lanes are from the same gel and blot and presented at the same exposure as the B/CC lanes. (D) Section of a sequence logo covering BMV aa160-170 generated by the SAM-T08 server from an input of BMV 1a aa1-410. Height of each letter indicates conservation of that amino acid at the given position among 1a homologs.

No RNA synthesis was detected in yeast expressing B/CC 3b. Region 3b contains one of the most highly conserved motifs among the Semliki forest-like alphavirus superfamily (excludes members of *Tymovirales*) [152]. Figure 10D shows a sequence logo from a multiple sequence alignment with BMV 1a aa1-410 [153]. This logo was generated by aligning sequences from over 150 diverse plant, insect, animal, and human viruses including tobacco mosaic virus, chikungunya virus, and hepatitis E virus. The letters above the X-axis are the most prevalent amino acids at that position and the height of the letter corresponds to its conservation.

DISCUSSION

Membrane-associated replication complexes are the central and essential machinery of (+)RNA virus RNA replication. Despite the variation in architecture and membranes utilized among different various, there is evidence that replication complex assembly may rely on conserved principles and mechanisms [125]. Thus, disruption of replication complex assembly could be a promising specific or broad spectrum antiviral target. For example, the anti-hepatitis C virus drug Daclatasvir inhibits assembly of the viral replication complex [70]. Endogenous membrane proteins responsible for shaping membranes often function as multimers. Similarly, many viral proteins critical for replication complex membrane rearrangements have been shown to multimerize or interact with other viral proteins in ways essential for RNA replication. Better understanding of how viral RNA replication proteins target and rearrange host membranes and how such proteins multimerize would bolster our ability to discover inhibitors of this process. Accordingly, to better understand how such oligomerization contributes to replication complex assembly, we have further mapped and characterized interactions within the BMV 1a protein, which is responsible for BMV replication complex assembly and studied the contributions of the implicated regions to RNA replication.

We examined interactions within the N-terminal domain of BMV 1a, which is sufficient for membrane localization, association, and oligomerization. We show that 1aN contains multiple self-interactions through at least two separate regions (Fig. 4.4B). We identified widely separated 1aN regions highly conserved within the alphavirus-like superfamily that are essential for RNA replication and that require genetic compatibility with each other for 1aN

localization. We also identified multiple BMV/CCMV hybrids that could form RNA replication-linked membrane rearrangements, but failed to induce RNA accumulation, implying an important role or roles for the N-terminal domain in recruiting viral RNAs to the replication complex.

BMV 1aN contains multiple, potentially competitive, sites of self-interaction

Although the BMV 1aN domain is not expressed naturally during BMV infection, it is homologous to alphavirus nsP1 which is cleaved from the viral nsP123/4 polyprotein during infection. BMV 1a localizes to and forms replication complexes on the ER and 1aN forms membrane-associated protein tubules associated with the ER. Alphavirus replication complexes are initially formed on the plasmid membrane. Interestingly, filament-like extensions have been observed along the plasmid membrane in cells infected with the alphavirus SFV and in cells expressing only nsP1 [137, 154]. Immunofluorescence microscopy revealed that the filaments contain nsP1, but not action or microtubules. Thus the ability to participate in assembly of both membrane vesicles and membrane-associated filaments is conserved between BMV 1a and SFV nsP1. Consistent with this conservation, multiple results indicate that the filament-forming interactions of BMV 1aN are essential for formation and function of the spherule RNA replication compartments [45]. Given the significant predicted secondary structure and functional conservation between BMV 1aN, SFV nsP1, and proteins across the alphavirus-like superfamily, the corresponding multimerizing interactions and their involvement in RNA replication complex assembly may also be broadly conserved.

We indentified two fragments of BMV 1aN, aa1-247 and aa367-557, capable of self-interaction in co-IP assays. Self-interaction indicates a role of these regions in intermolecular interaction. The two regions were also able to interact with each other which could represent an inter- or intra- molecular interaction. Interestingly, aa1-247 did not pull down with 1aN, although 1aN was precipitated with aa1-247. When aa1-247 was used as the bait the self-interaction band was stronger than the band for 1aN, despite 1aN being present at much higher levels in the total lysate. The aa1-247 fragment may compete poorly in trans- against the 1aN-

1aN interactions that are also occurring. The small pool of aa1-247-1aN interactions would be missed if the immunoprecipitation of the highly expressed 1aN was not 100% efficient.

Though these results enhance our understanding of 1aN interactions, the aa1-247 and aa367-557 fragments are still quite large and may contain multiple interactions within themselves. For example, the homo- and hetero- typic interactions of these two fragments could be directly competitive or may occur simultaneously through different sites within the fragments. We were unable to detect expression at any level for several smaller fragments that we attempted to express. Additionally, it was not feasible to test all possible combinations of interactions, for example we did not test the interaction of any internal fragments such as aa159-367. It is likely that the interactions of 1aN are even more complex than presented here. Future experiments may require novel approaches such as mutational analysis or fusion proteins, although these techniques present their own challenges.

BMV/CCMV hybrid 1a proteins are inhibited for RNA replication at multiple different steps

As a further approach to map and illuminate 1a interactions and 1a functions, we generated hybrid proteins between the similar BMV and CCMV 1a proteins. None of the hybrids supported wildtype levels of replication and several were inhibited at different stages of replication which should prove valuable for future studies of 1a function. Of the hybrids that supported RNA replication, the ratio of negative-strand to positive-strand RNA was similar to that of wildtype 1a, so there was no defect specific to positive-strand synthesis. A defect in capping activity would also be expected to have less (+)RNA as it would be more rapidly degraded in the cytoplasm. The defect in B/CC 2 may be primarily in RNA recruitment as it induced less RNA3 accumulation than the other replicating hybrids, but retained the highest level of RNA replication. Mutants B/CC 1, 5, and 6 all failed to recruit RNA, thus additional defects at later stages cannot be ruled out.

Recruitment of RNA3 to the replication complex depends on the presence of a functional cis-acting element in the RNA, 1a helicase activity, and replication complex assembly. Several mutations in the 1aN domain have been previously reported to effect RNA template recruitment, although the specific mechanistic contributions of this domain to recruiting RNA

remain unknown. BMV 1a RNA-capping activity is not required for RNA recruitment. In fact, two mutations that abolish methyltransferase activity, L52P and H80A, increase 1a-dependent BMV RNA3 accumulation above the levels induced by wildtype 1a [121]. Mutations of the membrane-associating amphipathic helix that do not disrupt membrane-association, but decrease interaction with the 2a polymerase and alter 1a-induced membrane rearrangements, also increase 1a-dependent RNA accumulation above wildtype levels [82]. The N-terminal domain could be involved in recognition of the RNA, conformational changes, or host factor interaction necessary for recruitment.

CCMV 1a supports replication of BMV RNA3 in plants [129], but has a yeast specific defect in recruiting BMV RNA3 (Chapter 3, this work). Further investigation of these hybrids may shed light on the contributions of both the 1a N-terminal domain and host factors essential for recruiting RNA.

B/CC 7 induced RNA accumulation, but no detectable RNA synthesis. Though the partial localization defects of B/CC 7 were restored by additional substitution of the surrounding regions and RNA accumulation was increased, RNA replication was not. Thus, the region has compatibility requirements beyond that required for replication complex assembly that may include interaction with the 2a polymerase or C-terminal domain of the protein.

Distal regions in BMV 1a require compatibility for proper membrane localization

Of all the BMV/CCMV hybrids only B/CC 3 abolished replication complex assembly and 1aN protein tubule formation. We were able to further narrow down the mutations responsible for loss of 1aN tubule formation to just five amino acids located near a highly conserved C-X(6)-C motif in the 1a methyltransferase domain. The exact role of these cysteines is unknown, although they have been shown to be important for methyltransferase and guanylyltransferase activity in SFV [155], are potentially involved in disulfide-linkage in tomato mosaic virus [156], and are essential for RNA replication in alfalfa mosaic virus [157] and BMV [96]. Cysteines in intracellular proteins rarely form disulfide bonds and are more often involved in binding metals, such as zinc, or as active site nucleophiles. Zinc fingers can contribute to the stability of a protein domain and can be involved in protein-protein interactions [158]. Decreased stability

and loss of protein-protein interactions could explain the loss of protein localization of the B/CC 3 chimera. There is no evidence that the cysteines of the C-X(6)-C motif play a direct role in the methyltransferase active site. Consistent with this, viruses in the *Tymovirales* branch of the alphavirus-like superfamily do not contain the C-X(6)-C motif. However, it is possible that the tymoviruses have adapted to use a different active site nucleophile.

Since B/CC 3 retains the conserved cysteines, our data shows that the context of the cysteines is also important. Substitution of the amino acids in region 3a and 3c surrounding the cysteine motif retained 1aN filament assembly and RNA replication, but the level of RNA replication was significantly lower than wildtype showing that as for region 7, restoration of 1aN interactions is not sufficient for RNA replication and the region is likely involved in other interactions or steps of RNA replication. Similarly, only 1aN localization of B/CC 3, but not RNA recruitment or replication, was complemented by additional substitution surrounding region 7.

B/CC 7 contains a known membrane-associating helix in BMV 1a. The homologous region in many related viruses including the plant cucumoviruses is predicted to contain a membrane-binding amphipathic helix. The alphaviruses also have a predicted helix at this position which contains the proven membrane-binding palmitoylated cysteine motif [81]. BMV 1aN protein tubule assembly and alphavirus nsP1 plasma membrane extensions depend on membrane-association of the amphipathic helix or cysteine palmitoylation in this region respectively [45, 110]. The requirement for compatibility between B/CC 3 and B/CC 7 may represent a requirement for compatibility between these two conserved functional motifs.

Overall, these studies have revealed two separated regions within the N-terminal domain of BMV 1a that are capable of self-interaction and interaction with each other. Within these regions we found that genetic compatibility between highly conserved motifs is essential for 1a localization, but that the regions have additional roles in supporting RNA replication as well. This work provides a foundation future studies of 1a interaction and hints at the possibility of conserved interactions within the alphavirus-like superfamily. Additionally, through the generation of BMV/CCMV hybrid proteins we've identified several 1a mutants that

fail to support replication at distinct steps that will be useful in dissecting the mechanism of 1a functions.

MATERIALS AND METHODS

Yeast and Plasmids

Culture and growth conditions for *S. cerevisiae* strain YPH500 were as described previously [31, 93]. Yeast were harvested at mid-log phase for all experiments. Tagged variations of BMV and CCMV 1a proteins and fragments were generated using standard molecular cloning techniques. All FLAG-tagged (DYKDDDDK) constructs for co-immunoprecipitation experiments were cloned into the PacI and BamHI sites of pB1YT3 [121] replacing the BMV 1a ORF; similarly, HA-tagged (YPYDVPDYA) constructs were cloned into the PacI and BamHI sites of pB1YT3L [45]. Chimeric B/CC proteins were generated using three-step overlap-extension PCR. All full-length chimeric proteins have a C-terminal HA-tag. All 1aN chimeric fragments have a C-terminal FLAG-tag. All clones were verified by sequencing.

Co-immunoprecipitation assays

Harvested yeast were resuspended in 50µl RIPA buffer (1% NP-40, 0.1% SDS, 0.5% sodium deoxycholate, 150mM NaCl, 50mM Tris pH 8.0, 5mM EDTA, 10mM NaF, 10mM NaPPi) with 50 µl of glass beads and lysed in a bead beater. RIPA buffer was added to 1 ml and the tubes were rotated for one hour; insoluble debris was pelleted by centrifugation at 14,000 rpm for 20 minutes. A 50µl aliquot of the supernatant was removed at this time as total lysate. Magnetic protein G dynabeads (Thermo Fisher) and the desired antibody were added to 700µl of supernatant. Samples were rotated for three hours prior to removal of the supernatant and washing with RIPA buffer via magnetic separation of the beads. Proteins were eluted from the beads by incubation at 50°C for 20 minutes in 50µl 1x SDS loading buffer. Mouse and rabbit antibodies against the FLAG and HA epitopes were purchased from Sigma (anti-HA clone HA-7, anti-FLAG clone M2, F7425, H6908). Mouse antibodies were used for immunoprecipitations and rabbit antibodies were used for detection by western blotting.

Electron and confocal microscopy

Electron microscopy was preformed as described for chemically fixed samples in Chapter 3 and elsewhere [17]. Confocal microscopy was done as described in Chapter 3. Monoclonal antibody against endogenous Pdi1p as an ER marker (clone 38H8) was purchased from ThermoFisher. All images are average projections of multiple adjacent confocal image planes.

RNA analysis

Northern blotting and luciferase assays were done as described in Chapter 3.

CHAPTER 5

Summary and future directions

Positive-strand RNA ((+)RNA) viruses are an important concern for human health, as highlighted by pandemic outbreaks in recent years. The development of antivirals, particularly broad spectrum antivirals, would bolster our ability to rapidly respond to pandemics and provide treatment where vaccines are unsuitable or unavailable. The replication of RNA in association with rearranged host membranes is conserved among all (+)RNA viruses and is essential for the intracellular lifecycle of (+)RNA viruses (For review see [124, 159]). For these reasons, disrupting formation of the replication complex is an attractive target for drug development. Previous studies of brome mosaic virus (BMV) have led to significant and substantial contributions to our understanding of viral RNA replication and replication complex assembly. In this thesis, we have expanded on those prior studies with a particular focus on BMV RNA replication protein 1a-membrane and 1a-1a interactions. This chapter reviews the main conclusions from these studies and outlines the major conceptual challenges and technical opportunities posed by this new foundation of results.

In chapter two we showed that a fraction of BMV 1a retains strong membrane association even after deletion of the proven membrane-associating amphipathic helix, helix A. Deletions and mutations at positions throughout the N-terminal domain disrupt 1a localization and membrane association. Appropriate membrane association of 1a likely depends on concerted action or appropriate conformation of the entire domain, as opposed to any single functional subdomain. In chapter three, we demonstrated that like BMV 1a, cowpea chlorotic mottle virus (CCMV) 1a is sufficient to induce perinuclear membrane rearrangements in the absence of other viral factors. Moreover, expression of CCMV 1aN in vivo assembles into ER-associated protein tubules identical to those formed by BMV 1aN. Our further demonstration that CCMV 1a+2a are capable of supporting RNA replication in yeast establishes an additional system to study conserved features of (+)RNA viruses. In chapter four, we showed that BMV 1aN contains multiple regions, involving conserved domains of the protein, that are capable of

homo- and hetero- typic interactions. Additionally, we identify an essential requirement for genetic compatibility between a highly conserved domain in the methyltransferase region of 1a and a distal region including helix A. These results expand our knowledge of how BMV 1a induces membrane rearrangements and provides strong foundations for future studies of replication complex assembly in BMV and related viruses, including the clinically important alphaviruses.

BMV 1a protein membrane association

BMV 1a is known to associate with membrane in part through an amphipathic helix, helix A, that inserts into the membrane [82]. Our work in chapter 2 shows that other regions within the N-terminal domain of 1a also have strong contributions to 1a membrane association. The exact mechanisms of helix A independent membrane association and their contributions to 1a function remain unknown. Alignment of BMV 1a with homologous proteins from the alpha-like virus superfamily suggests that BMV may contain at least two membrane-associating helixes in addition to helix A [81]. These include a predicted amphipathic helix immediately C-terminal of helix A and a putative amphipathic helix near the end of the methyltransferase core domain. BMV 1a fragments containing the region near the methyltransferase core domain did not demonstrate significant membrane association in gain-of-function experiments [112]. However, the homologous region in alphaviruses was shown to require multiple copies of the helix for membrane association in similar gain-of-function experiments [111]. Further analysis of the contributions of these newly predicted regions to membrane interaction and RNA replication is a clear future direction for the investigation of BMV 1a membrane association.

The ability to analyze protein-lipid interactions in vitro has been extremely informative in the study of many membrane proteins, including the helix A fragment of BMV 1a. Biochemical purification of 1a for use in such studies and other purposes would be extremely valuable, though previous attempts have been unsuccessful. Semliki forest virus nsP1 protein expressed in *E. coli* and in vitro translation assays has been used to identify some of the lipid requirements for nsP1 membrane association and function [160]. Sindbis virus nsP1 has been successfully purified to homogeneity and was found not to require membrane association for

methyltransferase or guanylyltransferase activity. The ability and requirements of purified Sindbis virus nsP1 to bind membrane were not determined in the study [161]. NMR spectroscopy and/or amino acid modification experiments of purified nsP1 interacting with liposomes could be used to identify regions of the protein that interact with membranes. Titration of lipid and nsP1 concentrations may provide some information regarding the cooperativity of membrane binding.

Recruiting RNA to the replication complex

For (+)RNA viruses, the infecting RNA must serve first as a template for translating RNA replication proteins and then as the initial template for genomic replication. The timing of this switch represents a crucial point during infection, as the virus must balance sufficient protein production against initiating RNA replication quickly. Currently, the mechanism of recruiting viral RNA from translation to the RNA replication complex is an important unanswered question. It is well established that recruitment of BMV RNA requires 1a NTPase activity and the presence of a functional recruitment element (RE) in the RNA [19, 84]. Since 1a NTPase activity may be linked to RNA helicase activity [84], this suggests that helicase-mediated RNA translocation may be involved. For BMV, it is unknown if the RNA is recruited concurrently or after formation of the replication complex. Additionally, although the Lsm1-7 proteins are known to be involved in recruitment [93], there may be other host contributions as well.

The defect in yeast in CCMV 1a recruitment of CCMV RNA3 relative to BMV 1a recruitment of BMV RNA3 could be a useful tool to study this process further. Examination of viral functions in restrictive hosts has been productive in many cases. Hybrid BMV/CCMV RNA3 constructs have been studied for their ability to replicate in plants [98], but the hybrids that did not replicate may have failed at RNA synthesis steps following recruitment. Examination of these or similar constructs in yeast could be used to determine if the defect in CCMV RNA3 recruitment in yeast is due to the absence of positive. The most direct assay currently used for measuring recruitment of bromovirus RNA templates to the RNA replication complex is measuring the level of nuclease-resistant membrane associated RNAs. Increased accumulation of viral RNA in the absence of viral RNA-dependent RNA polymerase is well

correlated with template recruitment and provides a technically easier and more commonly used measurement. Both of these are endpoint assays and do not definitively demonstrate that the protected RNA is in fact localized to the replication complex. Thus, fully following RNA trafficking or RNA localization will require the development of new techniques.

Visualization of RNA is commonly achieved by the addition of multiple MS2 stemloops and the co-expression of a fluorescent MS2-fusion protein. This approach has been used to localize BMV RNAs in the absence of BMV 1a [162]. Such a construct could be problematic in localizing viral RNA to the replication complex if the MS2-fusion protein is excluded from the spherule interior or if the addition of multiple stable stemloops inhibits RNA recruitment. The Broccoli RNA aptamer is an alternative mechanism to visualize RNA localization that does not depend on the binding of a fluorescent protein to the RNA and allows for the addition of a smaller foreign sequence [163]. This engineered RNA sequence binds and greatly enhances the fluorescence of a cell-permeating small-molecule fluorophore allowing for the localization of RNA by immunofluorescence microscopy. Given the relatively small size of the RNA aptamer, Broccoli containing BMV RNA templates may serve as functional RNA replication templates. If so, this would allow us to follow RNA localization and recruitment to the ER during RNA replication in yeast and plants.

Determine the functional role of BMV induced membrane rearrangements

BMV RNA replication has been shown to occur in ~70-80 nm spherules by IEM of chemically fixed and dehydrated yeast [17]. In this work we examined yeast expressing BMV 1a by high pressure freezing and freeze substitution (HPF-FS), a technique that has allowed for visualizing membrane rearrangements poorly preserved by chemical fixation in EAV. We observed both a larger number of cells containing spherules and a larger number of spherules per cell compared to chemical fixation. In particular, we observed a large number of 30-40 nm spherules in addition to the larger ~70 nm spherules. A previous study of chemically fixed BMV infected barley cells also identified populations of 30-40 nm spherules in addition to 80-90 nm spherules [30]. The presence of these smaller spherules raises important questions regarding their source and function.

One possibility is that these smaller spherules are precursors to the larger spherules known to support RNA replication. Pulse-chase and immuno-EM experiments using BrUTP to label active RNA synthesis could be used to determine if synthesis was limited to spherules of a given size. Time course experiments examining the abundance and ratio of spherule sizes may be done, taking advantage of the tightly regulated, inducible yeast *GAL1* promoter. The spherule size of Semliki forest virus is dependent upon the size of the replicated template [34], suggesting spherule size may be more dynamic than previous models for BMV indicate. We are well poised to study this further in BMV, as BMV 1a+2a efficiently support the trans-replication of templates of a variety of sizes.

Alternatively, the smaller spherules may represent a dead-end membrane rearrangement incapable of assembling a functional replication complex. The reticulon homology domain (RHD) containing family of proteins is involved in the maintenance of tubular ER. Expression of BMV 1a relocalizes these proteins to sites of 1a accumulation on the perinuclear ER [65]. Deletion of individual RHD proteins results in reduced average diameter of BMV spherules and decreased RNA replication. If host RHD proteins, or a similarly acting host factor, are limiting relative to BMV 1a abundance, excess 1a may induce this population of smaller spherules. In this case, one might expect an increase in smaller spherules at late time points following 1a expression in contrast to the precursor model. The relative abundance of specific lipid species may also be a limiting factor effecting spherule size and functional replication complex assembly. Deletion of acyl-coA-binding protein results in smaller BMV spherules, while deletion of phosphatidylethanolamine N-methyltransferase increased the average spherule diameter [62, 136]. Deletion of either reduced the level of RNA replication.

Tomato bushy stunt virus (TBSV), like BMV, is a well-studied (+)RNA plant virus that supports RNA replication in yeast [164]. As for BMV, a number of studies have found that deleting host membrane shaping or lipid synthesis proteins alters the function and membrane ultrastructure of TBSV replication complexes [63, 165]. It has been proposed that TBSV uses the depletion of essential host proteins and lipids as a sensor to regulate procession through the various stages of viral replication [166].

Finally, the 30 nm BMV spherules may be functionally equivalent to the 80 nm spherules. The interior of the 30 nm spherule would still provide enough space for viral replication proteins and a genomic template. The average diameter of Semliki forest virus spherules induced by replication of a 3 kB template, the approximate size of BMV genomic RNAs, was 42 nm [34]. Natural variations in the local density of 1a or host factors could result in a range of spherule sizes that are similarly functional for RNA replication. In support of such a possibility, overexpression of the BMV 2a polymerase results in a drastically different membrane ultrastructure that supports normal levels of RNA replication [68].

Advanced light and electron microscopy

Though HPF-FS is considered to introduce less artifacts than chemical fixation and dehydration of samples for EM, there is considerable variability in the preservation of certain features depending upon the fixative, resin, and substitution protocol. For example, the addition of 2-5% water to the substitution media is essential for the preservation of BMV replication complex membranes, but other cellular membranes are preserved in the absence of water (this work, data not shown). Regardless of the fixation method, the visualization of resin embedded samples requires heavy metal staining either en bloc, post-sectioning, or both. Again, the choice and timing of metal stains can have a significant impact on the ability to resolve structures of interest. Heavy metal stains provide excellent sample contrast, but mask true cellular densities limiting the potential resolution.

Cryo-electron microscopy is an alternative to resin embedded EM that allows for the visualization of stain free samples preserved in an aqueous state . In cryo-EM the sample is grown on or transferred to an EM grid that is subsequently plunge frozen in liquid ethane to preserve the sample in a thin layer of vitreous ice. The sample is then maintained at liquid nitrogen temperatures throughout imaging, including while in the microscope column through use of a specialized liquid nitrogen chilled holder. The sample must be very thin, <~500 nm, to prevent excessive damage from electron scattering. In some circumstances, events along the plasma membrane can be visualized in whole cells if the edge of the cell is sufficiently flat. In many instances, the object of interest must be isolated from cells or the sample must cryo-

sectioned. Cryo-EM of FHV replication complexes using isolated mitochondria has revealed structures in the interior and at the spherule neck not observed in fixed sections [167]. We have been able to successfully cryo-section and observe HPF yeast pellets by cryo-EM. The next step will be to examine cells expressing BMV 1a and BMV 1a+2a+RNA3.

Correlative light/electron microscopy can be used to identify cells with high levels of RNA replication, e.g. by using RNA templates encoding fluorescent reporters. Correlative microscopy can also be used to localize specific proteins to structures observed in EM. Newer super resolution light microscopy techniques allow for resolution below the diffraction limit. Structured illumination microscopy can achieve resolutions around 100 nm in XY. Photoactivated localization microscopy and stimulated emission depletion microscopy techniques can provide resolution <30 nm [168]. These resolutions may be sufficient to determine if proteins are localized solely to the spherule neck or throughout the spherule. Such approaches could also determine if 1a or other proteins of interest are present on areas of the ER with no replication complexes. It has been hypothesized that the ESCRT and RHD containing proteins, which are required for BMV spherule formation, may be localized to the neck [65, 75]. Models of BMV and alphavirus spherules with the polymerase localized predominantly at the spherule neck, rather than throughout the interior, have been proposed as well. Functional fluorescently tagged versions of the 2a polymerase, RHDs, and ESCRT proteins have been identified that would be suitable for super resolution microscopy. Previous attempts to fluorescently tag BMV 1a protein have all resulted in substantially reduced function and many disrupt 1a localization. Small tags in the proline-rich linker region (i.e. FLAG, 1.0 kDa) do not inhibit 1a function, but larger tags (One-STrEP-3xFLAG, 5.9 kDa) in this region do (Sibert, Nishikiori, unpublished results). There may be other internal sites that would allow for larger protein tags that could be useful in such super-resolution approaches to help resolve this critical question of 1a localization.

Final Conclusions

All together, we have identified multiple 1a-1a interactions within the 1a N-terminal domain. Our data suggests these interactions are well conserved across bromoviruses and potentially

across much of the alphavirus-like superfamily and that 1a-1a interaction and 1a membrane-association are likely closely intertwined. This is consistent with models of RNA replication complex assembly that require extensive multimerization of membrane-associated 1a for membrane rearrangement. Thus, while further study is needed, we have identified candidate regions for interaction that can be tested in the clinically relevant alphaviruses. Such studies may reveal a broadly conserved protein ultrastructure and assembly mechanism for RNA replication complex assembly within the diverse alphavirus-like superfamily.

REFERENCES

1. Murray, C.J.L., et al., *Disability-adjusted life years (DALYs) for 291 diseases and injuries in 21 regions, 1990-2010: a systematic analysis for the Global Burden of Disease Study 2010 (vol 380, pg 2197, 2012).* Lancet, 2013. **381**(9867): p. 628-628.

2. Parkin, D.M., *The global health burden of infection -associated cancers in the year 2002.* International Journal of Cancer, 2006. **118**(12): p. 3030-3044.

3. Minor, P.D., *Live attenuated vaccines: Historical successes and current challenges.* Virology, 2015. **479-480**: p. 379-92.

4. Treanor, J.J., et al., *Efficacy and safety of the oral neuraminidase inhibitor oseltamivir in treating acute influenza - A randomized controlled trial.* Jama-Journal of the American Medical Association, 2000. **283**(8): p. 1016-1024.

5. Beaucourt, S. and M. Vignuzzi, *Ribavirin: a drug active against many viruses with multiple effects on virus replication and propagation. Molecular basis of ribavirin resistance.* Curr Opin Virol, 2014. **8**: p. 10-5.

6. Thompson, M.A., et al., *Antiretroviral Treatment of Adult HIV Infection 2012 Recommendations of the International Antiviral Society-USA Panel.* Jama-Journal of the American Medical Association, 2012. **308**(4): p. 387-402.

7. Afdhal, N., et al., *Ledipasvir and Sofosbuvir for Untreated HCV Genotype 1 Infection.* New England Journal of Medicine, 2014. **370**(20): p. 1889-1898.

8. Miller, W.A. and L. Rasochova, *Barley yellow dwarf viruses.* Annu Rev Phytopathol, 1997. **35**: p. 167-190.

9. Knight-Jones, T.J.D. and J. Rushton, *The economic impacts of foot and mouth disease - What are they, how big are they and where do they occur?* Preventive Veterinary Medicine, 2013. **112**(3-4): p. 161-173.

10. Holtkamp, D.J., et al. *Economic Impact of Porcine Reproductive and Respiratory Syndrome Virus on U.S. Pork Producers*. Animal Industry Reports, 2012. **AS 658**.

11. Kraemer, M.U.G., et al., *The global distribution of the arbovirus vectors Aedes aegypti and Ae. albopictus.* eLife, 2015.

12. Romero-Brey, I. and R. Bartenschlager, *Membranous replication factories induced by plus-strand RNA viruses.* Viruses, 2014. **6**(7): p. 2826-57.

13. Knoops, K., et al., *SARS-coronavirus replication is supported by a reticulovesicular network of modified endoplasmic reticulum.* PLoS Biol, 2008. **6**(9): p. e226.

14. Welsch, S., et al., *Composition and three-dimensional architecture of the dengue virus replication and assembly sites.* Cell Host Microbe, 2009. **5**(4): p. 365-75.

15. Fogg, M.H., N.L. Teterina, and E. Ehrenfeld, *Membrane requirements for uridylylation of the poliovirus VPg protein and viral RNA synthesis in vitro.* J Virol, 2003. **77**(21): p. 11408-16.

16. Sethna, P.B. and D.A. Brian, *Coronavirus genomic and subgenomic minus-strand RNAs copartition in membrane-protected replication complexes.* J Virol, 1997. **71**(10): p. 7744-9.

17. Schwartz, M., et al., *A positive-strand RNA virus replication complex parallels form and function of retrovirus capsids.* Mol Cell, 2002. **9**(3): p. 505-14.

18. Miyanari, Y., et al., *Hepatitis C virus non-structural proteins in the probable membranous compartment function in viral genome replication.* J Biol Chem, 2003. **278**(50): p. 50301-8.

19. Sullivan, M.L. and P. Ahlquist, *A brome mosaic virus intergenic RNA3 replication signal functions with viral replication protein 1a to dramatically stabilize RNA in vivo.* J Virol, 1999. **73**(4): p. 2622-32.

20. Aizaki, H., et al., *Characterization of the hepatitis C virus RNA replication complex associated with lipid rafts.* Virology, 2004. **324**(2): p. 450-61.

21. Geiss, B.J., T.C. Pierson, and M.S. Diamond, *Actively replicating West Nile virus is resistant to cytoplasmic delivery of siRNA.* Virol J, 2005. **2**: p. 53.

22. Venter, P.A. and A. Schneemann, *Assembly of two independent populations of flock house virus particles with distinct RNA packaging characteristics in the same cell.* J Virol, 2007. **81**(2): p. 613-9.

23. Gamarnik, A.V. and R. Andino, *Switch from translation to RNA replication in a positive-stranded RNA virus.* Genes Dev, 1998. **12**(15): p. 2293-304.

24. Lanman, J., et al., *Visualizing flock house virus infection in Drosophila cells with correlated fluorescence and electron microscopy.* J Struct Biol, 2008. **161**(3): p. 439-46.

25. Kopek, B.G., et al., *Three-dimensional analysis of a viral RNA replication complex reveals a virus-induced mini-organelle.* PLoS Biol, 2007. **5**(9): p. e220.

26. Kujala, P., et al., *Biogenesis of the Semliki Forest virus RNA replication complex.* J Virol, 2001. **75**(8): p. 3873-84.

27. Kim, K.S., *Ultrastructural-Study of Inclusions and Disease Development in Plant-Cells Infected by Cowpea Chlorotic Mottle Virus.* Journal of General Virology, 1977. **35**(Jun): p. 535-543.

28. Martelli, G.P. and M. Russo, *Virus-Host Relationships*, in *The Plant Viruses*, R.I.B. Francki, Editor 1985, Springer US. p. 163-205.

29. Burgess, J., F. Motoyoshi, and E.N. Fleming, *Structural changes accompanying infection of tobacco protoplasts with two spherical viruses.* Planta, 1974. **117**(2): p. 133-44.

30. Diaz, A., *Formation, structure, and organization of the RNA replication compartments of brome mosaic virus*, 2009, University of Wisconsin-Madison. p. 166.

31. Janda, M. and P. Ahlquist, *RNA-dependent replication, transcription, and persistence of brome mosaic virus RNA replicons in S. cerevisiae.* Cell, 1993. **72**(6): p. 961-70.

32. Nagy, P.D. and J. Pogany, *The dependence of viral RNA replication on co-opted host factors.* Nature Reviews Microbiology, 2012. **10**(2): p. 137-149.

33. Quinkert, D., R. Bartenschlager, and V. Lohmann, *Quantitative analysis of the hepatitis C virus replication complex.* J Virol, 2005. **79**(21): p. 13594-13605.

34. Kallio, K., et al., *Template RNA length determines the size of replication complex spherules for Semliki Forest virus.* J Virol, 2013. **87**(16): p. 9125-34.

35. Frolova, E.I., et al., *Functional Sindbis virus replicative complexes are formed at the plasma membrane.* J Virol, 2010. **84**(22): p. 11679-95.

36. Gillespie, L.K., et al., *The endoplasmic reticulum provides the membrane platform for biogenesis of the flavivirus replication complex.* J Virol, 2010. **84**(20): p. 10438-47.

37. McCartney, A.W., et al., *Localization of the tomato bushy stunt virus replication protein p33 reveals a peroxisome-to-endoplasmic reticulum sorting pathway.* Plant Cell, 2005. **17**(12): p. 3513-3531.

38. Cao, X.L., et al., *Morphogenesis of Endoplasmic Reticulum Membrane-Invaginated Vesicles during Beet Black Scorch Virus Infection: Role of Auxiliary Replication Protein and New Implications of Three-Dimensional Architecture.* J Virol, 2015. **89**(12): p. 6184-6195.

39. Bienz, K., et al., *Structural and functional characterization of the poliovirus replication complex.* J Virol, 1992. **66**(5): p. 2740-7.

40. Suhy, D.A., T.H. Giddings, Jr., and K. Kirkegaard, *Remodeling the endoplasmic reticulum by poliovirus infection and by individual viral proteins: an autophagy-like origin for virus-induced vesicles.* J Virol, 2000. **74**(19): p. 8953-65.

41. Belov, G.A., et al., *Complex dynamic development of poliovirus membranous replication complexes.* J Virol, 2012. **86**(1): p. 302-12.

42. Snijder, E.J., et al., *Ultrastructure and origin of membrane vesicles associated with the severe acute respiratory syndrome coronavirus replication complex.* J Virol, 2006. **80**(12): p. 5927-40.

43. Knoops, K., et al., *Ultrastructural characterization of arterivirus replication structures: reshaping the endoplasmic reticulum to accommodate viral RNA synthesis.* J Virol, 2012. **86**(5): p. 2474-87.

44. O'Reilly, E.K., J.D. Paul, and C.C. Kao, *Analysis of the interaction of viral RNA replication proteins by using the yeast two-hybrid assay.* J Virol, 1997. **71**(10): p. 7526-32.

45. Diaz, A., A. Gallei, and P. Ahlquist, *Bromovirus RNA replication compartment formation requires concerted action of 1a's self-interacting RNA capping and helicase domains.* J Virol, 2012. **86**(2): p. 821-34.

46. Gosert, R., et al., *Identification of the hepatitis C virus RNA replication complex in Huh-7 cells harboring subgenomic replicons.* J Virol, 2003. **77**(9): p. 5487-5492.

47. Paul, D., et al., *NS4B Self-Interaction through Conserved C-Terminal Elements Is Required for the Establishment of Functional Hepatitis C Virus Replication Complexes.* J Virol, 2011. **85**(14): p. 6963-6976.

48. Cho, M.W., et al., *Membrane Rearrangement and Vesicle Induction by Recombinant Poliovirus 2c and 2bc in Human-Cells.* Virology, 1994. **202**(1): p. 129-145.

49. Teterina, N.L., et al., *Evidence for functional protein interactions required for poliovirus RNA replication.* J Virol, 2006. **80**(11): p. 5327-5337.

50. Dye, B.T., D.J. Miller, and P. Ahlquist, *In vivo self-interaction of Nodavirus RNA replicase protein A revealed by fluorescence resonance energy transfer.* J Virol, 2005. **79**(14): p. 8909-8919.

51. Kopek, B.G., et al., *Nodavirus-induced membrane rearrangement in replication complex assembly requires replicase protein a, RNA templates, and polymerase activity.* J Virol, 2010. **84**(24): p. 12492-503.

52. Spuul, P., et al., *Assembly of alphavirus replication complexes from RNA and protein components in a novel trans-replication system in mammalian cells.* J Virol, 2011. **85**(10): p. 4739-51.

53. Carette, J.E., et al., *Cowpea mosaic virus infection induces a massive proliferation of endoplasmic reticulum but not Golgi membranes and is dependent on de novo membrane synthesis.* J Virol, 2000. **74**(14): p. 6556-63.

54. Perez, L., R. Guinea, and L. Carrasco, *Synthesis of Semliki Forest virus RNA requires continuous lipid synthesis.* Virology, 1991. **183**(1): p. 74-82.

55. Chuang, C., et al., *Inactivation of the host lipin gene accelerates RNA virus replication through viral exploitation of the expanded endoplasmic reticulum membrane.* PLoS Pathog, 2014. **10**(2): p. e1003944.

56. Berger, K.L., et al., *Hepatitis C virus stimulates the phosphatidylinositol 4-kinase III alpha-dependent phosphatidylinositol 4-phosphate production that is essential for its replication.* J Virol, 2011. **85**(17): p. 8870-83.

57. Heaton, N.S., et al., *Dengue virus nonstructural protein 3 redistributes fatty acid synthase to sites of viral replication and increases cellular fatty acid synthesis.* Proc Natl Acad Sci U S A, 2010. **107**(40): p. 17345-50.

58. Lee, W.M. and P. Ahlquist, *Membrane synthesis, specific lipid requirements, and localized lipid composition changes associated with a positive-strand RNA virus RNA replication protein.* J Virol, 2003. **77**(23): p. 12819-28.

59. Cherry, S., et al., *COPI activity coupled with fatty acid biosynthesis is required for viral replication.* PLoS Pathog, 2006. **2**(10): p. e102.

60. Moradpour, D., F. Penin, and C.M. Rice, *Replication of hepatitis C virus.* Nat Rev Microbiol, 2007. **5**(6): p. 453-63.

61. Lee, W.M., M. Ishikawa, and P. Ahlquist, *Mutation of host delta9 fatty acid desaturase inhibits brome mosaic virus RNA replication between template recognition and RNA synthesis.* J Virol, 2001. **75**(5): p. 2097-106.

62. Zhang, J., et al., *Host acyl coenzyme A binding protein regulates replication complex assembly and activity of a positive-strand RNA virus.* J Virol, 2012. **86**(9): p. 5110-21.

63. Barajas, D., Y. Jiang, and P.D. Nagy, *A unique role for the host ESCRT proteins in replication of Tomato bushy stunt virus.* PLoS Pathog, 2009. **5**(12): p. e1000705.

64. Tang, W.F., et al., *Reticulon 3 binds the 2C protein of enterovirus 71 and is required for viral replication.* J Biol Chem, 2007. **282**(8): p. 5888-98.

65. Diaz, A. and P. Ahlquist, *Role of host reticulon proteins in rearranging membranes for positive-strand RNA virus replication.* Curr Opin Microbiol, 2012. **15**(4): p. 519-24.

66. Rust, R.C., et al., *Cellular COPII proteins are involved in production of the vesicles that form the poliovirus replication complex.* J Virol, 2001. **75**(20): p. 9808-18.

67. Romero-Brey, I., et al., *Three-dimensional architecture and biogenesis of membrane structures associated with hepatitis C virus replication.* PLoS Pathog, 2012. **8**(12): p. e1003056.

68. Schwartz, M., et al., *Alternate, virus-induced membrane rearrangements support positive-strand RNA virus genome replication.* Proc Natl Acad Sci U S A, 2004. **101**(31): p. 11263-8.

69. Diaz, A., X. Wang, and P. Ahlquist, *Membrane-shaping host reticulon proteins play crucial roles in viral RNA replication compartment formation and function.* Proc Natl Acad Sci U S A, 2010. **107**(37): p. 16291-6.

70. Berger, C., et al., *Daclatasvir-like inhibitors of NS5A block early biogenesis of hepatitis C virus-induced membranous replication factories, independent of RNA replication.* Gastroenterology, 2014. **147**(5): p. 1094-105 e25.

71. Ahlquist, P., *Parallels among positive-strand RNA viruses, reverse-transcribing viruses and double-stranded RNA viruses.* Nature Reviews Microbiology, 2006. **4**(5): p. 371-82.

72. Briggs, J.A., et al., *Structure and assembly of immature HIV.* Proc Natl Acad Sci U S A, 2009. **106**(27): p. 11090-5.

73. Ono, A., et al., *Phosphatidylinositol (4,5) bisphosphate regulates HIV-1 Gag targeting to the plasma membrane.* Proc Natl Acad Sci U S A, 2004. **101**(41): p. 14889-94.

74. Stuchell, M.D., et al., *The human endosomal sorting complex required for transport (ESCRT-I) and its role in HIV-1 budding.* J Biol Chem, 2004. **279**(34): p. 36059-71.

75. Diaz, A., et al., *Host ESCRT Proteins Are Required for Bromovirus RNA Replication Compartment Assembly and Function.* PLoS Pathog, 2015. **11**(3): p. e1004742.

76. Ahlquist, P., *Bromovirus RNA replication and transcription.* Curr Opin Genet Dev, 1992. **2**(1): p. 71-6.

77. Wierzchoslawski, R., et al., *Characterization of a novel 5′ subgenomic RNA3a derived from RNA3 of Brome mosaic bromovirus.* J Virol, 2006. **80**(24): p. 12357-66.

78. Chaturvedi, S. and A.L. Rao, *Live cell imaging of interactions between replicase and capsid protein of Brome mosaic virus using Bimolecular Fluorescence Complementation: implications for replication and genome packaging.* Virology, 2014. **464-465**: p. 67-75.

79. Dohi, K., et al., *Brome mosaic virus replicase proteins localize with the movement protein at infection-specific cytoplasmic inclusions in infected barley leaf cells.* Arch Virol, 2001. **146**(8): p. 1607-15.

80. Ahola, T. and P. Ahlquist, *Putative RNA capping activities encoded by brome mosaic virus: methylation and covalent binding of guanylate by replicase protein 1a.* J Virol, 1999. **73**(12): p. 10061-9.

81. Ahola, T. and D.G. Karlin, *Sequence analysis reveals a conserved extension in the capping enzyme of the alphavirus supergroup, and a homologous domain in nodaviruses.* Biol Direct, 2015. **10**: p. 16.

82. Liu, L., et al., *An amphipathic alpha-helix controls multiple roles of brome mosaic virus protein 1a in RNA replication complex assembly and function.* PLoS Pathog, 2009. **5**(3): p. e1000351.

83. Ahlquist, P., et al., *Sindbis virus proteins nsP1 and nsP2 contain homology to nonstructural proteins from several RNA plant viruses.* J Virol, 1985. **53**(2): p. 536-42.

84. Wang, X., et al., *Brome mosaic virus 1a nucleoside triphosphatase/helicase domain plays crucial roles in recruiting RNA replication templates.* J Virol, 2005. **79**(21): p. 13747-58.

85. Dinant, S., et al., *Bromovirus RNA replication and transcription require compatibility between the polymerase- and helicase-like viral RNA synthesis proteins.* J Virol, 1993. **67**(12): p. 7181-9.

86. Ishikawa, M., et al., *In vivo DNA expression of functional brome mosaic virus RNA replicons in Saccharomyces cerevisiae.* J Virol, 1997. **71**(10): p. 7781-90.

87. Krol, M.A., et al., *RNA-controlled polymorphism in the in vivo assembly of 180-subunit and 120-subunit virions from a single capsid protein.* Proc Natl Acad Sci U S A, 1999. **96**(24): p. 13650-5.

88. Nagy, P.D., *Yeast as a model host to explore plant virus-host interactions.* Annu Rev Phytopathol, 2008. **46**: p. 217-42.

89. Kushner, D.B., et al., *Systematic, genome-wide identification of host genes affecting replication of a positive-strand RNA virus.* Proc Natl Acad Sci U S A, 2003. **100**(26): p. 15764-9.

90. Gancarz, B.L., et al., *Systematic identification of novel, essential host genes affecting bromovirus RNA replication.* PLoS One, 2011. **6**(8): p. e23988.

91. Yi, G., K. Gopinath, and C.C. Kao, *Selective repression of translation by the brome mosaic virus 1a RNA replication protein.* J Virol, 2007. **81**(4): p. 1601-9.

92. Janda, M. and P. Ahlquist, *Brome mosaic virus RNA replication protein 1a dramatically increases in vivo stability but not translation of viral genomic RNA3.* Proc Natl Acad Sci U S A, 1998. **95**(5): p. 2227-32.

93. Diez, J., et al., *Identification and characterization of a host protein required for efficient template selection in viral RNA replication.* Proc Natl Acad Sci U S A, 2000. **97**(8): p. 3913-8.

94. Chen, J., A. Noueiry, and P. Ahlquist, *Brome mosaic virus Protein 1a recruits viral RNA2 to RNA replication through a 5' proximal RNA2 signal.* J Virol, 2001. **75**(7): p. 3207-19.

95. Chen, J., A. Noueiry, and P. Ahlquist, *An alternate pathway for recruiting template RNA to the brome mosaic virus RNA replication complex.* J Virol, 2003. **77**(4): p. 2568-77.

96. Yi, G. and C. Kao, *cis- and trans-acting functions of brome mosaic virus protein 1a in genomic RNA1 replication.* J Virol, 2008. **82**(6): p. 3045-53.

97. Pacha, R.F., R.F. Allison, and P. Ahlquist, *cis-acting sequences required for in vivo amplification of genomic RNA3 are organized differently in related bromoviruses.* Virology, 1990. **174**(2): p. 436-43.

98. Pacha, R.F. and P. Ahlquist, *Use of bromovirus RNA3 hybrids to study template specificity in viral RNA amplification.* J Virol, 1991. **65**(7): p. 3693-703.

99. Mackenzie, J., *Wrapping things up about virus RNA replication.* Traffic, 2005. **6**(11): p. 967-77.

100. Allison, R., C. Thompson, and P. Ahlquist, *Regeneration of a functional RNA virus genome by recombination between deletion mutants and requirement for cowpea chlorotic mottle virus 3a and coat genes for systemic infection.* Proc Natl Acad Sci U S A, 1990. **87**(5): p. 1820-4.

101. Bamunusinghe, D., J.K. Seo, and A.L. Rao, *Subcellular localization and rearrangement of endoplasmic reticulum by Brome mosaic virus capsid protein.* J Virol, 2011. **85**(6): p. 2953-63.

102. Restrepo-Hartwig, M. and P. Ahlquist, *Brome mosaic virus RNA replication proteins 1a and 2a colocalize and 1a independently localizes on the yeast endoplasmic reticulum.* J Virol, 1999. **73**(12): p. 10303-9.

103. Difranco, A., M. Russo, and G.P. Martelli, *Ultrastructure and Origin of Cytoplasmic Multivesicular Bodies Induced by Carnation Italian Ringspot Virus.* Journal of General Virology, 1984. **65**(Jul): p. 1233-1237.

104. Mackenzie, J.M., M.K. Jones, and P.R. Young, *Immunolocalization of the dengue virus nonstructural glycoprotein NS1 suggests a role in viral RNA replication.* Virology, 1996. **220**(1): p. 232-40.

105. Magliano, D., et al., *Rubella virus replication complexes are virus-modified lysosomes.* Virology, 1998. **240**(1): p. 57-63.

106. Kim, M.J., H.R. Kim, and K.H. Paek, *Arabidopsis tonoplast proteins TIP1 and TIP2 interact with the cucumber mosaic virus 1a replication protein.* J Gen Virol, 2006. **87**(Pt 11): p. 3425-31.

107. Miller, D.J. and P. Ahlquist, *Flock house virus RNA polymerase is a transmembrane protein with amino-terminal sequences sufficient for mitochondrial localization and membrane insertion.* J Virol, 2002. **76**(19): p. 9856-67.

108. Egger, D., et al., *Expression of hepatitis C virus proteins induces distinct membrane alterations including a candidate viral replication complex.* J Virol, 2002. **76**(12): p. 5974-84.

109. Tsujimoto, Y., et al., *Arabidopsis TOBAMOVIRUS MULTIPLICATION (TOM) 2 locus encodes a transmembrane protein that interacts with TOM1.* EMBO J, 2003. **22**(2): p. 335-43.

110. Ahola, T., et al., *Effects of palmitoylation of replicase protein nsP1 on alphavirus infection.* J Virol, 2000. **74**(15): p. 6725-33.

111. Spuul, P., et al., *Role of the amphipathic peptide of Semliki forest virus replicase protein nsP1 in membrane association and virus replication.* J Virol, 2007. **81**(2): p. 872-83.

112. den Boon, J.A., J. Chen, and P. Ahlquist, *Identification of sequences in Brome mosaic virus replicase protein 1a that mediate association with endoplasmic reticulum membranes.* J Virol, 2001. **75**(24): p. 12370-81.

113. de Jong, A.S., et al., *Determinants for membrane association and permeabilization of the coxsackievirus 2B protein and the identification of the Golgi complex as the target organelle.* J Biol Chem, 2003. **278**(2): p. 1012-21.

114. Drozdetskiy, A., et al., *JPred4: a protein secondary structure prediction server.* Nucleic Acids Res, 2015. **43**(W1): p. W389-94.

115. O'Reilly, E.K., et al., *Interactions between the structural domains of the RNA replication proteins of plant-infecting RNA viruses.* J Virol, 1998. **72**(9): p. 7160-9.

116. Kroner, P.A., B.M. Young, and P. Ahlquist, *Analysis of the role of brome mosaic virus 1a protein domains in RNA replication, using linker insertion mutagenesis.* J Virol, 1990. **64**(12): p. 6110-20.

117. Gyuris, J., et al., *Cdi1, a human G1 and S phase protein phosphatase that associates with Cdk2.* Cell, 1993. **75**(4): p. 791-803.

118. Stapleford, K.A., D. Rapaport, and D.J. Miller, *Mitochondrion-enriched anionic phospholipids facilitate flock house virus RNA polymerase membrane association.* J Virol, 2009. **83**(9): p. 4498-507.

119. Dick, R.A., E. Kamynina, and V.M. Vogt, *Effect of multimerization on membrane association of Rous sarcoma virus and HIV-1 matrix domain proteins.* J Virol, 2013. **87**(24): p. 13598-608.

120. Chen, J. and P. Ahlquist, *Brome mosaic virus polymerase-like protein 2a is directed to the endoplasmic reticulum by helicase-like viral protein 1a.* J Virol, 2000. **74**(9): p. 4310-8.

121. Ahola, T., J.A. den Boon, and P. Ahlquist, *Helicase and capping enzyme active site mutations in brome mosaic virus protein 1a cause defects in template recruitment, negative-strand RNA synthesis, and viral RNA capping.* J Virol, 2000. **74**(19): p. 8803-11.

122. Restrepo-Hartwig, M.A. and P. Ahlquist, *Brome mosaic virus helicase- and polymerase-like proteins colocalize on the endoplasmic reticulum at sites of viral RNA synthesis.* J Virol, 1996. **70**(12): p. 8908-16.

123. Golemis, E.A., et al., *Interaction trap/two-hybrid system to identify interacting proteins.* Curr Protoc Cell Biol, 2001. **Chapter 17**: p. Unit 17 3.

124. den Boon, J.A., A. Diaz, and P. Ahlquist, *Cytoplasmic viral replication complexes.* Cell Host Microbe, 2010. **8**(1): p. 77-85.

125. Paul, D. and R. Bartenschlager, *Architecture and biogenesis of plus-strand RNA virus replication factories.* World J Virol, 2013. **2**(2): p. 32-48.

126. Spuul, P., et al., *Phosphatidylinositol 3-kinase-, actin-, and microtubule-dependent transport of Semliki Forest Virus replication complexes from the plasma membrane to modified lysosomes.* J Virol, 2010. **84**(15): p. 7543-57.

127. Mise, K., et al., *Bromovirus movement protein genes play a crucial role in host specificity.* J Virol, 1993. **67**(5): p. 2815-23.

128. Ding, X.S., et al., *Characterization of a Brome mosaic virus strain and its use as a vector for gene silencing in monocotyledonous hosts.* Mol Plant Microbe Interact, 2006. **19**(11): p. 1229-39.

129. Allison, R.F., M. Janda, and P. Ahlquist, *Infectious in vitro transcripts from cowpea chlorotic mottle virus cDNA clones and exchange of individual RNA components with brome mosaic virus.* J Virol, 1988. **62**(10): p. 3581-8.

130. Allison, R.F., M. Janda, and P. Ahlquist, *Sequence of cowpea chlorotic mottle virus RNAs 2 and 3 and evidence of a recombination event during bromovirus evolution.* Virology, 1989. **172**(1): p. 321-30.

131. Furusawa, I., *Infection with Bmv of Mesophyll Protoplasts Isolated from 5 Plant Species.* Journal of General Virology, 1978. **40**(Aug): p. 489-491.

132. Rakotondrafara, A.M., et al., *Preparation and electroporation of oat protoplasts from cell suspension culture.* Curr Protoc Microbiol, 2007. **Chapter 16**: p. Unit 16D 3.

133. Giddings, T.H., *Freeze-substitution protocols for improved visualization of membranes in high-pressure frozen samples.* J Microsc, 2003. **212**(Pt 1): p. 53-61.

134. Romero-Brey, I. and R. Bartenschlager, *Viral Infection at High Magnification: 3D Electron Microscopy Methods to Analyze the Architecture of Infected Cells.* Viruses, 2015. **7**(12): p. 6316-45.

135. French, R., M. Janda, and P. Ahlquist, *Bacterial gene inserted in an engineered RNA virus: efficient expression in monocotyledonous plant cells.* Science, 1986. **231**(4743): p. 1294-7.

136. Zhang, J., et al., *Positive-strand RNA viruses stimulate host phosphatidylcholine synthesis at viral replication sites.* Proc Natl Acad Sci U S A, 2016.

137. Laakkonen, P., et al., *Alphavirus replicase protein NSP1 induces filopodia and rearrangement of actin filaments.* J Virol, 1998. **72**(12): p. 10265-9.

138. Kiiver, K., et al., *Properties of non-structural protein 1 of Semliki Forest virus and its interference with virus replication.* J Gen Virol, 2008. **89**(Pt 6): p. 1457-66.

139. Quadt, R., et al., *Formation of brome mosaic virus RNA-dependent RNA polymerase in yeast requires coexpression of viral proteins and viral RNA.* Proc Natl Acad Sci U S A, 1995. **92**(11): p. 4892-6.

140. Pacha, R.F. and P. Ahlquist, *Substantial portions of the 5′ and intercistronic noncoding regions of cowpea chlorotic mottle virus RNA3 are dispensable for systemic infection but influence viral competitiveness and infection pathology.* Virology, 1992. **187**(1): p. 298-307.

141. Janda, M., R. French, and P. Ahlquist, *High efficiency T7 polymerase synthesis of infectious RNA from cloned brome mosaic virus cdna and effects of 5' extensions on transcript infectivity.* Virology, 1987. **158**(1): p. 259-62.

142. Leeds, P., et al., *The product of the yeast UPF1 gene is required for rapid turnover of mRNAs containing a premature translational termination codon.* Genes Dev, 1991. **5**(12A): p. 2303-14.

143. Grdzelishvili, V.Z., et al., *Mutual interference between genomic RNA replication and subgenomic mRNA transcription in brome mosaic virus.* J Virol, 2005. **79**(3): p. 1438-51.

144. French, R. and P. Ahlquist, *Intercistronic as well as terminal sequences are required for efficient amplification of brome mosaic virus RNA3.* J Virol, 1987. **61**(5): p. 1457-65.

145. Mastronarde, D.N., *Dual-axis tomography: an approach with alignment methods that preserve resolution.* J Struct Biol, 1997. **120**(3): p. 343-52.

146. Schindelin, J., et al., *Fiji: an open-source platform for biological-image analysis.* Nat Methods, 2012. **9**(7): p. 676-82.

147. Gorbalenya, A.E. and E.V. Koonin, *Viral proteins containing the purine NTP-binding sequence pattern.* Nucleic Acids Res, 1989. **17**(21): p. 8413-40.

148. Froshauer, S., J. Kartenbeck, and A. Helenius, *Alphavirus RNA replicase is located on the cytoplasmic surface of endosomes and lysosomes.* J Cell Biol, 1988. **107**(6 Pt 1): p. 2075-86.

149. Lim, P.J., et al., *Correlation between NS5A dimerization and hepatitis C virus replication.* J Biol Chem, 2012. **287**(36): p. 30861-73.

150. Choi, M., et al., *A hepatitis C virus NS4B inhibitor suppresses viral genome replication by disrupting NS4B's dimerization/multimerization as well as its interaction with NS5A.* Virus Genes, 2013. **47**(3): p. 395-407.

151. Goregaoker, S.P., D.J. Lewandowski, and J.N. Culver, *Identification and functional analysis of an interaction between domains of the 126/183-kDa replicase-associated proteins of tobacco mosaic virus.* Virology, 2001. **282**(2): p. 320-8.

152. Rozanov, M.N., E.V. Koonin, and A.E. Gorbalenya, *Conservation of the putative methyltransferase domain: a hallmark of the 'Sindbis-like' supergroup of positive-strand RNA viruses.* J Gen Virol, 1992. **73 (Pt 8)**: p. 2129-34.

153. Karplus, K., et al., *SAM-T04: what is new in protein-structure prediction for CASP6.* Proteins, 2005. **61 Suppl 7**: p. 135-42.

154. Laakkonen, P., T. Ahola, and L. Kaariainen, *The effects of palmitoylation on membrane association of Semliki forest virus RNA capping enzyme.* J Biol Chem, 1996. **271**(45): p. 28567-71.

155. Ahola, T., et al., *Critical residues of Semliki Forest virus RNA capping enzyme involved in methyltransferase and guanylyltransferase-like activities.* J Virol, 1997. **71**(1): p. 392-7.

156. Nishikiori, M., T. Meshi, and M. Ishikawa, *Guanylylation-competent replication proteins of Tomato mosaic virus are disulfide-linked.* Virology, 2012. **434**(1): p. 118-28.

157. Vlot, A.C., A. Menard, and J.F. Bol, *Role of the alfalfa mosaic virus methyltransferase-like domain in negative-strand RNA synthesis.* J Virol, 2002. **76**(22): p. 11321-8.

158. Krishna, S.S., I. Majumdar, and N.V. Grishin, *Structural classification of zinc fingers: survey and summary.* Nucleic Acids Res, 2003. **31**(2): p. 532-50.

159. Miller, S. and J. Krijnse-Locker, *Modification of intracellular membrane structures for virus replication.* Nature Reviews Microbiology, 2008. **6**(5): p. 363-74.

160. Ahola, T., et al., *Semliki Forest virus mRNA capping enzyme requires association with anionic membrane phospholipids for activity.* EMBO J, 1999. **18**(11): p. 3164-72.

161. Tomar, S., et al., *Heterologous production, purification and characterization of enzymatically active Sindbis virus nonstructural protein nsP1.* Protein Expr Purif, 2011. **79**(2): p. 277-84.

162. Beckham, C.J., et al., *Interactions between brome mosaic virus RNAs and cytoplasmic processing bodies.* J Virol, 2007. **81**(18): p. 9759-68.

163. Filonov, G.S., et al., *In-gel imaging of RNA processing using broccoli reveals optimal aptamer expression strategies.* Chem Biol, 2015. **22**(5): p. 649-60.

164. Panavas, T. and P.D. Nagy, *Yeast as a model host to study replication and recombination of defective interfering RNA of Tomato bushy stunt virus.* Virology, 2003. **314**(1): p. 315-25.

165. Sharma, M., Z. Sasvari, and P.D. Nagy, *Inhibition of phospholipid biosynthesis decreases the activity of the tombusvirus replicase and alters the subcellular localization of replication proteins.* Virology, 2011. **415**(2): p. 141-52.

166. Nagy, P.D., *Viral sensing of the subcellular environment regulates the assembly of new viral replicase complexes during the course of infection.* J Virol, 2015. **89**(10): p. 5196-9.

167. Short, J.R., et al., *The Role of Mitochondrial Membrane Spherules in Flock House Virus Replication.* J Virol, 2016.

168. Nienhaus, K. and G.U. Nienhaus, *Where Do We Stand with Super-Resolution Optical Microscopy?* J Mol Biol, 2016. **428**(2 Pt A): p. 308-22.